CUSTOMIZED DESIGN AND DEVELOPMENT OF TRANSTIBIAL PROSTHETIC SOCKET FOR IMPROVED COMFORT USING REVERSE ENGINEERING & ADDITIVE MANUFACTURING

Ph.D. Thesis

CHITRESH NAYAK

(2012RME9543)

DEPARTMENT OF MECHANICAL ENGINEERING

MALAVIYA NATIONAL INSTITUTE OF TECHNOLOGY

JAIPUR

JLN MARG, JAIPUR – 302017, INDIA

July, 2017

CUSTOMIZED DESIGN AND DEVELOPMENT OF TRANSTIBIAL PROSTHETIC SOCKET FOR IMPROVED COMFORT USING REVERSE ENGINEERING & ADDITIVE MANUFACTURING

CHITRESH NAYAK

(2012RME9543)

Thesis submitted

as a partial fulfillment of the requirements of the degree of

Doctor of Philosophy

to the

Department of Mechanical Engineering

Malaviya National Institute of Technology, Jaipur

Jaipur – 302017, India

July, 2017

Dedicated to

My Parents

Malaviya National Institute of Technology, Jaipur
Mechanical Engineering Department

CERTIFICATE

This is to certify that the thesis entitled "**Customized Design and Development of Transtibial Prosthetic socket for Improved Comfort using Reverse Engineering & Additive Manufacturing**" being submitted by **Mr. Chitresh Nayak (Roll No: 2102RME9543)** in partial fulfilment of the requirements for the award of **Doctor of Philosophy** in **Mechanical Engineering** to the **Malaviya National Institute of Technology**, **Jaipur** is an authentic record of research work carried out by him under my supervision and guidance. To the best my knowledge, the results contained in this thesis have not been submitted, in part or in full, to any other University or Institute for the award of any Degree or Diploma.

<table>
<tr><td>Dr. Amit Singh</td><td>Dr. Himanshu Chaudhary</td></tr>
<tr><td>(Supervisor)</td><td>(Co-Supervisor)</td></tr>
<tr><td>Assistant Professor</td><td>Associate Professor</td></tr>
<tr><td>Mechanical Engineering Department</td><td>Mechanical Engineering Department</td></tr>
<tr><td>MNIT, Jaipur-302017 (Rajasthan)</td><td>MNIT, Jaipur-302017 (Rajasthan)</td></tr>
</table>

The Ph.D. viva voce examination of Mr. **Chitresh Nayak** has been conducted by the Oral Defense Committee (ODC) constituted by the Dean (Academic Affairs), as per 9.4.3, vide letter No: F.4 (P) Ph.D./Acad/MNIT/2016/1611 dated 5th July 2017 on wednesday, condect the viva-voce examination dated 20th July, 2017. The ODC declares that the student has successfully defended the thesis in the viva-voce examination.

Dr. Prashant Kumar Jain
(External Examiner)
Associate Professor
Mechanical Engineering Department
IIITDM, Jabalpur

ACKNOWLEDGEMENTS

Chitresh Nayak
Department of Mechanical Engineering
Malaviya National Institute of Technology, Jaipur

ABSTRACT

The main objective of this thesis is to design and develop of transtibial prosthetic socket to improve patient's comfort. The manufacturing of residual limb prosthesis socket that is comfortable for the amputee depends on prosthetic practitioner's knowledge of socket biomechanics and skill. It involves multistage manual corrections depending upon the clinical condition of the patient's residual limb which may be affected by shrinkage or possible damage of Plaster of Paris (PoP) mold.

The research reported in this thesis involves five parts: The first part consists of process simplified through digitization, it integrates conventional PoP processes, reverse engineering (RE), and additive manufacturing (AM) technologies to design and develop a socket. The stereolithography (STL) file generated from the scan data was modeled on a fused deposition modeling (FDM) based AM. The second part consists of identification of optimum pressure distribution of the prosthetic socket under specific load using finite element analysis (FEA). Plaster of Paris (PoP) sockets of different clinical cases and below Knee (BK) amputees having different stump geometries have been considered in this thesis. The quantification of location, intensity, and distribution of stress-strain on the socket leads to improved socket design. The third part predicts the pressure distribution/ pressure measurement around the lower limb/prosthetic socket with the help of Fuji film. Also, a sensor based methodology for effective pressure measurement at the stump-socket interface integrating regression technique and genetic algorithm (GA). An experimental setup is developed for force investigation of the lower limb socket using the FlexiForce sensor. The fourth part evaluates the effects of patient-specific physiological parameters viz. height, weight, and stump length on pressure development at the transtibial prosthetic limb/socket interface. The measured maximum pressure data related to subject's physiological parameters is used to develop the (ANN) model. The fifth part consisting of fitment of socket based on topology optimization was assessed with the help of INSPECTPLUS and GEOMAGIC reverse engineering tools.

Technological advances in prosthetics have attracted the curiosity of researchers in monitoring design and developments of the sockets to sustain maximum pressure without any soft tissue damage, skin breakdown, and painful sores. This approach takes the guess work out of prosthetic practitioner's job, ensures better fitment, and shortens

the total fabrication time leading to improved patient satisfaction. This study will provide an important platform for the design and development of patient-specific prosthetic socket which can ensure the maximum pressure conditions at stance and ambulation conditions. This will help the prosthetist in developing an accurate socket in the first trial providing comfort for the patients by adequate socket fitting.

TABLE OF CONTENTS

LIST OF FIGURES

LIST OF TABLES

_____

ABS	Acrylonitrile Butadene Styrene
AK	Above Knee
ANOVA	Analysis of Variance
AM	Additive manufacturing
AP	Antero-Posterior
ANN	Artificial Neural Network
BK	Below knee
BMVSS	Bhagwan Mahaveer Viklang Sahayata Samiti
BPNN	Backpropagation neural network
CAE	Computer Aided Engineering
CAM	Computer Aided Manufacturing
CASD	Computer-aided socket design
CASM	Computer-aided socket manufacture
CPU	*Central Processing Unit*
CT	Computed Tomography
DAQ	Data acquisition
FE	Finite Element
FEM	Finite element method
FEA	Finite Element Analysis
FDM	Fused Deposition Modeling
GA	Genetic algorithm
HB	Higher-the-better
HDPE	High-density polyethylene
HT	Height
KP	Kick point
LB	Lower-the-better
LDPE	Low-density polyethylene
LT	Lateral tibia
LG	Lateral Gastrocnemius
ML	Medio-Lateral
MG	Medial Gastrocnemius
MT	Medial tibia
MRI	Magnetic Resonance Imaging
NB	Nominal-the-best
NGO	Non-governmental organization
POP	Plaster of Paris
PD	Popliteal depression
PPT	Pain-pressure tolerance
PT	Patellar tendon
PTB	Patellar Tendon Bearing
RP	Rapid Prototyping
RE	Reverse Engineering
SLA	Stereo lithography Apparatus
STL	Stereo lithography
SLS	Selective Laser Sintering
ST	Stump Length

TSB	Total Surface Bearing
TTA	Transtibial Amputee
TT	Transtibial
WT	Weight
1D	One dimensional
2D	Two dimensional
3D	Three dimensional

CHAPTER 1

INTRODUCTION

This thesis concerns the customized design of lower limb prosthesis socket for below knee amputees, called "trans-tibial". The process and procedures employed for prosthesis design are crucial to improve the quality of fit, affecting the quality of the amputee's life. In following section, background and motivation for research work is briefly discussed; finally, an overview of thesis organization is described.

1.1   Background and motivation

Artificial arms and legs, or prostheses, are designed to restore a degree of natural function to amputees. Mechanical devices that allow amputees to walk again or continue to use two hands have probably been in use since ancient times, the most notable one being is the simple peg leg. A surgical procedure for amputation, however, was not widely successful until around 600 B.C. At present, the prosthetic socket is easily manufactured within a day. The prosthetic socket has radically improved the life-quality of millions of amputees globally. Currently, there are more than 30 millions of people worldwide who have amputations (Alcaide et al. 2013), with the help of prosthesis amputees can improve the quality of life. Most involve the lower limb at the transtibial level (Murdoch et al.; 1996, Wilson et al.; 1989). Amputation can occur at any stages of their lives. The loss of a limb represents a very traumatic event in one's life. After China, India has the highest number of diabetic people in the world. In developing countries, including India, the amputation rate is about 45% of diabetic foot problems, with an estimated 50,000 amputations occurring per year (Peters et al. 2016).

Amputation has important economic costs and strong physiological effects due to the loss of functionality. Prosthetic devices represent the best solution to restore lost functions to individuals that have undergone an amputation after diseases or accidents. The prosthesis is an artificial extension that substitutes a missing body part such as an upper or lower body extremity. The amputee needs a prosthetic device and services which become a permanent event. They have a deep

interaction with the human body and their functionality, comfort, and fit, depends on the way in which the device is interfaced with the residual limb.

The number of lower-limb amputees is increasing every year globally (Dilingham et al. 2002). Patients wearing prosthetic socket often experience discomfort. During the last decades, there has been a steady increase in the number of amputations due to peripheral vascular disease (54%) including diabetes mellitus and peripheral arterial disease, trauma (45%) and cancer (less than 2%) including tumors and congenital defects (Ziegler-Graham et al., 2008). Although not all causes of limb loss are avoidable, the leading causes of amputation, difficulties from diabetes and peripheral artery disease which can often prevented, and then reduced through patient edification, disease management and regular foot screening.

In India, Bhagwan Mahaveer Viklang Sahayata Samiti (BMVSS), also known as *Jaipur Foot organization*, a non-governmental organization (NGO), a non-profit organization, is a major developer and distributor of prosthetic, orthotic, and assistive devices throughout the developing world. The organization was started in Jaipur, India in 1975 and now has 16 centers throughout India and some free camps held every year in various locations of the country. With the help of BMVSS, Jaipur Foot camps also have been conducted in 25 countries as shown in Table 1.1. The Jaipur Foot fabricated and fitted approximately 23,000 patients annually. BMVSS services about 80,000 patients each year by providing all artificial limbs, calipers, crutches, ambulatory aids like wheelchairs, hand paddled tricycles and other assistances and appliances entirely free of cost to the physically challenged people. Using an outside funding source, they distribute all their products free to amputees. (www.Jaipurfoot.org).

Table-1.1: Jaipur limb fitments of artificial limb throughout the world

Continent	Country	Patients with prosthesis
Asia	Afghanistan	3738
	Bangladesh	1588
	Indonesia	1398
	Iraq	882
	Lebanon	381
	Nepal	200
	Philippines	3000
	Pakistan	987
	Shri Lanka	2373
	Vietnam	600
Africa	Liberia	271
	Malawi	250
	Mauritius	567
	Nairobi	500
	Rwanda	500
	Senegal	607
	Somalia	1000
	Sudan	1800
	Zambia	121
	Zimbabwe	250
Australia	Papua New Guinea	170
North America	Dominican Republic	500
	Honduras	400
South America	Trinidad	200
Oceania	Fiji	300
Total		**23,483**

(Source: Jaipur Foot)

1.2   Transtibial amputation

This research focuses on one particular group of amputees, specifically lower limb, below knee (BK) amputees, also referred to as transtibial amputees. As compared to the upper limb amputees, lower limb amputees experience more changes in their life after the amputation (Demet et al. 2003). The incidence of lower limb amputation is also greater than the upper limb (Ziegler-Graham et al. 2008).

Trans-tibial amputations have a clear benefit over higher-level leg amputations since the knee joint remains the artificial leg replaces functional and less mass. However, the bony structure and the low, soft tissue coverage make it susceptible to pressure and friction related injuries.

Amputees need a prosthetic device after limb surgery, which is an artificial extension that replaces a missing body part. The pressure interface between the residual limb and prosthetic socket has a significant influence on an amputee's satisfaction and comfort. The customized socket is fitted around the amputee's residual limb that supports body weight bearing throughout specific regions. Traditionally, fitment of socket depends on prosthetic practitioner's knowledge of socket biomechanics and skill. The contact pressure distribution at the socket-socket interface has been a critical consideration for the practice of socket design. Lower limb prosthetic socket offers interaction between the patient's stump and the prosthesis (Powelson et al. 2012 and Ryait et al. 2012).
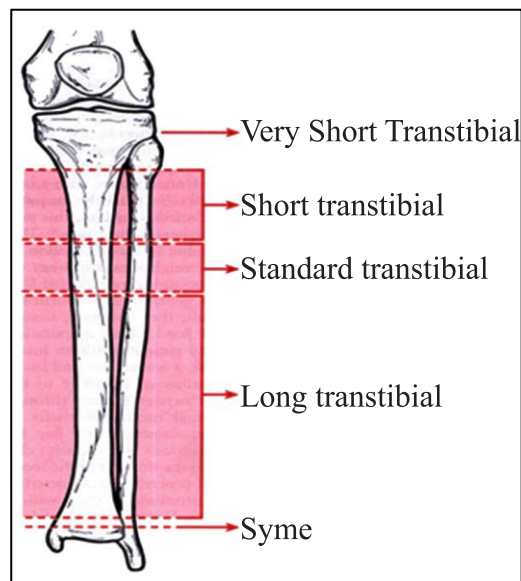
Figure-1.1: Amputation regions on below-knee (Seymour, 2002)

1.3   Transtibial Prosthetic sockets

The trans-tibial prosthetic socket is used for lower-limb amputees, who have their leg amputated below the knee, i.e. across the tibia. Prosthetic is an artificial add-on that substitutes a lost human body part. The socket portion of the trans-tibial

prosthesis is the crucial element which determines the successful rehabilitation of the patient (Sewell et al. 2012). The design of prosthesis socket is a challenge due to the complex geometry of the stump which differs from one amputee to other. Prosthesis socket aims to performance as an interface between the amputee's limb and his prosthesis (Mak et al. 2001 and Moo et al. 2009).

The socket offers a perfect interface between prosthesis and residual limb, which is designed to provide comfort, proper load transmission, and efficient moment control. The appropriate pressure distribution between the limb/socket interfaces is a significant factor in the socket design and fit (Mak et al. 2001). The bone closer to the surface is one of the subtle areas which should not be exposed to high pressure; on the other hand, pressure must be sustained by the limb's areas of thick tissue. The prosthesis socket has critical importance as the residual limb does not possess the same weight-bearing competencies as foot (Goh et al. 2004). The trans-tibial prosthetic patients experience pressure between socket and stump while performing routine actions. Therefore, a pressure measurement at the limb-socket interface provides key information on processes of socket manufacturing, fitting and modification. The prosthetics select the best socket design depending on the patient's skin integrity and situation of the residual limb. Achieving a good socket-stump interface, provides a comfortable transmission of body weight, supporting the amputee's limb during the standing phase and walking, sufficient control of motion and transfer forces from the residual limb to the prosthesis during patient's daily activities, it desires to be lightweight.

The purpose of a prosthetic socket is to integrate the prosthesis as a well-designed extension of the residual limb by providing coupling between the stump and the prosthesis. The entire load from the residual limb is transferred to prosthesis through the stump's soft tissues in contact with prosthetic socket, liner and socks. The primary factor in determining the comfort of prosthesis and its effectiveness in restoring the amputee mobility is the fit of prosthetic socket. Prosthetic replacement is one of the most significant rehabilitation programs for amputee loses their limbs. The transtibial prosthesis is collected primarily from three parts: socket, shank and foot as shown in Figure 1.2.
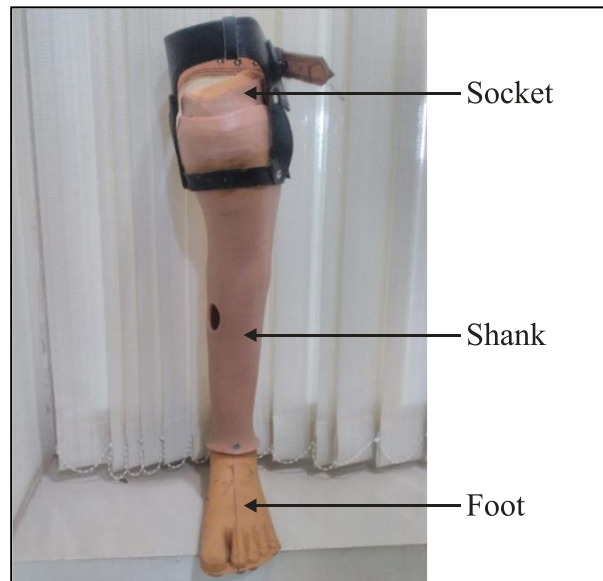
Figure-1.2: Transtibial Prosthetic socket

Thickness of Prosthetic Socket

- Prosthetic socket is typically composed of a relatively stiff material, such as polypropylene or polyester, and is approximately 3 to 6 mm thick [Silver-Thom et al. 1996].

- System proposes the final socket thickness according to the following empirical formula:

  Socket thickness [mm]

  $$= \frac{\text{Patient weight [kg]}}{20} \quad \text{[Colombo et al. 2013]}$$

- Equation used to define the overall thickness of the socket wall is given by [Roark et al. 1975 and Pilkey et al. 1994]

  $$t = \frac{qR^2 + \frac{p}{2}vRL}{E\Delta Rmax}$$

Where q is the normal pressure load, R is the radius of the cylinder, p is the transferred shear stress, v is Poisson's ratio, L is the cylinder length, E is Young's modulus, and $Rmax$ is the maximum desired radial expansion.

1.4   Importance of socket fitting

Fitting a socket is a craftsmanship that continues to progress. If the socket doesn't fit correctly, it will cause pain, sores, and blisters to the person wearing it and prosthesis will feel heavy and cumbersome. The socket is the main interface between prosthesis and residual stump of the patient. It helps to transfer load from above i.e. head-trunk and swinging limb to prosthesis during walking. The other important function of the socket is to control the residual joint motion (the main joint which is saved after the amputation). An optimum socket fitment will cause minimum pseudo-joint motion (motion due to slippage or stump socket poisoning). But the residual stump, not a symmetrical structure and it varies from one individual to another.

A new amputee will have gradual changes in the residual stump. These changes in stump shape take place for a number of reasons and varying degree, depending on patient's activities, weight, amputation procedure, health and other issues. Therefore, each patient will have a unique condition of the stump which requires specific socket fitment to accommodate these changes.

Traditional socket making becomes a hit and trial approach as check socket is prepared based on subjective feedback from amputee and the skill of the prosthetic practitioner. The main reason for this time-consuming socket fitting process is the various sources of pain in stump due to interface pressure. Stump-socket friction during walking varies depending upon socket design; material also affects the comfort of the residual limb. Also, ill-fit prosthesis causes severe discomfort due to uncontrolled pressure on the already distressed residual limb. Therefore, to improve the patient condition in prosthetic fitment advance technology can play a crucial role.

Conventional techniques used externally obtained anthropomorphic data to produce prosthetic socket through a laborious, experience-based artisan skill. Reverse Engineering (RE) has the competence to shorten the product development cycle time by process integration and manual intervention. A topographical image of the stump is acquired using an optical digitizer and eventually creates a positive

mold. Furthermore, researchers have applied the concept of Reverse Engineering using CAD technology for possibilities of developing prosthetic sockets through Additive Manufacturing. Tay et al. (2002) described a CASD/CASM method for prosthetic socket manufacturing. It was found that FDM provided excellent fabrication results, but a major drawback is long construction time (about 30 hrs) which was not reflected to be cost-effective. Patient-specific prosthetic socket using RP technique proved that the socket fabricated using this method is beneficial in durability, time saving, cost and accuracy of the socket than other manual methods. However, comfortable prosthetic sockets manufactured by 3D printing have been used in preliminary fittings with patients. One of the principle benefits of FDM technology is the use of various materials which includes ceramic materials, polymers (synthetic and natural), metals and biodegradable materials with a promising avenue for cost reduction in the development of prosthetic socket (Herbert et al. 2005, Hsu et al. 2010, Sengeh et al. 2013 & Tzeng et al. 2015).

A good custom-made model can only be achieved if the measurement and the casting of the stump are precise and manufacturing is accurate. The traditional manual production of artificial limbs is carried out by first creating negative, and a positive cast of the asymmetric shaped residual limb which may lead to inaccuracy and ultimately results in the pain and difficulty in prosthetic use (Bowker et al., 1992 and Rogers et al. 2007).

Integration of advanced tools like reverse engineering, CAD, and FEM plays an essential role in improving the design, analysis, and manufacturing of the socket. Finite element method (FEM) is applied to predict pressure and stress occurring in prosthetics in Clinical Biomechanics (Krishna et al. 2015 & Jia et al. 2004). The behavior of prosthetic socket has been studied based on certain assumptions, such as ignoring the friction/slip at the limb-socket coupling and the pre-stressed produced by donning the limb into a shape-modified socket (Zachariah et al. 2000 & Zhang et al. 2000). FE models for BK amputees have also been originated to manifest the stress-strain coupling among socket and stump (Lee et al. 2007 & Portnoy et al. 2009). In another approach, contact interface is modeled considering the friction/slip

circumstances and pre-stresses applied to the limb within a correct socket (Lee et al. 2004).

At present, automation has been used to help fit amputees with prosthetic limbs. Eighty-five percent of prosthetic facilities prepare a mold from the design of a model of the patient's lower limb, using CAD/CAM. Laser-guided measuring and fitting are also available. The advent of digital technology for prosthetic and orthotic practice plays a significant role in the clinical treatment. Pressure is one of the most important factors for proper fit, comfort, and capability to bearing the load of the prosthetic socket. Fuji film has been determined to be an exact and reliable method for determining contact areas and stresses within the stump-socket. The possibility of using the Fujifilm pressure measurement system providing reliable information on socket fit. The method discussed can be used for designing, fabrication, and application of the transtibial prosthetic socket.

Prosthetic socket is a freeform shape in which numerous control factors collectively find out the performance output (i.e. Pressure), and there is enormous scope in it for application of opposite statistical techniques for process optimization. But unfortunately, no studies were found on the relation between amputee's physiological parameters and the maximum pressure measured at the limb/socket interface. The present work addresses this aspect by adopting regression technique, genetic algorithm (GA) and statical method to optimize the process parameters. An experimental setup is developed for force investigation of the lower limb socket using the FlexiForce sensor. The pressure values at the limb/socket interface were clinically measured during stance and walking conditions of different patients using strain gauges placed at critical locations of the stump for each patient. But when we require characterizing all the likely combinations of the prosthetic socket, a prediction model based on Artificial Neural Network (ANN) can be formed. A well trained or designed prediction model can be used to predict the output (Pressure) for any combinations of the input variables (height, weight, and stump length).

Against this background, the present research work has been undertaken to study the customized prosthetic socket design and optimization of the interface

pressure between stump-socket. For this, firstly develop a novel digital process for customized prosthetic socket design and afterward effective pressure measurement at the stump-socket interface under different loading conditions, evaluation of amputee's physiological parameters, and statistical interpretation of the various test results.

1.5   Thesis Statement

This thesis presents a CAD/CAE based approach for producing a topology optimized prosthetic socket for transtibial amputees using anthropomorphic data obtained from surface scanning. The fundamental goal of a comfortable socket design is to maintain reduced socket interface pressure on anatomical landmarks including the fibula head, tibia, medial tibial flare, lateral femoral condyle and the medial femoral condyle. Increasing compliance over these locations while maintaining structural integrity for dynamic walking activities is crucial. Unlike previous works, this thesis presents a novel approach for developing a CAD model of Prosthesis socket. Based on finite element analysis and experimental pressure measurements, interface contact peak pressures at the anatomical features were predicted. The resulting peak pressures were redistributed using topology optimization and finally, the improved socket design was 3D printed using FDM-based additive manufacturing technology. The accuracy of the resulting socket was verified using the traditional methodology.

1.6   Hypothesis

A CAD/CAE based fabricated topology optimized socket using a transtibial mapping generated from the quantitative 3D anthropomorphic data of a residual limb will maintain reduced socket-residual limb interface peak contact pressures for an amputee. Improved comfort resulting from lower peak pressures is anticipated in a topology optimized socket over a conventional socket.

1.7 Thesis organization

This thesis contains eight chapters which are arranged as follows:

Chapter One: Introduction

The background, motivation and significance of the research work to develop a customized prosthesis socket design are presented in this chapter. It also highlights the outlines the organization of the thesis.

Chapter Two: Literature Review

This chapter included a literature review and developed for the customized prosthetic socket to deliver a summary of the base of knowledge previously available including the issues of interest. It presents the research works on lower limb prosthesis sockets as well as the various technologies employed by various investigators.

Chapter Three: Reverse Engineering (RE) and Computer Aided Design (CAD) based Customized Prosthetic Socket Design

This chapter discusses the traditional and innovative approach to developing a customize socket design. It presents the detail fabrication of below-knee socket at Bhagwan Mahaveer Viklang Sahayata Samiti (BMVSS).

Chapter Four: Finite Element Analyses of CAD Model of Socket Obtained using Reverse Engineering

This chapter presents a new perspective for identifying stress to optimize and improve socket design using finite element analysis (FEA) method. The method to reduce the stress on socket through topology optimization is also presented.

Chapter Five: Experimental Pressure measurement between stump and socket

This chapter presents a discussion on results of pressure distribution around the residual limb under different loading conditions. It includes two different types of sensors for optimized pressure between stump-socket interfaces.

Chapter Six: Prosthetic socket pressure prediction using ANN

This chapter includes, predicting the pressure under different operating condition using artificial neural networks (ANN) technique and the compared with experimental results. Finally, the outcomes of pressure behavior optimized by Taguchi experimental design and the most significant factor are determined by ANOVA.

Chapter Seven: Additive manufacturing of socket based on Topology optimization

This chapter presents, the dimensional evaluation of AM socket based on topology optimization

Chapter Eight: Conclusions and Future Scope

The experimental and analytical results obtained are summarized in this chapter. It also addresses the contributions and future scope of the research work.

Chapter Summary

This chapter describes the background, motivation, and significance of the research work and it also contains brief information about the seven chapters of the thesis.

CHAPTER 2
LITERATURE REVIEW

Introduction

This chapter presents an extensive literature review which provides background information on the research topics of the current investigation. This is a multidisciplinary research covering a broad range of subjects including pressure sensors, additive manufacturing and FEM Analysis with reverse engineering of customized prosthesis socket design. Several review papers such as Sander (1995), Cummings (1996), Silver-Thorn et al. (1996), Zhang et al. (1998), Mak et al. (2001), Linde et al. (2004), Baars et al. (2005), Collins et al. (2006), Sagawa et al. (2011), Sander (2011), Gholizadeh et al. (2014), Andrysek (2010) Sang et al. (2016), Al-Fakih et al. (2016) has been published on prosthetic socket design & manufacturing, stump-socket interface stress measurement and evaluation considerations for prostheses in the developing world. In a previous study, researchers have integrated the rapid product design and development with an goal to treat many concepts of 3D scanning, CAD-based modeling, and 3D printing, 3D scanning technique combined with RE and rapid prototyping (RP) principles for inspection of part quality, introduced an approach that combines scanning technology, computer aided design, and Rapid Prototyping.

Traditional fabrication of these sockets has always been a time-consuming and complicated task. However, recent studies and investigation have shown the feasibility of using scanning technology, computer aided design (CAD), Finite Element Analysis and 3D Printing techniques in prosthetics. Therefore, the goal of this thesis was to use existing technologies to improve the current procedure for prosthesis socket design.

The methods available in the literature can be classified as follows:
- On the basis of prosthetic socket fit and design
- On the basis of geometry acquisition and CAD based digitization of socket
- On the basis of optimization of the socket using Finite Element Analysis
- On the basis of pressure measurement and stress distribution
- On the basis of additive manufacturing

At the end of the chapter, a summary of the literature survey and the knowledge gap in the previous investigations are presented.

2.1 On the basis of prosthetic socket fit and design

Traditional prosthetic socket manufacturing processes invariably is an artistic and a labour intensive process. In this method prosthetist must know the complete topology of the amputee's stump and needless to say, many factors affect the design and quality of fit. A suction socket for the above-knee prosthesis was created at the University of California (UC), Berkeley by (Eberhart et al., 1954). Additionally, several corrections/innovations in below-knee socket design created by prosthetic practitioners in several parts of the developing country (Radcliffe and Foort; 1961, Berlemont et al., 1969, Kay et al., 1975, Michael et al., 1986).

2.1.1 Residual limb volume measurement techniques

Amputee wears prosthetic socket which must oblige a broad range of function because of the residual limb volume changes during the entire day. It is required that the socket, adjust to accommodate changes in volume to maintain proper fit and comfort. Wilson et al. (1987) describe a preliminary prosthesis socket design with six amputees, by fabrication techniques for adjustable volume trans-tibial socket. The authors defined the purpose of their socket as custom fitted; using existing prosthetic molding, modification, and fabrication techniques; control volume equally or selectively between proximal and distal parts of the residual limb; have standard prosthetic Cosmesis, and be light but durable. The main problems arrive at maintaining the prosthesis socket comfortable and an accurate fit. It is due to changes in residual limb volume and shape due to edema and muscle atrophy occurring post-amputation (Golbranson et al., 1988).

Insufficient control of residual limb volume leads to delay prosthetic fitting. The advantage of early fitting with a prosthesis have been suggested to include achieving a more normal gait re-education; accomplishing a more independent life; undertaking more active physical training; gaining psychological advantages such as better acceptance of the amputation and restoration of body image; hastening the maturation of the residual limb; and adapting the residual limb form to the definitive socket (Lilja et al., 1997). Day-to-day changes in the volume of the residual limb

can cause discomfort and pain for the person using lower limb prostheses. It was found that the volume of the residual is affected by muscle contraction. Specifically, muscle contraction in the TTA residual limb increased its volume by 3.5 and 5.8% with and without a silicone liner, respectively (Lilja et al. 1999).

(a) Transtibial length caliper

(b) GPM anthro-pometer

(c) Universal anterior-posterior–medial-
lateral caliper
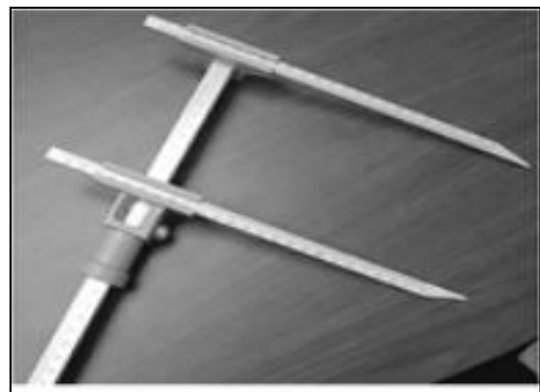
(d) VAPC caliper

(e) Standard tape

(f) Spring tape

Figure-2.1: **Measurement devices (Geil 2005)**

The accurate measurement of the residual limb at different anatomical landmark which, depending on the tools such as transtibial length caliper, universal anterior-posterior–medial-lateral caliper, standard tape, spring tape, and circumferential tape as shown in Figure 2.1 (Geil, 2005 and Boonhong 2007). It also depends on the Prosthetic practitioner's skill (Vannier et al., 1997), on the measurement condition of the patient's stump. Markers on the limb identify standard anthropometric dimensions, usually in correspondence with the articulation, the critical parameters are observed to be such as stump length (from the under patella support to tibia apex) and femoral condyle position. Further, casting reliability following the shape of the socket with the control of manual dexterity during refinement has also been reported to be a major factor (Buis et al., 2003 & Convery et al., 2003).

2.1.2 Prosthesis socket fabrication

Prosthetic socket is the primary interface between the amputee's residual limb and the artificial leg. Unlike other components, such as knee links and foot, which are modular, the socket is custom made on the stump. A good custom-fit model can only be achieved if the measurement and the casting of the stump are precise and manufacturing is accurate. State-of-the-art socket developed has its limitations. Prosthetic socket manufacture is carried out exclusively according to the external shape of the amputation stump using manual casting methods (Foot at al. 1979, Radcliffe et al. 1957).

To create a socket by traditional manufacturing, the prosthetist has to capture the free-form profile of the residual limb by wrapping a cast around it; either the residual limb is loaded or unloaded. It depends on the performance and skills of the prosthetist. Initially, creating negative and a positive cast of the asymmetric shaped residual limb led to inaccuracy and ultimately results in the pain and difficulty in prosthetic use (Bowker et al., 1992 & Rogers et al., 2007) as shown in Figure 2.2. The effusion of the cast creates a positive model which serves as a negative form to shape the prosthetic socket using plastic material (Lee et al. 1997). Alterations can be done on the negative mold before a positive mold completely from it. However, modifications are commonly made to the positive mold. The anatomical points of

interest are identified on the positive mold and extra material is either added to relieve pressure at sensitive areas, or removed, to increase pressure at the specific load bearing positions (Muller et al. 2007). A test socket is shaped from the improved positive mold to be tried by the patient before a final socket manufactured. This is repeated and could last several weeks or months up to adaptable comfort is accomplished as practiced by the amputee. Patient use soft liner is made of 5 mm thickness polyethylene (PE), it acts as an interface between the stump-socket. The traditional methodology used to design prosthetic socket is time-consuming and complicated, by this, is estimated that nearly hundred present of amputees experience socket discomfort (Saunders et al. 1985).
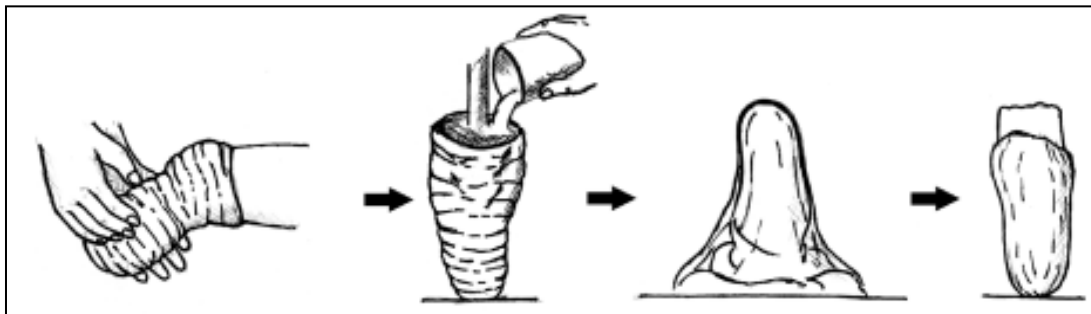
Figure-2.2: Socket design based on a plaster cast (Ng et al. 2002)

Jensen et al. (2004) examine the outcome application of the high-density polyethylene (HDPE), Jaipur prosthetic construction in fitting transfemoral amputees. The study includes three countries in Honduras, Uganda, and India. One hundred and fifty-eight (158) amputees had been offered with the HDPE Jaipur prosthesis and of these 72 were seen for a clinical and technical follow-up after a median of 32 months. It was found that amputees are unsatisfactory both technically and clinically. This was a reflection of the insufficiencies of the prosthetic manufacture, mostly the knee joint, and the inadequate training of prosthetic practitioner's which involved in the fabrication and fitting. Jensen et al. (2005) suggested a sand-casting technique for below-knee socket was practical to twenty-eight amputees, provides a better fit and offers an alternative to plaster of Paris casting.

2.1.3 Types of prosthetic socket

There are two types of prosthetic sockets: a Patella Tendon Bearing (PTB) socket, and Total Surface Bearing (TSB) socket. It has been observed that the type

of prosthetic socket used by an amputee affects the physical and the biomechanical situation of the residual limb.

Patella Tendon Bearing (PTB) Sockets

Patella Tendon Bearing (PTB) (See Figure 2.3) Socket is also known as Specific Weight Bearing sockets, as the socket is molded to forces or load onto specific areas of the stump. Created from work done at the Symposium of below Knee Prosthetics at Berkeley, California in 1957 were formally introduced in 1959 (Radcliffe and Foort, 1961).

Figure-2.3: Patellar Tendon Bearing Socket

PTB socket design work on the principles of total contact and selective loading theory. The design of PTB socket has changed little over the years. Total contact theory states that all surfaces of the stump are in contact with inner walls of the socket which does not mean total support of body weight. Selective loading theory states to determine the pressure tolerant or intolerant of the stump. Selective loading theory refers to the identification of specific areas of the stump that are tolerant or intolerant of pressure. Biomechanics of the stump is described by (Murphy et al. 1962). Pressure tolerant areas are Patella tendon, the medial flare of tibia and popliteal area/ gastrocnemius belly. Pressure intolerant areas are a Tibial crest, including tibial tuberosity, distal ends of the tibia and fibula, Head of the fibula & peroneal nerve. The PTB socket design assists in controlling pressure distribution,

which changes throughout the gait cycle. (Sanders et al. 1997) was found that maximal pressure at the anterior distal and mid portion of the stump in the first 50% of stance, and this is shifted to anteromedial and lateroproximal sites through late stance.

Total Surface Bearing (TSB) sockets

A total surface bearing socket design (See Figure 2.4), all portions of residual limb evenly share the pressure distribution and weight bearing of the prosthesis. PTB sockets are manufactured using a pressure casting system, and fit can be inspected through the use of clear check sockets. However, (Dumbleton et al., 2009) found higher interface pressures with a pressure cast TSB compared to a manually cast PTB. In spite of this finding, the wearers did not complain of discomfort. However, steeper pressure gradients in PTB sockets compared to TSB sockets were found, suggesting higher levels of localized shear forces in the PTB sockets.

Figure-2.4: Total Surface Bearing Socket

Use of TSB sockets may cause a loss in stump volume of up to 6.5% with use (Staats et al., 1987), which causes worsening in the fit of the socket and increases the risk of skin irritation. However, adding vacuum assist pumps to the suction socket was found to lead to a net gain in stump volume (Goswami et al., 2003), which is recommended to ensure a good fit. However, (Selles et al., 2005) found a TSB socket functioned similarly to a PTB regarding patient satisfaction,

ADL's, and gait characteristics. In TSB socket, there is a greater range of knee flexion, less traumatisation of the skin and lighter than a PTB, It has less pistoning than a PTB (Yigiter et al., 2002). Manufacturing and fitting pressure cast TSB sockets can be less time consuming than PTB sockets (Hachisuka et al., 1998).

Comparison of PTB and TSB socket

In the below-knee prosthesis, suction is a mode of suspension that can only be maintained through an accurately fit the socket. In this section, we have compared the two techniques whereby such a fit can be achieved. In order to understand differences, Stump/Socket interface gap between the TSB and the more traditional PTB sockets has been made. The basic idea of the patellar tendon bearing below-knee prosthesis can be stated as follows:

Table-2.1: Comparison between PTB and TSB socket

Parameters	Patellar Tendon Bearing Socket (PTB)	Total Surface Bearing Sockets (TSB)
Weight bearing / Shape / Volume	Cause stress concentration in a specific region may result in discomfort. Shape and volume change are likely to be affected by the pattern of stress distribution due to different socket styles.	Weight is distributed over the entire surface of the residual limb on the contact surface maintained during the gait cycle. The shape of the stump remains same as the uniform distribution of pressure provided by the TSB socket design.
Prosthetic mobility	It has decreased intact step length; slow functional mobility	It has increased entire step length; faster functional mobility
Suspension	Socket pistoning is likely, due to the accommodation of pressure sensitive areas.	A Reduced socket volume, which leads to reduced pistoning and hence better suspension.
Peak pressures	300 to 400 kPa; this is because of classical PTB socket design is based on soft tissue firmness (pressure sensitive and pressure tolerant).	200 kPa; the less average pressure in TSB design is because of pressure distributed all over the stump more evenly.

Parameters	Patellar Tendon Bearing Socket (PTB)	Total Surface Bearing Sockets (TSB)
Proprioception	Diminished proprioception, which may result in less control movement.	Enhanced proprioception, therefore more controlled movement.
Pressures Distribution	Uneven distribution of pressure along the entire residual limb-socket interface and hence, large forces applied to small areas.	Even distribution of pressure along the entire residual limb-socket interface and forces are applied to the whole area of the stump.
Blood Circulation	Improper blood circulation within the stump due to uneven distribution of pressure.	Blood flow is seen to be enhanced inside the stump.
Material	Low-cost interface material can be used for PTB socket manufacturing. Ex. EVA can be used.	High-cost interface material is required for making a standard TSB socket. Ex. Silicone liner is used as a soft insert.
Fitting/ Comfort	Socket comfort or fitting are compromised, and Ill-fitting sockets may result in deterioration of the stump, excessive shrinkage or edema.	Socket fitting is far better as compared to PTB Socket.
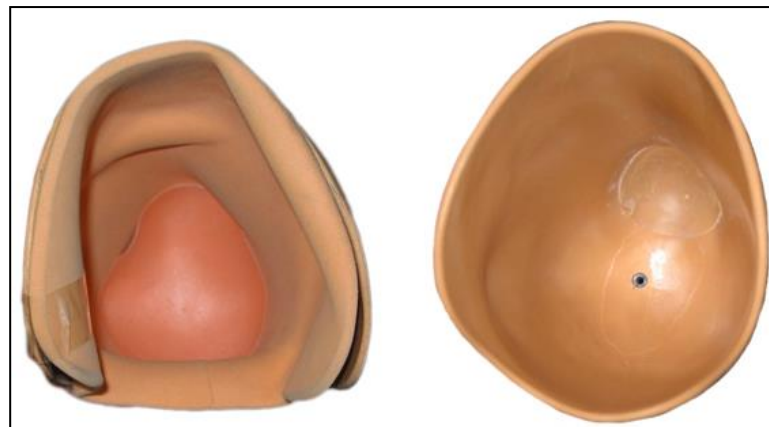
Figure 2.5: PTB & TSB Socket

Despite differences (See Figure 2.5), PTB and TSB socket performed equally well regarding patient satisfaction, comfort, ease of flexing the knee, slippage, less skin irritation, better appearance and grit performance. Material cost is higher in the TSB group, whereas the manufacturing time in the TSB group was low. The prosthetic socket, being a human-device interface, should be designed so as to

achieve flexible, lightweight, optimal load transmission, stability, and efficient control of motion. Some early designs of the prosthetic socket such as the "plug fit," were designed as a simple conical shape with very little biomechanical rationale involved. Over the years, it became obvious that a biomechanical understanding of the interaction between the prosthetic socket and the residual limb is crucial to improving the socket design. With an understanding of the residual limb anatomy and the biomechanical principles involved, more flexible designs soon came about.

2.2 On the basis of geometry acquisition of socket and CAD based digitization of socket

The residual lower limb focuses on constant morphological changes (Nawijn et al. 2005), both in short and long term; these changes require a new socket realization when any significant variation occurs. A variety of image processes has been explored for the application in socket design. At present, there are different techniques existing to acquire internal and external geometry of residual limb.

2.2.1 Internal geometries

The main methods for obtaining residual limb parts (bone, muscle, soft tissue, skin and blood vessels) Computed Tomography (CT) (Smith et al. 2001) (Lacroix et al. 2011), Magnetic Resonance Imaging (MRI) (Buis et al. 2006) (Douglas et al. 1998), and Ultrasound (Douglas et al. 2002) that have been integrated into CAD/CAM socket design. These noninvasive methods create cross-section geometrical images of the residual limb, and it is possible to analytical/reconstruct and to visualize 3D the inner part of a limb by the apparatus using computers.

Computed Tomography is a part of traditional radiology. CT scan makes use a wide beam of ionizing radiation in the form of X-rays. Computer handled combinations of many X-ray images taken from a different angle to produce cross-sectional images of specific areas, 3D model of the residual limb, permitting the user to see both soft and hard tissues inside the limb without cutting (Webb, 1988). The results of the CT are better than the traditional radiology regarding diagnostic imaging of soft tissue, with using a quite high radiation dose for the patient.

Previous studies depicted that CT scan has a precision and accuracy value of 0.88 mm and 2.2 mm respectively (Commean, 1996). CT data acquisition offers faster scanning less than a minute as compared to 3D geometry created by the FEM model of the prosthetic stump is about 8-10 minutes (Kovacs et al. 2010). Computed tomography (CT) permitted the integration of patient-specific stump-socket geometry into a CAD/CAM system, performing modifications, and milling a positive plaster likeness. In spite of being static analyses, these studies offered high image quality and the benefit of seeing the skin. However, significant CT disadvantages from movement artifacts were reported (Smith et al. 1995 & 1996).

Similar to CT, MRI requires the patient to adopt a horizontal position. This posture suffers the effect of gravitational forces on the soft tissue distribution of the residuum in connection with the skeletal structure. Nowadays, alternative MRI scanner designs, such as upright systems, allow the patient to be also acquired in a vertical position, avoiding the soft tissues flattering. MRI images look similar to a CT image; however, in MRI images bones are dark in color. MRI used for learning the shape and volume of the residual limb (Zhang et al. 1998). MRI provides high-resolution images that show a clear difference between the tissues. However, it is expensive and requires a longer scan time: for the whole residual limb, due to which a compromise solution between details and scan time (approximately 10 minutes) is obtained by using a slice thickness of 2 mm associated with 0.6 mm of in-plane resolution (Buis et al. 2006).

Ultrasound offers the potential for imaging internal residual limb structures, therefore contribution new vision not achieved with any of the previous technology. However, ultrasonic imaging is a very time-consuming process, with a scanning time of 13 minutes, creation it highly disposed to subject tremor and movement (He et al. 1996 & 1997). One additional investigation has been reported on limb prosthetics using ultrasound (Singh et al. 2007).

The limitations of the technology are a few such as it takes a long time to produce an image, high cost and a scan involve ionizing radiation (Faulkner et al. 1989). Ionizing radiation (x-rays or γ-ray) contain sufficient energy to ionize atoms

and molecules within the body, causing serious and lasting biological damage. The absorbed dose, measured per unit mass of the body, is usually considered acceptable, but it strictly depends on the time of exposition (Dougherty, 2009). Frequent discussions and extensively scanned areas lead to incremental considerably the absorbed dose, making this technique harmful and then unsuitable. Smith et al. (2013) evaluated the accuracy of the image segmentation process, printing process, and bone surface reconstruction.

2.2.2 External geometries

After various attempts to get a customized socket, scanning is found to be one of the best methods. However, scanning of the live residual limb is a challenging task. It may lead to inconvenience to the patient and has a psychological impact and physical fatigue because of holding the patient in the same posture for a long time and patients often tend to be skeptical of scanner rays. (Varady et al. 1997) reported the possibility and problems of use of 3D scanning in interpreting topology of simple geometries

There are two methods used to execute optical scanning is silhouetting (Schreiner et al. 1995 & Smith et al. 1995) and fringe projection (Commean et al. 1996). With the help of silhouetting, the outline of the residual limb is observed from different angles. By fringe projection, a fringe is used to view from different angles of the residual limb. Both methods create 3D digital images taken from various locations around the limb which help to calculate the volume of the residual limb. An optical scanner is having the fast processing time, scanner acquired images in 1.1 seconds (Schreiner et al. 1995), in 1.5 seconds (Sender et al. 2008) and 0.75 seconds (Commean et al. 1996). By collecting 3D numerical data describing the surface of the limb and specific modification site locations; a positive mold is produced with the help of a high-resolution numerical control (NC) milling machine (Engsberg et al. 1992).

Another approach based on reverse engineering employs a non-contact scanner to get the digitized point cloud data of the lower limb. Fernie et al. (1985) and Oberg et al. (1989) introduced laser scanning for residual limb volume

measurement in the field of prosthetics and orthotics. Then, Lilja et al. (1995) and Johansson et al. (1998) calculated the volume of residual limb taking images at multiple positions of the limb. The advantage of this design is that the laser light is perpendicular to the surface of the residual limb which causes minimum distortion with scanning time 10 seconds. The strength of laser scanning approaches is that there is no uncertainty in identifying features in the images (Turner-Smith 1997).

The CAD/CAM technology is based on three-dimensional digital programs, on where the less possibility of human error with the rapid fabrication of the final socket. At present, the reconstructive and corrective medicine is based on virtual reality. A computer-aided socket design (CASD) and manufacture (CASM) method for lower limb amputees have been established at the Medical Engineering Resource Unit (MERU) of the University of British Columbia at Vancouver (Novicov et al. 1982 & Dean et al. 1985). The CASD system is a collaborative software package written in PASCAL. (Sunders et al. 1985) reported the design of below-knee sockets improved comfort for the amputee through software controlling. (Krouskop et al. 1987) Extended this method to investigate CAD technology can be used to design socket for above-knee amputees. The CAD/CAM method offers a controlled method for shape capturing of patient's lower limb with modification, an accurate method for positive mould fabrication, a decrease in manufacture time, determines manual correction areas, quality of fit, and an easy to sending the physical model efficiently over the hand cast model techniques (Torres Moreno e*t al.,* 1995; Lemaire and Johnson, 1995 & 1996). A physical model of socket obtained after 3D scanning that can convert into a CAD model using a commercial software system such as CANFIT, CAPOD, CADVIEW, rapid-Form. However, some limitations, several non-contact scanners generate an enormous amount of point data. This leads to a massive file size that needs an extensive finishing time and makes difficult to transfer it from one place to another. Moreover, enormous time and skill are required for surface operation on these point data.

Computer-aided design (CAD) system to construct the CAD model of that residual limb (Hsu et al. 2001) under static and dynamic conditions. The scanned socket model is transferred directly through a CAD interface used for rapid product

development. Varady et al. (1997) reported the possibility and problems of use of 3D scanning in interpreting topology of simple geometries. As per after mentioning, direct scanning of the human stump either with Magnetic Resonance Imaging (MRI), Computed Tomography (CT), the 3D scanner was involved (Bibb et al. 2000). Cugini et al. (2006) and Colombo et al. (2006) integrated reverse engineering non-contact laser scanning and two medical imaging technologies, computer tomography (CT) and magnetic resonance imaging (MRI) tools to optimize reconstruct a 3D lower limb socket prosthesis design. Also, a key role is played by the digital geometric model of the residual limb, which replaces the plaster cast socket design. Virtual Socket Laboratory (VSL) (Facoetti et al. 2010) prepares the socket virtual prototype directly on the digital model of the patient's residual limb and simulates the real activities. The benefits of laser scanning are fast scanning process, accuracy, consistency and clean.

Various studies demonstrated the benefits of CAD/CAM systems to design and manufacture prosthetic socket (Spaeth et al. 2006, Oberg et al. 1993, McGarry et al. 2005 & Hsu et al. 2000). Houston et al. (1992) conducted subjective knowledge-based on the design of CAD/CAM studies with the below-knee prosthetic socket. Geil et al. (2007) recorded six basic anthropometric dimensions from CAD shape files of three positive foam models of the residual limbs of persons with transtibial amputations. Smith et al. (2001) found no significant differences between manual and CAD/CAM socket designs. Similarly, Sanders et al. (2007 & 2011) compared manufactured socket profile and CAD data file shapes by central fabrication facilities for a collection of below knee amputee sockets. CAD/CAM methodology has been used for lower limb amputees providing seamless variable impedance prosthetic (VIPr) socket (Sengeh & Herr, 2013). Lilja et al. (1995) found a linear, almost constant systematic error of +2.5 percent, which could easily be corrected for, and a small random error, represented by a CV of less than 0.5 percent. Sander et al. (2011) used different computed metrics for error evaluation (volume, shaping and size) and made the decision about clinical judgment by comparing with these computed metrics.

The prosthesis socket having close interaction with the residual limb required a highly customized product to accomplish comfort (Frillici et al. 2008). Colombo et al. (2010) presented 3D model, develop a special custom-fit prosthesis socket for lower limb amputees. Based on the same approach, Colombo et al. (2013) introduced the virtual digital limb of patients using digital models and virtual tools. By using human-design interface, prosthetist could modify the socket quickly and manufacture. After various attempts to get a customized socket, scanning is found to be one of the best methods. However, scanning of the live residual limb is a challenging task. It may lead to inconvenience to the patient and has a psychological impact and physical fatigue because of holding the patient in the same posture for a long time and patients often tend to be skeptical of scanner rays. The current process of prosthetic socket design in orthopedic technology with the integration of modern techniques helps to achieve patient-specific socket.

2.3 On the basis of finite element analysis socket optimization

Finite element (FE) analysis is a powerful technique for assessing the effectiveness of the developed prosthesis socket model in the last three decades. The main advantage of using FE is to predict stress, strain, and displacement of free-form shape for understanding load transfer in the prosthesis. Also, estimate the interface stresses between prosthetic socket and stump. Furthermore, FE analysis eliminates the need of building physical prosthesis by systematically investigating different parameters. These FE models can be classified into three main parts. The first category comprises of linear static analysis considering assumptions of linear material properties, infinitesimal deformation and linear boundary condition without taking any interface friction and slip. These types of models involve comparatively small CPU time. The second category includes nonlinear analysis, considering the nonlinear material properties, significant deformation, and nonlinear boundary conditions, comprising friction/slip contact boundary. This kind of nonlinear FE analysis usually needs specific iterative procedures. These nonlinear methodologies mostly provide highly accurate solutions, however, requires more CPU time. The third category includes dynamic models. Investigation of this type involves taking

into account dynamic loads, material inertial effects and time-dependent material properties.

Krouskop et al. (1987) proposed a finite element method as a possible tool to create a prosthetic socket design shape for above-knee (AK) amputees. In a parallel effort, Steege et al. (1987a, b) established the first FE model for below-knee (BK) residual limb and predict interface pressure between stump and socket. Subsequently, simplified through readily accessible commercial FE computer software (Lee et al. 1992), numerous FE models have been established. If the model is not a valid representation of the real situation, the result will be misleading. Hence, the development of the FE model for stump/socket interface needs to be carefully monitored, critically assessed and validated. Silver-Thorn et al. (1996) presented a review of stress investigation engaged in experimental measurement methods and computational model of the prosthetic socket. In another review, Zachariah, and Sanders (2000) discussed in details FE model, then compared to experimental data and sensitivity analysis of the model. Zhang et al. (1998) review of FE model developing between 1987-1996 of lower limb prostheses on the basis of below-knee and above-knee. Also, described generations of modeling: simple linear, nonlinear, and dynamic. The meshed geometries of the residual limb, prosthetic socket and bones are shown in Figure 2.6.
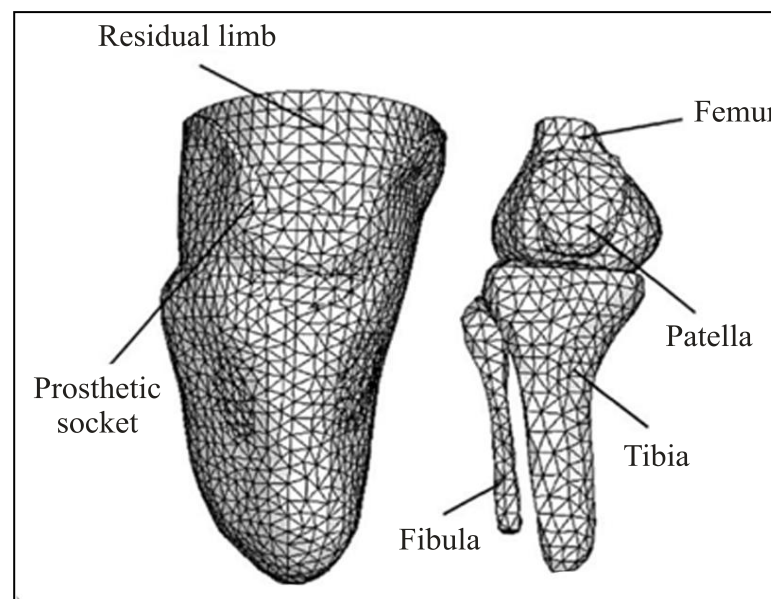
Figure-2.6: **FE mesh model of residual limb, Prosthetic socket and bones (Lee et al. 2004)**

Many studies have investigated the integration of advanced technology to evaluate the prosthesis socket design (Colombo et al. 2013). Pandey et al. (2014) Analysis of traditional and reverse engineering (RE) based fabrication of sockets used in artificial limbs is presented using the real data from amputees. The FEA tool is used for parametric study and evaluation of prosthetic socket mechanisms (Geil et al. 2002 & Saunders et al. 2003). Wu et al. (2003) Proposed finite element analysis (FEA) technique for the evaluation protocol using pain-pressure tolerance (PPT) of soft-tissue to determine socket design parameters. It is useful for better understanding of the actual socket fabrication from design. Colombo et al. (2006) used RE techniques to obtain a digital model, which includes both the external shape and the inner parts to integrate rapid prototyping technology. Colombo et al. (2010) Used an integration of computer aided design (CAD), and FEA approaches to analyze the residual limb-socket interaction over the stump. They created digital models of the stump-socket and performed simulations for the realization of the physical prototype.

In the field of biomechanics, FEM uses to analyze the behavior structures of the prosthesis socket to investigate the contact pressure between computer-interfaced prosthesis (Shankar et al. 2013, 2014). Compliant feature designs were analyzed, using FEM to relieve pressure between the residual limb and socket under quasi-static loading condition (Faustini et al. 2006). Similarly, Portnoy et al. (2007) developed a patient-specific FE parametric biomechanical model of the residual limb that predicts stresses transmitted through the muscle flap by the shin bones during static and dynamic loading. The calculations of stress-strain condition at the interface of the socket and stump of five transfemoral amputees were proposed by Lacroix et al. (2011). They used patient-specific geometrical data acquired from CT and laser scans in socket donning methodology for FEM based modeling

To identify possible structure design, topology optimization technique is used for reducing mass and improving the performance of socket. Prasanna et al. (2011) described the structural topology accounting for different material, mechanical properties and weight of the socket. Faustini et al. (2005 & 2006) identifying optimal compliant features using topology optimization, then integrating

these features within the geometry of the socket. Nicholas et al. (2009) present a framework using topology optimization methods to develop new prosthetic feet manufactured using selective laser sintering as shown in Figure 2.7.

Figure-2.7: **Optimized prosthetic feet using SLS technology (Nicholas 2009)**

2.4 On the basis of pressure measurement and stress distribution

Several studies have utilized experimental equipment such as sensors to measure stump-socket interface pressures and then validate to the FE forecast results. Winaski and Pearson (1987) developed a diaphragm deflection strain gauge combining a matrix equation and least-squares algorithm to measure the normal pressures and the values of the flexion-extension moment of the prosthesis. Williams et al. (1992) mounted a sensor, including three disks and a resistor, located in a socket hole to measure interface stresses on three axes as demonstrated in Figure 2.8 (a, b)**.** These sensors, though, increased prosthetic weight and the amputee obligatory increased effort to control the prosthesis while walking. Engsberg et al. (1992) developed a pressure sensing system that consisted of a thin pressure mat, which is small enough to comfortably fit between the socket and the residual limb. This system could measure pressure for both small and large regions. Sander et al. (1992) designing a custom three orthogonal axial transducer using strain gauges (6.35 mm diameter) mounted to the socket, so the face of the transducer is flush with the liner. Then, Sanders and Daly (1993) using similar strain gauge, compare finite element (ANSYS) results with experimental measurement to measure normal and shear stresses as shown in Figure 2.9. The sensors were placed on the inner wall of a socket. As the sensors increased prosthetic weight, the amputee necessarily required increased force to control the prosthesis while walking. As these sensors increased

prosthetic weight, the amputee necessarily used increased force to control the prosthesis while walking. Convery and Buis (1998) used force sensing resistors (FSR) (Figure 2.10), measurement of dynamic interface pressures between stump-socket, during the stance phase of gait with a trans-tibial amputee. The sensors were located on the inner wall of a PTB socket, and the data on ground reaction forces was obtained from a force platform. The interface pressure distributions measured at the stance phase in four surfaces of a stump, i.e. anterior surface, a lateral surface, posterior surface and medial surface. Then, Convery et al. (1999) used the same system, the resulting outcomes the pressure gradients within the hydrocast socket were less than those within the hand cast PTB socket.
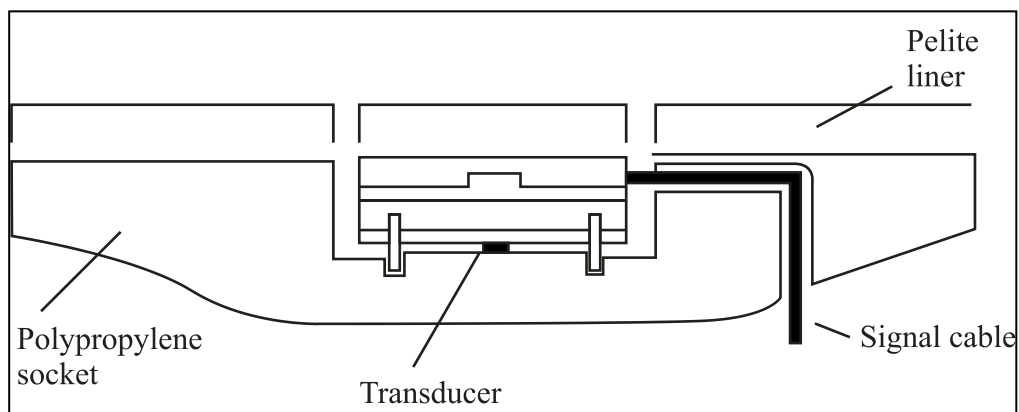
(a) Experimental components

(a)

(b)   (c)
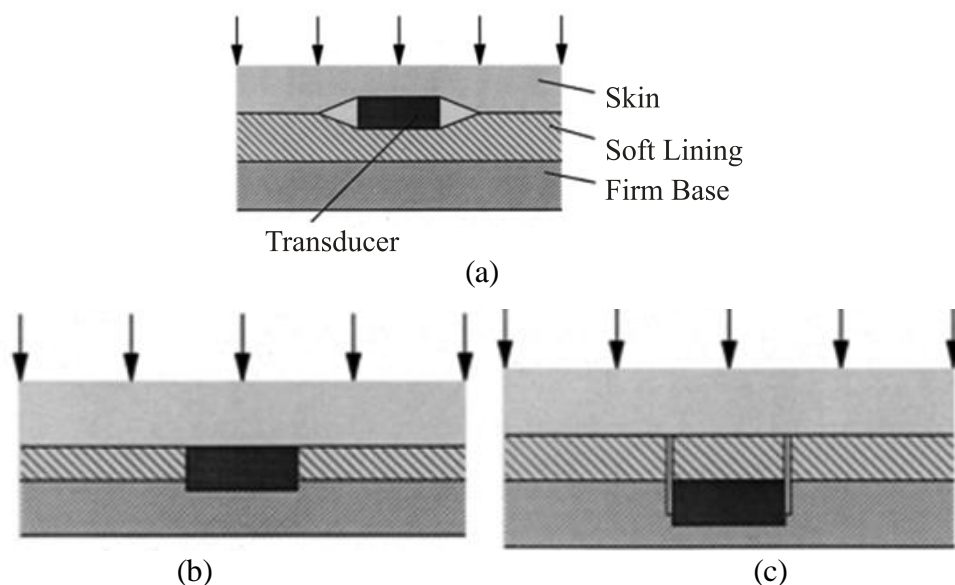
Figure-2.8: **Experimental equipment (Williams, 1992)**
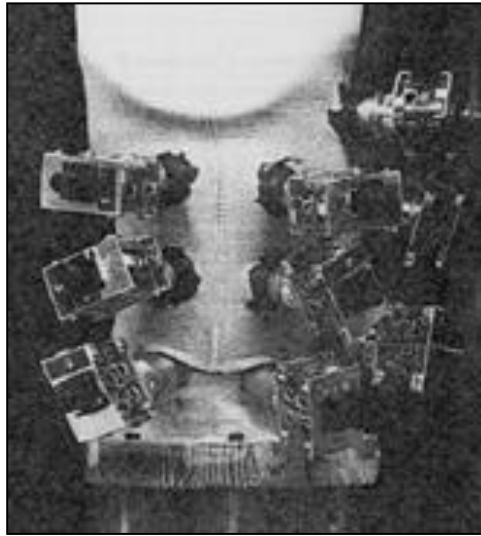
Figure-2.9: Experimental Sensor (Sanders, 1993)
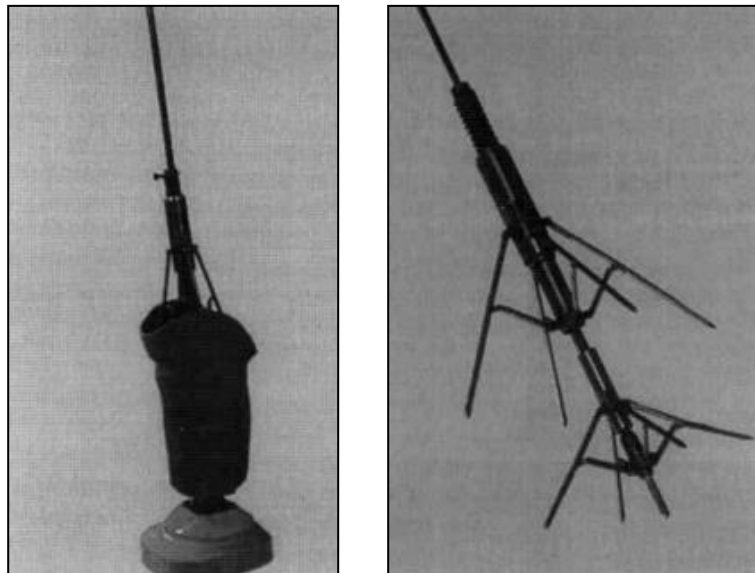
Figure-2.10: Socket axis locator (Convery, 1998)

Zhang et al. (1996) investigated the pressure distribution with the Tekscan sensor in specific regions at lower limb prosthesis socket. It was found that interface pressure increase with the decrease of friction while walking four steps, and maximum pressure occurs over the patellar tendon area (212 kPa). Then, Zhang et al. (1998, 2000) designed a conventional strain-gauge diaphragm method for the effective measurement of normal force on the below-knee stump with a prosthesis (Figure 2.11). The data was collected at 200 Hz for 20 seconds. A self-made tool using force transducers measured normal and shear stresses. Two receivers captured two phases of heel strike and toe off. However, these sensors increased prosthetic

weight and required enhanced force to control the prosthesis while walking. The peak pressure over the patella tendon (215 kPa) and longitudinal shear stress were measured over the lateral tibia (44 kPa). Sanders et al. (1997) investigated the interface pressure and shear stresses at thirteen sites on two subjects with unilateral transtibial amputation using PTB sockets. The results were suggested that skin across the distal tibial crest was in tension at the time of the first and second peaks in the shank axial force. Kim and Newman (2003) evaluated the effectiveness of the patellar tendon bar using an experimental device, P-Scan pressure transducers, to measure interface pressures between the below-knee residual limb and prosthetic socket.
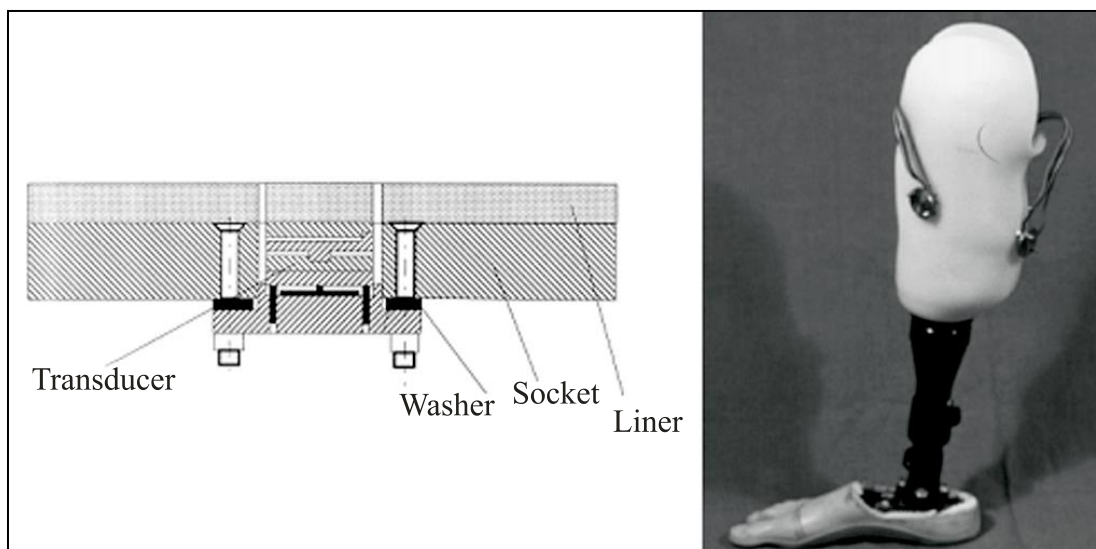
(a) Experimental sensor layout   (b) A sensor mounted on the socket
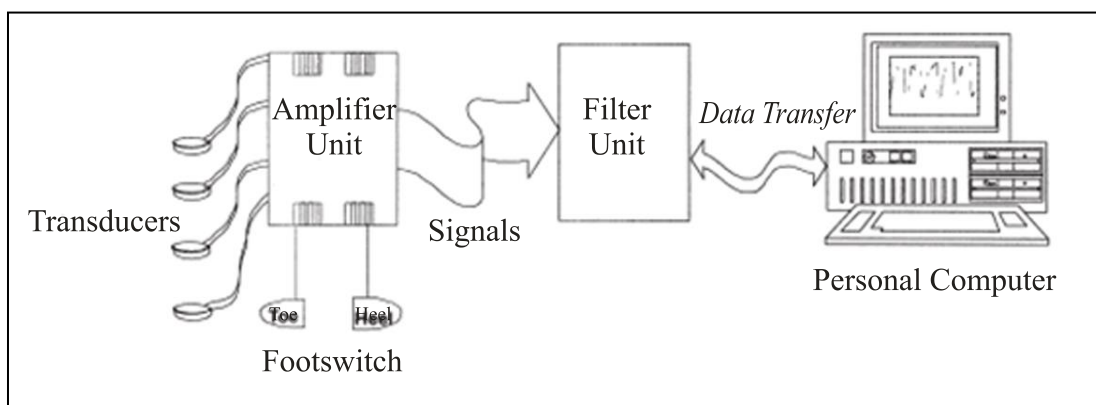
(c) Installation of equipment

Figure-2.11: Experimental devices (Zhang, 1998)

Zachariah and Sanders (2001) determined the interface stress ratio of standing to walk at the same position of the residual limb. It was found that

correlation coefficient of 0.88 during standing with full weight bearing on the prosthetic limb and peak stress. The fit of the socket used to interface an external prosthesis to an amputee's residual limb has been manifest to be of vital importance to prosthesis users (Legro et al. 1999, Dillingham et al. 2001) Presented in a study of 78 trauma-related amputees that, although 95% tended to wear their prostheses extensively (>80hr/week), only 43% reported satisfaction with prosthetic comfort. Similarly, (Nielsen et al. 1991) found that out of 109 amputees, 57% reported moderate to severe pain most of the time while wearing their prosthesis. Then, polliack et al. (2002) developed 4x4 matrix array of 16 capacitance pressure mounted on a silicon substrate had an acceptable level of accuracy error, hysteresis error and drift error.
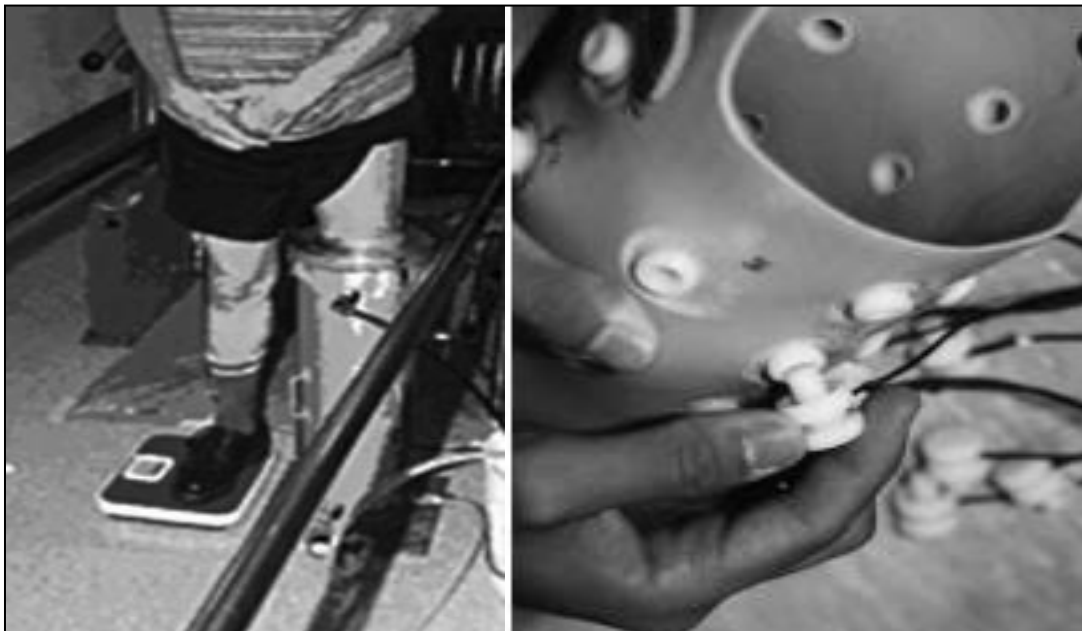
Figure-2.12: **Pressure transducer mounted on the measurement site of PCast system (Goh, 2003)**

Goh et al. (2003) used piston-type transducers to investigate the interface pressure distribution of five amputees wearing a TSB socket developed by a pressure profile of the PCast prosthetic socket technique (See Figure 2.12). It was found that the hydrostatic pressure profile was not observed during standing or gait, nor was there a standard pressure profile for the PCast socket. Zhang et al. (2000) measured limb-socket surface forces during different activities such as standing up from a chair or walking. Also, Dou et al. (2006) used portable, real-time, Pliance

sensors that examined the stump/socket interface stress have been restricted to controversial stance and natural gait. Further, compared with a natural gait, the mean peak pressure, and sustained sub-maximal load increased notably over the patellar tendon. Then, analyzed interface pressure during walking on stairs and non-flat road. Then, Ali et al. (2013) used F-socket transducer (See Figure 2.13) measuring interface pressure in the transtibial socket throughout ascent and descent on stairs with effect on patient satisfaction.
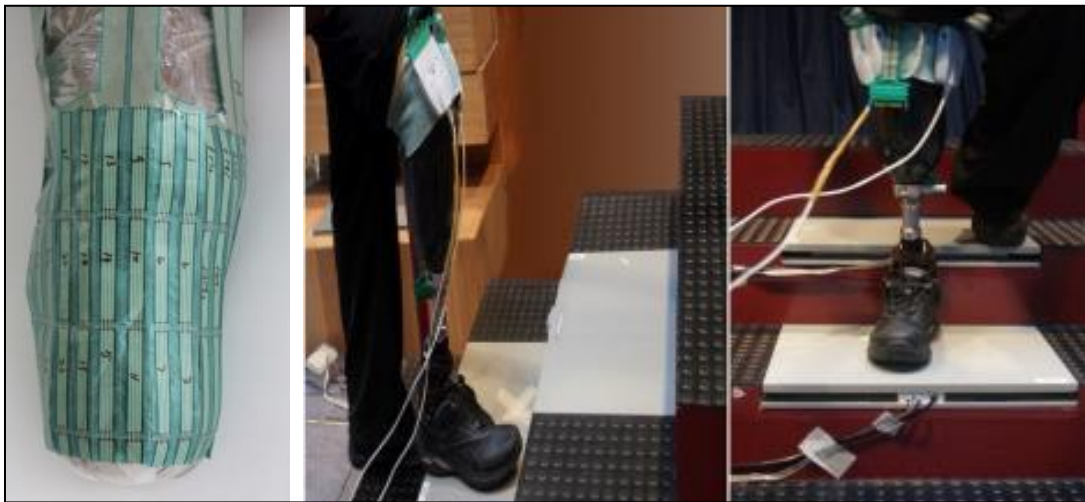
Figure 2.13: (a) Sensor placement on limb (b) Strain ascent; (c) Stair descent (Ali, 2013)

Sanders et al. (2005) compared diurnal and long-term (5 weeks to 6 months) interface stress changes as well as the variance in the change in the cross-sectional area down the length of the residual limb. Simultaneously, measured interface pressures and shear stresses at 13 custom-designed transducers, using strain gauges mounted on a socket on eight below-knee amputees, patients using patella tendon bearing prostheses. Kang et al. (2006) investigated the pressure distribution patterns in anterior and posterior areas (proximal, mid, and distal respectively) of the stump/socket interface when socket used the F-socket system to measure static and dynamic pressure in stump/socket interface as shown in Figure 2.14. These studies assumed that high surface pressures endanger the integrity of the residual limb and compare persons with transtibial amputation using Patella tendon bearing (Shrivastava et al. 2015).
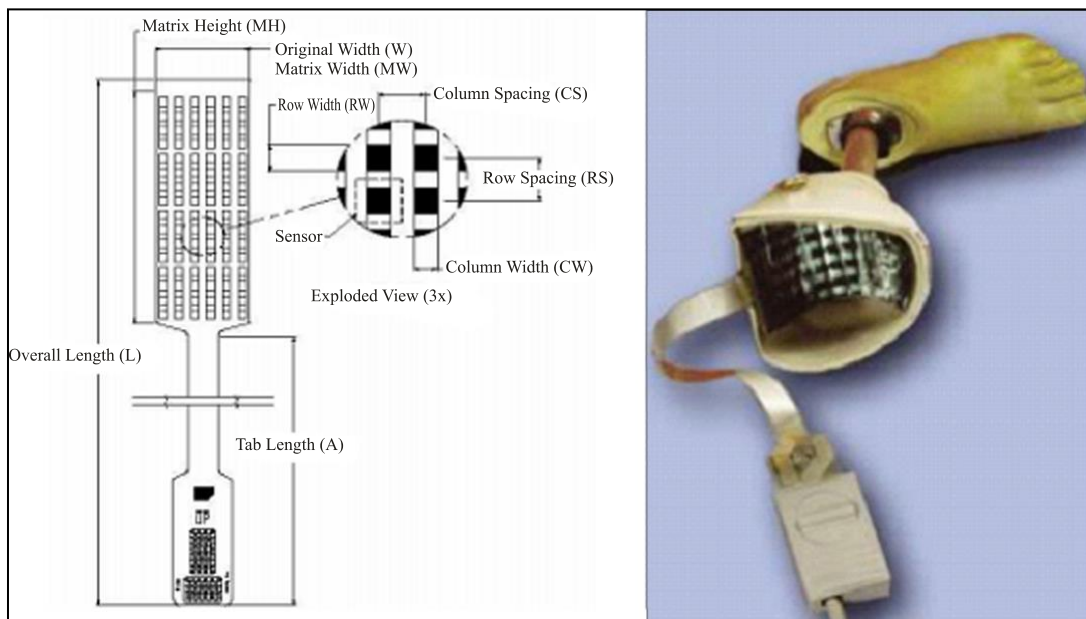
Figure-2.14 (a) F-socket sensor and (b) Sensors placed inside the socket

(Kang, 2006)

Skin problems are common in transtibial amputees and are exacerbated as 70% of amputees suffer from vascular diseases and associated comorbidities. The anterior distal tibia is a common area of skin breakdown due to increased pressure at loading response. The internal stresses are monitored between the residuum of transtibial amputation prosthetic during their daily activities (Portnoy et al. 2012). Nowadays, Electromyography (EMG) signals are widely used for the clinical/biomedical application. EMG signals acquired from residual limb muscles require advance methods. Transmission techniques for acquisition of the EMG (Electromyogram) signal using LabVIEW is a useful tool (Dev et al. 2015) that quantifies the coordination between hip-thigh muscles (Bansal et al. 2011). Piezoelectric sensors identify different phases during a gait cycle for, sit to stand, and stair ascent (Sayed et al. 2015).

In prostheses, the interaction between stump-socket occurs due to improper design which increases pressure/friction and subsequent surface damage to the soft tissue. This damage is manifested in local that increases in the temperature of the affected area. The socket is considered as an element of primary importance in the makeup of prosthesis. Each socket is a tailor- made the device, designed to fit the

unique geometry of the patient's residual limb. However, if the prosthetic socket fits improperly, it results in external conditions stem from the frictional interaction between the soft tissue of the residual limb and the prosthetic socket. These circumstances lead the amputee to suffer pain, blisters, edema, ulcers, and osteomyelitis (Lyon et al. 2000, Mak et al. 2001).

Abu Osman (2010) has positioned SG-based transducers at 16 sites (Figure 2.15), which is relatively more in comparison with previously reported studies, at all the interesting sites, including those located on the high-curvature regions. They investigated to what extent the changing indentation depth at the PT area would affect the pattern of interface pressure distribution and then assessed the correlation that may exist between the pressure magnitudes at PT bar and other sites within the socket (Abu Osman et al. 2010). The PT bar of ten patients was indented inward at 2-mm each, but not more than 4 mm from the original position. The results revealed that altering the indentation depth at PT bar had no effect on the pressure distribution at all sites within the socket, and the subjects who participated in this study experienced no pain or discomfort from removing the PT bar, concluding that the PT bar could be eliminated during the socket fabrication.

Anterior   Medial   Posterior   Lateral
Figure-2.15: **Location of strain gauge on socket, Abu Osman (2010)**

Sewell et al. (2012) clinically tested the artificial intelligence approach to the determination of the forces at the stump-socket interface under different static and dynamic loading conditions (See Figure 2.16). Ebrahim et al. (2013) FBG element(s) were recoated and surrounded by a thin layer of epoxy material to form a sensing pad, which was in turn fixed in a silicone polymer material to form a

pressure sensor. Rajtukova et al. (2014) study the anterior side of the stump, three loadable and two non-loadable areas was monitored using the TACTILUS tactile pressure sensor (Sensor Products Inc., Madison, New Jersey, USA).

Figure 2.16: **(a) Strain gauge based transducer (b) Pressure being applied on socket (Sewell, 2012)**

2.5 On the basis of additive manufacturing

Presently, the prosthetic socket is manufactured by thermoforming plastic over positive plaster mold. A digital process starts with 3D scanning, collecting data from the surface of the socket and generate a 3D model file to CAD software for 3D printing. Modifications are made electronically rather than manually, which replace the conventional fabrication of the prosthetic socket. Squirt-shape is a rapid prototyping of a prosthetic socket was accompanied by (Rovick in 1992) at Northwestern University. The SLA and its CAD and computer-aided manufacturing (CAM) software had been just available for implementation in AM of custom Orthotists and Prosthetists practitioners. The wooden CNC carved socket, plaster residual limb model, and SLA socket from this well-recognized innovative application of AM in O&P is shown in Figure 2.17 (a). In this research, the socket is fabricated by the layer-to-layer concept (See Figure 2.17 (b)) to fabricate a socket

(Figure 2.17 (c)) was demonstrated. The mechanical digitizer was applied to obtain the 3D geometry of the plaster residual limb model.
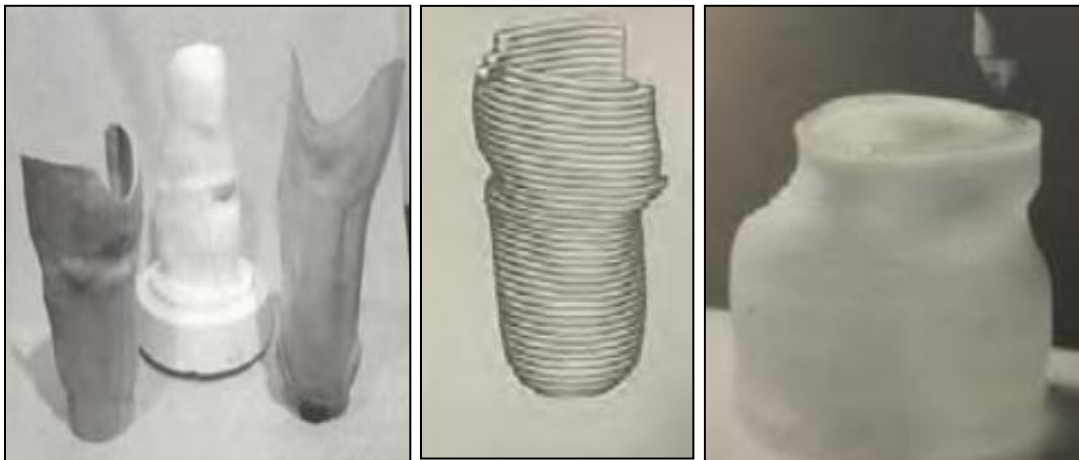
Figure-2.17: **AM of the socket**

(a) wooden and SLA sockets and the plaster mold, (b) layer-by-layer deposition concept and (c) socket by AM (Rovick et al. 1992).

The emergence of rapid prototyping is novel technology, which revolutionizes research within prosthetic/orthotics and clinical practice. Researchers have designed, developed and fabricated a variety of prosthetic sockets using various types of RP machines that include stereo lithography Apparatus (SLA), selective laser sintering (SLS) fused deposition modeling (FDM), and droplet/binding processes (i.e. 3D printing) (Gibson 2005 & Rogers et al. 2007).

Montgomery et al. (2010) fabricated prosthetic socket by selective laser sintering (SLS) for which the volume will actively change as the residual limb changes shape. RM of the medical device using Freeform fabrication techniques such as fused deposition modeling has been explored, although this approach requires the development and validation of new materials. Rogers et al. (2000) fabricating double-wall socket using SLS and compared to a conventional socket. Faustini et al. (2006) developed a framework for a patient-specific prosthetic socket for trans-tibial amputees using the SLS method with duraform material as shown in Figure 2.18. It was found that allowing for systematic and controlled design modification in the socket shape or volume. Faustini et al. (2008) further exploring

the feasibility of using an SLS-based manufacturing to identifying the most appropriate material for socket manufacturing.

Figure-2.18: **Prosthetic Socket manufactured by SLS technology (Faustini 2008)**

The rapid socket manufacturing machine (RSMM) and fused deposition modeling (FDM) were compared with traditional socket manufacturing processes and studied with respect to the accuracy, labour-intensive, fabrication data, and biological evaluation of the new socket throughout the gait (Gho et al. 2002, Ng et al. 2002 and Fuh et al. 2005). Hopkinson et al. (2003) reported on cost analysis; that was achieved to compare a traditional manufacturing route with layer manufacturing processes (stereolithography, fused deposition modeling and laser sintering) regarding the unit cost for parts made in several quantities. Then, results showed that, for some geometry, it was more economical to use layer manufacturing methods than it used traditional approaches for production in the thousands. However, comfortable prosthetic sockets manufactured by 3D printing have been used in preliminary fittings with patients. One of the principle benefits of FDM technology is the use of various materials which includes ceramic materials, polymers (synthetic and natural), metals and biodegradable materials with a promising avenue for cost reduction in the development of prosthetic socket.

Table-2.2: Summary of FE modeling methodologies

Investigator (year)	Method (Static / Dynamic)	Socket type/ amputation level	Shape acquisition/ Geometry source	Elements/ Nodes	Software	Meshes	Measure	Peak Interface pressure
Peter (1991)	Static	PTB/BK	Sagittal plane Profile	655 elements & 63 nodes	-	Quadrilateral and triangular	Normal and shear stresses	961& 463 KPa
Zhang (1995)	Static	PTB/BK	Digitizing biplanar X ray	1854 elements & 2421 nodes.	ABAQUS	Triangular prism	Pressure and shear stress	226 & 53 kPa at patellar tendon
Zhang (1996)	Static	PTB/AK	Sagittal plane Profile	2D 4-node solid elements	ABAQUS	2D 4-node solid elements	Pressure distributions	65 kPa Anterior & 63 Posterior
Silver-Thorn (1996)	Static	PTB/BK	Anthropometric	1688 elements & 2221 nodes	MARC	Hexahedron	Stress distribution	Patellar tendon
Zachariah (2000)	Static	PTB	CT and MRI	1826 elements & 2386 nodes	MARC	Hexahedral	-	-
Zhang (2000)	Static	PTB/BK	Biplanar X-rays	2304 elements & 2421 nodes	ABAQUS	3D 8-node brick element	Pressures and shear stress	226 kPa at the patellar tendon & the shear stress 50 kPa at the anterolateral tibia
Wu (2003)		KBM & TSB/BK	CT	14776 elements & 14904 nodes	ANSYS	3D 8-node Hexahedron brick element	Pressure	230 kPa at patellar tendon

Investigator (year)	Method (Static / Dynamic)	Socket type/ amputation level	Shape acquisition/ Geometry source	Elements/ Nodes	Software	Meshes	Measure	Peak Interface pressure
Lin (2005)	Static	KBM/BK	CT images	11788 elements	ANSYS	Tetrahedral	Interface stresses and sliding distance	590, 230, 660 & 190 Kpa on the anterior, lateral, posterior and medial surfaces of the stump,
Lee (2004)	Dynamic	PTB/AK	MRI	22301 elements & 6030 nodes	ABAQUS	Tetrahedral structural	Normal and shear stresses	250, 109 & 205 kPa at the patellar tendon, popliteal depression & medial tibia
Jai (2004)	Dynamic	PTB/BK	MRI	22301 elements & 6030 nodes	ABAQUS	Tetrahedral structural	Pressure and shear stress	292 kPa at the middle patella tendon (PT)
Goh (2005)	Static	BK	CAPOD prosthetic workstation	9477 elements & 14140 nodes	Developed In-house CAD soft.	Tetrahedral structural	Pressure distribution	80.1 kPa
Jeffrey (2006)	Dynamic	BK	CT	111 672 elements and 20 481 nodes.	-	Tetrahedral structural	Temperature	34 ^{0}C at Popliteal depression

Investigator (year)	Method (Static / Dynamic)	Socket type/ amputation level	Shape acquisition/ Geometry source	Elements/ Nodes	Software	Meshes	Measure	Peak Interface pressure
Faustini (2006)	Dynamic	PTB	ShapeMaker 3000 laser scanning	7582 elements & 22 570 nodes.	CAD software	Tetrahedral structural	Stress	45.2 Mpa
Lee (2007)	Dynamic	PTB/BK	ShapeMaker 4.3 laser scanning	22301 element	ABAQUS 6.4	tetrahedral structural	Pressure distribution	260 at Popliteal muscle, 230 at mid Patellar tendon, 200 at Anteromedial tibia & 160 at anterolateral tibia
Portnoy (2007)	Static/ Dynamic	BK	Slice	290 triangles (3-node) elements	MSC NASTRAN 2003	Phantom mesh	Stress	Patellar tendon
Prasanna (2011)	Static	PTB/BK	White light scanner	15017 elements & 7678 node	ANSYS/ COMET, 250	Shell 63 and solid 92	Pressure and shear stress	173 at Patellar tendon & 79 at Popliteal area
Linlin Zhang (2013)	Static	TSB/AK	CT	19592 elements	Mimics v10.01/ Altair	Tetrahedral elements	Normal stress	80.57 kPa
Colombo (2014)	Dynamic	AK	MRI	64042 element &13096 node	Abaqus package V 6.9	3-noded triangular elements	Pressure	200 Kpa

Table-2.3 Pressure transducers used in transtibial socket

Investigator (year)	Method (Static / Dynamic)	No. of Subject/ socket type	Reason for Amputation/ Liner	Positioning of the sensor	Sensor type/ Instrument	Measurement sites	Parameters to measure	Highest Pressure Area
Sanders (1992)	Dynamic	03/PTB	Trauma/ Pelite liner	Skin/Soft tissue	Diaphragm strain gauge	Anterior Sites & Posterior Sites	Normal & shear stress	205 kPa & 54 kPa
Sanders (1993)	Dynamic	03/PTB	Trauma/ Pelite liner	Skin/Soft tissue	Piston-type Strain gauge	Anterior Sites & Posterior Sites	Normal & shear stress	Interface stress waveforms
Zhang (1995)	Static	01/PTB	Unknown/ Pelite liner (1.5 mm)	Socket/skin	Tekscan (Version 3.6)	Anterior, posterior, medial & lateral	Frictional action	Patellar tendon area (212 kPa)
Sanders (1997)	Dynamic	02/PTB	Traumatic / Pelite liner	Mounted on socket wall	Piston-type Strain gauge	13 sites	Pressure and shear stress	Anterior sites
Convery (1998)	Dynamic	01/ PTB & Hydrocast	Unknown/ Silicone sleeve	Stump/socket	Piezoresistive (F-socket)	Overall impression of the interface	Pressure distribution	Patellar tendon area (244 kPa)

Investigator (year)	Method (Static / Dynamic)	No. of Subject/ socket type	Reason for Amputation/ Liner	Positioning of the sensor	Sensor type/ Instrument	Measurement sites	Parameters to measure	Highest Pressure Area
Zhang (1998)	Static and Dynamic	05/PTB and TSB	Unknown/ Pelite liner	Skin/Soft tissue	Force transducer	Anterior & posterior	Pressures and bi-axial shear stresses	During walking 320 kPa at Popliteal area & 61 kPa at medial tibia area
Convery (1999)	Dynamic	01/PTB	Traumatic Injury/ No liner	Sump/socket interface	Tekscan, Force sensing resistors (FSR)	Overall impression of the interface	Pressure distribution	Patellar tendon area (244 kPa)
Sanders (2000)	Dynamic	01/PTB	Traumatic Injury/ Ply sock	Skin/Soft tissue	Custom designed sensors	13 sites	Changes in interfaces stresses & stump shape over time	-
Goh (2003)	Dynamic	05/PTB & PCast	Peripheral Vascular disease and Traumatic injuries/ Silicon liner	Mounted on socket wall	Piston-type Strain gauge	16 sites	Pressure distribution	81.32 at 25% of gait cycle

Investigator (year)	Method (Static / Dynamic)	No. of Subject/ socket type	Reason for Amputation/ Liner	Positioning of the sensor	Sensor type/ Instrument	Measurement sites	Parameters to measure	Highest Pressure Area
Sanders (2005)	Dynamic	08/PTB and TSB	Traumatic Injury/ silicone liner (6 mm)	Soft tissue /socket	Force transducer	13 sites	Pressure & shear stress	99.4 kPa & 11.7
Dou (2006)	Dynamic	01/PTB	Pressure ulcers/ silicone liner (6 mm)	Stump/socket	Capacitive (Pliance pressure system)	Antero-posterior & Medio-lateral planes	Pressure distribution	215.8 kPa over the Patella tendon
Kang (2006)	static and dynamic	10/TSB	Vascular diseases, trauma & diabetes mellitus/ Silicone Liner	Stump/socket	F-socket	Anterior and posterior area	Pressure distribution	Anterior Proximal (230.6)
Portnoy (2008)	Static	01/PTB	Unknown/ Unknown	Socket/ limb	Piezoresistive sensors	Anterior and posterior area	Pressure and shear strain	100kPa at tibia crest
Wolf (2009)	Dynamic	12/TSB	Trauma and Tumor/ Silicone liner	Socket/ limb	Pliance S 2052, Novel	Stair-up/down, ramp-up/down & walking	Pressure	244.73 kpa at the calf muscle

Investigator (year)	Method (Static / Dynamic)	No. of Subject/ socket type	Reason for Amputation/ Liner	Positioning of the sensor	Sensor type/ Instrument	Measurement sites	Parameters to measure	Highest Pressure Area
Dumbleton (2009)	Dynamic	48/PTB & Hydrocast	Unknown/ silicone liner and Pelite liner	Attached to the inner socket wall	Piezoresistive (F-socket)	Overall impression of the interface	Pressure distribution	118 kPa at lateral
Papaioannou (2010)	Dynamic	10/PTB	Unknown/ Silicon liner	Stump/skin	Biplane Dynamic Roentgen Stereogrammetric Analysis	Overall impression of the interface	Dynamic slippage of skin tissue/ shear	151 mm
Abu Osman (2010)	Dynamic	10/PTB	Unknown/ No liner	Mounted on socket wall	Strain gauge and Electrohydraulic technologies	16 sites	Pressure distribution	203 to 230 kPa at Patella tendon
Boutwell (2012)	Dynamic	Unknown/ PTB and TSB	Unknown/ Silicon liner	Residual limb/ liner interface	Capacitive pressure sensor	Patellar tendon, distal anterior tibia, distal end of the tibia, fibular head & medial gastrocnemius	Shear and pressure distributions	496 kPa at Patella tendon
Philip (2012)	Static and Dynamic	Unknown	Unknown/ Gel liner	Residual limb/socket interface	Strain gauge based transducer	Overall impression of the interface	Pressure measurement	637 kPa at Patella tendon

Investigator (year)	Method (Static / Dynamic)	No. of Subject/ socket type	Reason for Amputation/ Liner	Positioning of the sensor	Sensor type/ Instrument	Measurement sites	Parameters to measure	Highest Pressure Area
Ali (2012)	Dynamic	9/TSB	Diabetic, trauma, patients/ Seal-In X5 liner	Stump/liner	Piezoresistive (F-socket)	Overall impression of the interface	Pressure measurement	86.5 kPa
Ali (2013)	Dynamic	10/TSB	Trauma, Diabetes and peripheral vascular diseases/ Seal-In liner X5	Stump/liner	Piezoresistive (F-socket)	Overall impression of the interface	Pressure measurement	Posterior proximal area
Eshraghi (2013)	Dynamic	12/ TSB	Diabetic, trauma, patients/ Seal-In X5 liner	Stump/liner	Piezoresistive (F-socket)	Overall impression of the interface	Pressure measurement	89.89 kPa
Ali (2014)	Dynamic	30/TSB & KBM	Seal-In X5 and Pelite liners	Stump/liner	Piezoresistive (F-socket)	Overall impression of the interface	-	-
Faklh (2013)	Dynamic	Unknown/ PTB	Polyethylene liner	Residual limb/socket	Fiber Bragg Grating Sensors	Overall impression of the interface	Pressure measurement	35 kPa at Patella tendon

Investigator (year)	Method (Static / Dynamic)	No. of Subject/ socket type	Reason for Amputation/ Liner	Positioning of the sensor	Sensor type/ Instrument	Measurement sites	Parameters to measure	Highest Pressure Area
Sayed (2014)	Static and Dynamic	1	No liner	Stump/Socket	Piezoelectric	Overall impression of the interface	Pressure measurement	27 kPa anterior proximal
Safari (2015)	Static	6/PTB	Discomfort, pain or poor socket fit/ Pelite liner	Stump/socket	Novel Pliance	Anterior distal, Fibular Head, Popliteal & Patella tendon.	Pressure measurement	404.76 kPa Patella tendon

Against this literature review, the present work has been undertaken to investigate the pressure measurement between the socket and residual limb. The focus has been on the fabrication of customized prosthesis socket to integrate advanced technology.

2.6   The Knowledge Gap in Earlier Investigations

This exhaustive literature review presented above reveals the following knowledge gap that helped to set the objectives of this research work:

1. Though much work has been reported on traditional prosthetic socket manufacturing. However, integration of using Reverse Engineering (RE), computer-aided design (CAD) and Additive Manufacturing (AM) is infrequent.

2. Study of computerized and FEM modeling assessments still do not match prosthetic evaluations with topology optimization and is scarcely reported in the literature.

3. Studies carried out worldwide on to measuring interface pressure between stump-socket. However, no study has been found particularly on clinically significant cases and its impact on the success of the prosthesis.

4. Taguchi method, in spite of being a simple, efficient and systematic approach to optimizing designs for performance, quality and cost, is used only in a limited number of applications worldwide. Its implementation in parametric appraisal of stump-socket interface pressure has hardly been reported.

5. The understanding of clinically meaningful changes in socket fit and its effect on biomechanical outcomes. Further, safe and comfortable pressure thresholds under various conditions should be determined through a systematic approach.

2.7   The objectives of this work are outlined as follows:

The scope of this present work is to design patient-specific prosthesis socket integrating reverse engineering, computer-aided design, additive manufacturing and pressure sensors. Therefore, the objectives of this research work are:

1. To overcome the limitations of traditional manufacturing process of socket by Semi-automating the existing process using Reverse Engineering (RE), computer-aided design (CAD) and Additive Manufacturing (AM).

2. To analyze the structural response of patella tendon bearing (PTB) socket designs with topology optimization using Finite Element Analysis (FEA) study.

3. To measure and predict pressures site at the amputee's stump/socket interface at low-cost to reduce potentially harmful contact pressure which leads to increase patient's comfort.

4. An experimental investigation to obtain critical pressure points for clinically significant cases such as a short-stump, long-stump, diabetic stump, peripheral vascular disease, traumatic injuries.

5. To establish a mathematical model using artificial neural networks (ANN) for the relationship between interface pressure and amputee's physiological parameters for PTB socket.

6. Development of Topology optimized socket using FDM-based Additive Manufacturing and to investigate the dimensional accuracy of the 3D Printed Socket.

Chapter Summary

The chapter reviews the literature available on plaster casting, geometry acquisition, FE analysis & method, experimental equipment principles and additive manufacturing. The following points summarize this chapter.

- Techniques of volume measurement for the residual limb and its effect on the fabrication of prosthesis socket were reviewed in section 2.1.

- Reviews of the literature regarding geometry acquire internal and external geometry of patients-specific residual limb is described in section 2.2.

- The three features of FE analysis were described in section 2.3, to assist the determination of suitable socket shape. Also, present a summary of FE modeling methodologies in Table 1.2.

- Several measurement techniques have been reported in section 2.4; which includes a strain gauge, capacitive, piezoresistive and optical sensors for pressure measurement and prediction at stump-socket interface (Table 1.3).

- In section 2.5, literature on the socket manufacturing using various RP machines were presented.

- The knowledge gap in past research.

- The objective of the present work.

CHAPTER 3
REVERSE ENGINEERING (RE) AND COMPUTER AIDED DESIGN (CAD) BASED CUSTOMIZED PROSTHETIC SOCKET DESIGN

Introduction

This chapter introduces an important aspect of an innovative approach to develop customized design process of below-knee prosthesis socket. As per the condition of each amputee stump, socket varies from one to another bone which needs to be customized. Computer-aided tools help in shortening and eradicating numerous repetitive tasks that reduce the gap between the digital model and the actual product. Use of these tools assists in realizing free-form objects such as custom fit products as described by a stringent interaction with the residual limb. In this chapter, the development of a semi-automated methodology which integrates traditional process and reverses engineering methodology for developing a CAD model of prosthesis socket is discussed. Also, chapter proposes an integrated methodology for measuring the accuracy of 3D models generated by RE employing commercial CAD tools. Determination of key factors and how they influence the 3D model accuracy from RE is evaluated. In order to the digital model accuracy, the correct use of the surface reconstruction process employed in RE is of vital importance. The stereolithography (STL) file generated from the scan data was modeled on a fused deposition modeling (FDM) based AM. Its fitment was assessed with the help of INSPECTPLUS and GEOMAGIC reverse engineering tools. The aim is to minimize manual operations for duplicating the plaster models of residual limbs and to accelerate the design and manufacturing process of the prosthetic socket with better quality of fit. Further, this chapter presents the computer-aided modeling of the prosthetic socket design.

3.1   Traditional methods of Prosthesis Socket Fabrication

The prostheses fabrication process presented in work is adapted from Bhagwan Mahaveer Viklang Sahayata Samiti (famous as Jaipur Foot), Jaipur, India. Traditional prosthetic socket fabrication is invariably an artistic or a labour intensive process, meeting fitness and consideration of amputee satisfaction. In this method, the prosthetic practitioner must know the complete topology of the amputee's stump

and many assumptions that ultimately affect the quality of fit are being made. Socket manufacturing is always custom-made because each patient presents a different level of amputation, specific healing states, various muscular tones, which lead to an essentially handcrafted production process and therefore may lack in accuracy. However, through hand casting there is a chance for the uncontrolled deformation of the soft tissues, leading to bad socket fit in the future. Fabrication of the prosthetic socket for below-knee (BK) amputees has always been a time-consuming and complicated task, and experience is not easily captured on the stump. As the conditions of each patient's stump are different. Therefore, each socket has to be customized to the patients. Thus, much expertise is also required on the part of the prosthetist. Due to its freeform shape, it's hard to perform design, analysis and automate the fabrication process of the socket. Fabrication of socket follows numerous steps: measurement, wrapping, casting, modification, Thermoforming, and assemble.

3.1.1 Stump Measurements

After, qualitative assessment such as muscle/limb strength, joint function, skin grafting, scarring, site of pain in the stump, the condition of limb etc. by the Prosthetic practitioner's, the measurement process starts. It has different steps to measure the length of leg, which include reference measurements of the sound limb to measurement on the residual limb from the medial tibial plateau to the heel/floor.

Figure-3.1: Stump measurement of amputee's limb in BMVSS, Jaipur, India

As shown in Figure 3.1, the circular width of the stump is measured at mid patella level, and further, it continues every one inch below, until the distal end of the stump. Similarly, the stump length is measured and recorded by measuring tape from the head of the fibula or lower end of the patella to distal end of the stump. The

AP (Antero-Posterior) and ML (Medio-Lateral) diametric measurement of the knee at the condylar level and the patellar tendon level are also measured by using AP and ML caliper. This technique helps a lot in making a positive mould with correct dimensions.

3.1.2 Plaster Casting method

The next step after the measurement is casting or molding procedures which are as displayed in Figure 3.2. Firstly, the stump is covered via cling film. The required number of six inches of PoP bandages is submerged (wet) in water and when sufficiently soaked, is taken out and excessive water is squeezed before use. Casting process starts with wrapping one or two layers of PoP bandages on the patient's stump using the figure of 8 wrapping method. It starts from the front slightly above the patella and spirally down till the end and starts again up in the back of the stump to the posterior crease of the knee. Smoothing of the plaster over the surface of the stump is done by moving the hand around the stump and working towards the knee.

Figure-3.2: Wrapping POP bandages, applies pressure on the pressure-tolerant areas at patella tendon in BMVSS, Jaipur, India

As the plaster starts solidifying, Prosthesis applies pressure of the thumb and fingers on the pressure-tolerant areas of the stump to outline different soft

tissue/bones landmark and redistribution of more load on those areas. The depth of the fingertip impression in the popliteal area serves as a measure of tissue firmness is and is indication of how much modification of the model is required. The geometry of the residual stump is captured through the casting which is a duplication of the topographic shape of the stump. The dried cast is safely removed from the patient's stump known as negative cast.

3.1.3   Modification of the mould

The obtained negative cast is then filled with PoP paste, supported by a rod (mandrel) at a bench-vice. When the plaster gets dried, the plaster bandage is cut lengthwise down the posterior surface and removed. In this way, the positive plaster mold is obtained. The socket model is manually modified in Figure 3.3, as to transmit an optimum weight of the residual bones to the prosthetic socket.

Before modifying this positive mould according to standard PTB total contact socket modification principles, initial girth measurement has been noted over this positive mould. These girth values are compared with the manually measured girth values of the patient's stump. Our aim is to increase stump-socket contact pressure on the pressure tolerant areas and to decrease contact pressure in sensitive areas. It's a general finding that for the positive mould, the volume gets increased in comparison to hand measurement as taken over the residual stump by 5-7%, therefore initially these extra materials are removed from all over the mould with the help of the flat Surform file. The inferior patellar tendon area which is one of the most important pressure tolerant areas is modified by cutting away the plaster model midway between the lower edge of the patella and the tubercle of the tibia to a certain depth according to the patient's stump condition.

The prosthetic practitioner accommodates the material allocation at "pressure sensitive" and bulk areas to relieve pressure at sensitive regions and to improve the pressure distribution. In the traditional method, the modification of the plaster is primarily performed on the basis of experiences, skill, and craftsmanship using manual measurement data taken on the patient's stump. As a result, current socket design and fitting are mostly subjective to wide variation.

Figure-3.3: Manually modifications at patella tendon area in BMVSS, Jaipur, India

3.1.4   Fabrication of soft plastic socket

After modification of the positive mold, the manufacture of the socket starts with the fabrication of soft liner using standard vacuum forming apparatus by sealing or draping method. This soft liner is the main interface between the patient's stump and soft plastic socket. The distal end of the mould is made with the thicker soft liner material and is known as the distal cap. The prosthetic socket is formed of polyethylene (PE) sheet having 330x330x8 mm^3 dimensions drape over the previously moulded soft liner, using the same vacuum forming apparatus. The

plastic sheet falls by itself on the mould with uniform thickness rather than being pulled down and shaped onto the PoP profile using felt blankets or asbestos gloves.

Figure-3.4: Fabrication and finishing of socket in BMVSS, Jaipur, India

A piece of HDPE pipe is hung on a rod with PE sheet placed in an electric oven as in Figure 3.4, which is heated to 200°C for 30 minutes. For this, the positive mould is kept inverted on a standard vacuum forming apparatus. Socket trial may be helpful in all cases, but mainly in old user cases where the patient already knows the comfortable level of pressure that he can bear. It also provides another chance to the

prosthetist to check fitting and re-draw the socket alignment line in a weight bearing condition of the patient. For socket trail, the soft plastic is removed out of the positive mould. The proximal brim of the soft socket is trimmed and buffed. A small hole of 2 cm diameter is made at the distal end of the socket for pulling stockinette during the trial.

3.1.5 Fitting of the Socket

To check the fitting of the socket as shown in Figure 3.5, the patient is made to lie in a supine position on the examination table with the patient's stump lying near to the side of the prosthesis. Stockinet is sleeved over the residual stump, and then the trail socket is sleeved over the residual stump, by pulling the distal end of the stockinet out of the hole created at the distal end of the socket. At this stage, it is observed whether the donning of the socket is difficult or ease. Once the socket is fitted onto the stump, the patient is made to stand on the sound side with the compensatory blocks beneath the wore socket.

Figure-3.5: Soft-socket trail with patient in supine

The distal bony end must be free from any socket pressure when the patient loads the prosthetic socket side. Any other area (bony, soft tissue) where the patient is feeling discomfort or pain is marked on the socket. The proximal trims line is also marked on the socket, depending upon the required socket design. This socket is then removed out of the stump, is corrected and trimmed at those marked areas. This trial socket is reinserted on the stump to check with the patient feedback.

3.2   Proposed Methodology for Prosthesis Socket Manufacturing

For using the advanced technology of rapid prototyping (RP), a CAD model of the stump is constructed to fabricate prosthetic socket for a below-knee amputee. The proposed methodology for a new concept of prosthetic socket design is based on digitization of the positive mould of an amputee's stump. Reverse engineering (RE) technology is used to acquire the point data of the profile by instruments. The 3D digital data developed by reverse engineering offers two different manufacturing methods: first is the integration of reverse engineering and rapid prototyping, and second is the integration of reverse engineering and computer-aided manufacturing (CAM). Reverse engineering (RE) system helps in creating a 3D CAD model from a point cloud of an existing physical object. Numerous applications of RE include replication of an object, when actual drawings or digital model does not exist; when testing and alterations are necessary for the improvement of a new product or a re-design of a part or where the geometries too intricate and challenging for direct modeling in a CAD system.

As detailed in the (Figure 3.6), the traditional procedure for manufacturing of socket has three main steps, namely the measurement and casting stage, modification stage, and manufacturing stage. Measurement of the stump requires peripheral and diametric database taken by individual prosthetics, which may have an intra-reliability issue. Overall casting and measurement take about 60 minutes. The modification is the second stage, and it takes around 120 minutes including all subprocess in the modification. Finally, the interface preparation and socket manufacturing stages involved in traditional manufacturing demand extensive handwork of Prosthetic practitioners. It takes a longer time of around 480 minutes using traditional material and method. Overall time consumption in the traditional method estimated around 360 minutes.
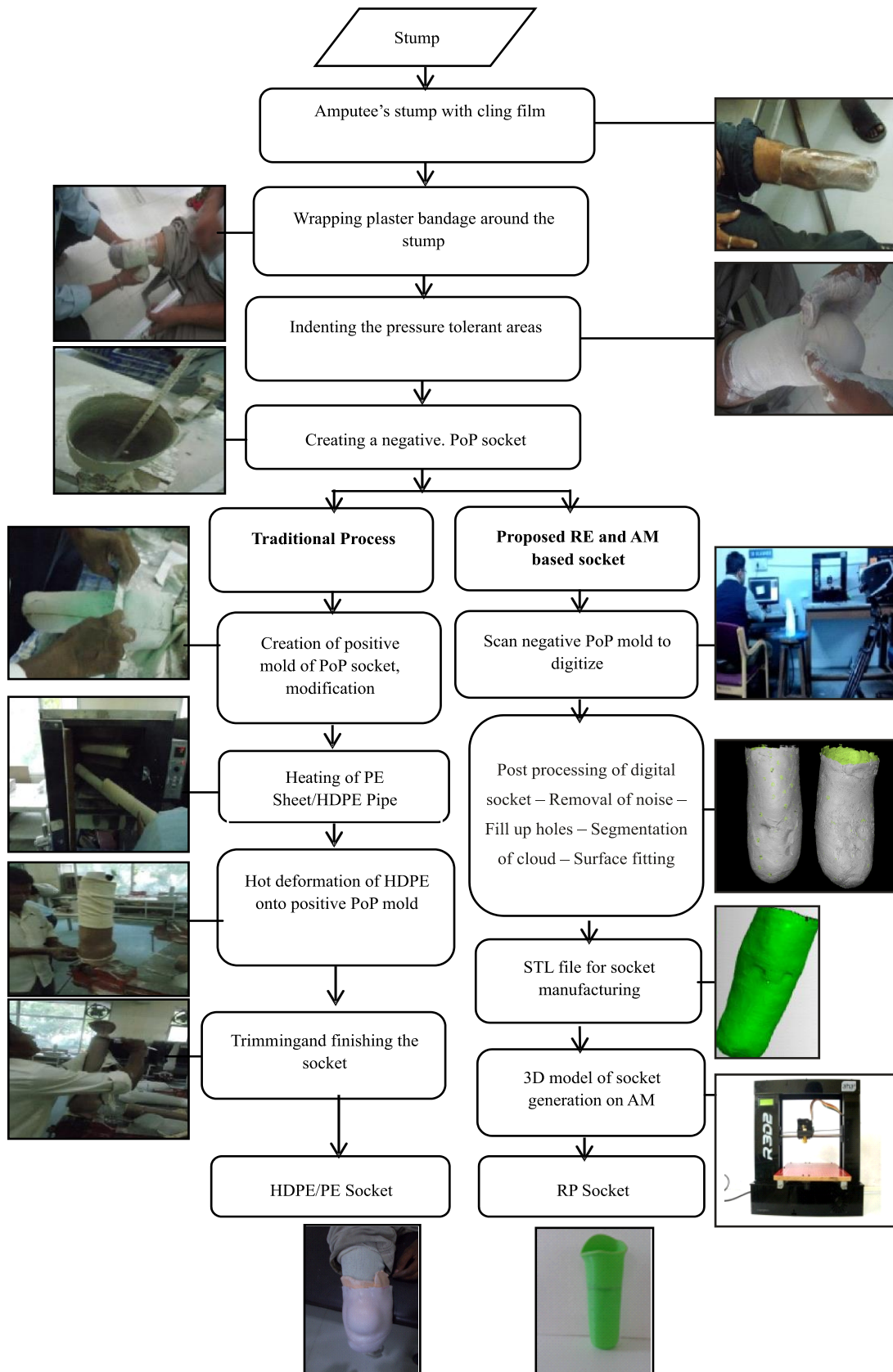
Figure-3.6: Comparison between traditional and proposed integrated RE and AM based socket

In the proposed method, the manufacturing of negative PoP mold is same as in the traditional method which is about 30 minutes. This is done with an intention to avoid direct scanning on the human body (residual stump) in proposed method. The scanning and Post Processing of the negative mold takes about 40 minutes.

```
         ┌──────────────────┐
         │   PoP Socket      │
         └──────────────────┘
                 │
         ┌──────────────────┐
         │  3D Measurement   │
         └──────────────────┘
                 │
      ┌────────────────────────────┐
      │ Post-processing of point cloud data │
      └────────────────────────────┘
                 │
      ┌────────────────────────────┐
      │   Surface reconstraction    │
      └────────────────────────────┘
                 │
         ┌──────────────────┐
         │ STL file generation│
         └──────────────────┘
                 │
         ┌──────────────────┐
         │  RP manufacturing │
         └──────────────────┘
                 │
         ┌──────────────────┐
         │    RP Socket      │
         └──────────────────┘
```
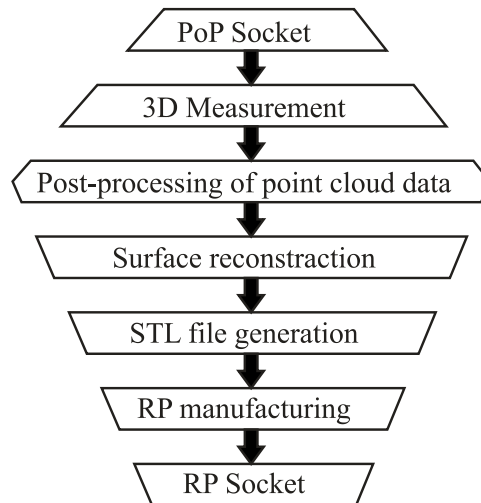
Figure-3.7: Flowchart of reverse engineering

The non-contact 3D laser scanner is used to scan each layer of the positive mould by rotating table and translating the sensor horizontally. After the first layer is scanned, the sensor moves vertically to the next layer, and a horizontal scanning process is repeated. Once the whole mould is completely scanned layer-by-layer, the external geometry of the positive mould is obtained. The output an STL format file obtained with the help of the solid modeling of the CAD software, it used in the RP machine to manufacture a prosthetic socket as shown in Figure 3.7. This present socket design approach, can decrease the training duration for prosthetists, lower production costs, and augment amputee care.

The 3D models with free-form socket profile are widely used in various medical applications such as surgery planning, customized inserts, and bio-mechanical work. In the same context, the design and development of prosthesis socket is a challenge due to the complex geometry of the stump which differs from one amputee to other. The precision of the produced 3D model is of utmost importance for the outcome of the result, particularly when different software processes the captured point data. So, it becomes important to examine the accuracy of the developed digital model with reference to the actual physical model. Several

RE software tools are available that suits the requirements needed by design personnel and operators. Prior using difficult mathematical approximations, they attempt to obtain the desired accuracy of 3D models by regulating various key factors through continuous approximations using commercially available CAD application tools.

3.2.1 Scanning processes

Employing the reverse engineering technology, the first stage is to obtain the point data of the residual limb by scanning. In the proposed approach, the 3D laser scanner can scan the geometry of residual limb easily and quickly. This method is novel as all the earlier scanning procedures involved direct scanning on the limb of the patient, which psychological fear of rays (ionizing radiation from MRI or CT scan) and have experienced a little vibration during scanning.

Figure-3.8: PoP Socket used for scanning

The object being a tubular segment, capturing the inside profile was not possible. Hence, it was decided to split it into two half's as shown in Figure 3.8. The socket size was not possible to accommodate in a single field of view. Hence, the complete acquisition of the PoP socket to capture the surface point clouds about

thirty scans, which is taken from different orientations. The tie point stickers were also used for proper surface earmarking. Respective cloud point segments were captured in steps and processed through INTEGRATION, and REGISTRATION option in the COMETPLUS software

3.2.2   Digitization (data capturing)

Digitization of lower limb PoP socket was scanned using a non-contact blue light scanner (Steinbichler's COMET L3D). The mean acquisition rate of the COMET L3D scanner is about 50,000 points per second. The version used in this study for data acquisition has a resolution of 1 Mpx and 1170 x 880 pixels. The socket was placed on a rotary table which makes the scanning process more efficient and faster. The complete digitization process for handling the point clouds was controlled by the 3D scanner software (COMET PLUS). To change the point of view between one scan to another scan, the part was fixed in the working volume and the scanner location was changed. No additional data processing was needed, since the RE software merges multiple scans in one point cloud either automatically or by manually selecting N points. For efficient scanning and identification of previous scans, tie points are placed on the socket surface uniformly. The 3D point cloud was exported in IGES format and the raw data of the socket composed of 11,585 points.

Figure-3.9: (a) Scanning of Plaster of Paris socket model

Figure-3.9: (b) 3D scanning arrangement

Once the negative PoP socket mold of a patient's stump is ready, then the proposed method begins with its digitization in Figure 3.9 (a). A scanner was used to scan the plaster cast (PoP) mold as shown in Figure 3.9 (b). The scanner scans each layer of the negative mold by rotating the mold on the plate, and the sensor is translated horizontally. The sensor was moved from location to location to cover the complete surface of the PoP socket with a tie spot as a referral point. This step eliminates direct scanning of the patient's stump and initiates digitization.

The study focuses on an accurate 3D surface generation of a complex profile. This free-form surface is generated from a plaster of Paris (PoP) socket model of an amputee. The external dimensions of the socket are 105 mm (maximum diameter) with a height of 252 mm.

3.2.3 Scanning of Clinically Significant Cases

Different clinically significant stump examples which require a different level of care and attention were considered as a case study, and the same is exhibited in Figure 3.10. All the five cases considered here are pertinent to patients in the age group of 35 to 45 who have been using Patellar Tendon Bearing (PTB) sockets for

10 to 12 years. Age, the cause of causality, the profile of the stump, etc. are all important in the diagnosis and design of prosthesis socket.

(a)   **(b)**   **(c)**   **(d)**   **(e)**
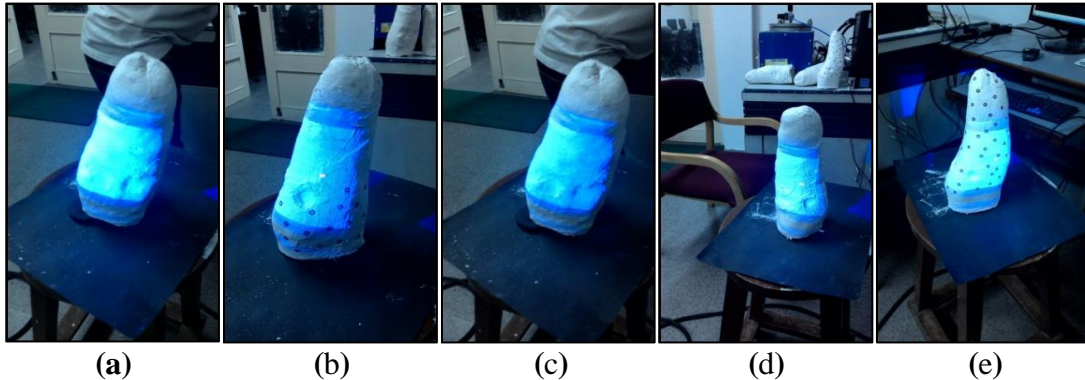
Figure-3.10: Stumps of different causalities–Case study
(a) Short stump, (b) Diabetic, (c) Peripheral vascular disease, (d),
(e) Traumatic injuries

Short Stump

The length of the residual limb is divided into three levels, i.e., short stump, normal stump and long stump. Short stump restricts control and alignment with prosthesis socket. It does not facilitate the revolving function and interferes with the grip and flexibility of the socket. This classification largely depends on the stump diameter-length ratio (Colombo et al. 2013). In the case of stump ratio greater than 1, it falls into the normal stump category. Normally, for comfortable fitment a stump of length 10 mm is required. For a short stumpy; 'Below Knee Amputee' stump ratio is almost unity or less than one and in such cases the stump becomes a dome shape and is unstable inside the prosthetic socket. A short stump inside a conventional PTB prosthesis hence causes strain, pain, and blisters on the patient.

Diabetic and Peripheral Vascular Disease Patient

Lower limb amputations make up to 90% of all amputations. They are most commonly caused by patients with diabetes and peripheral vascular disease. (Baars et al., 2008) mentioned that the patient could not walk continually and comfortably, hence needed frequent consultation. Diabetic patients suffer from open blisters on the distal part of the stump due to rigid fitting and donning of the prosthesis. It can cause sensations like an electric shock or even trigger phantom limb pain. This can result in infection and ulcers. Vascular disease with poor blood circulation is also

more frequent. The limb where the tumor exists is removed to prevent the incidence of cancer. All the above factors cumulatively could lead to further amputation.

3.2.4 Post Processing of Point Cloud Data

This step enhances the quality and accuracy of digital socket model. The primary output from any of the scanning or measuring techniques discussed before it's become a large set of X-Y-Z coordinates cloud, maybe incomplete with tessellated surface definitions. The post processing of the cloud data was done with the post processing software COMETPLUS[*].

Data acquisition of PoP socket requires multiple scans; during which surface outside of the intended object can also get captured. This unintended data is called noise. Noise removal is a necessary task to acquire the desired accuracy of socket model. The next step is filling with holes in the scanned socket model that may have been introduced due to the occlusion; different views scan during scanning. A curvature-based filling option ensures that the polygonal structure used to fill holes in high-curvature. After that, tetrahedral meshes are created by using an iterative closing algorithm available in RE interface. A tetrahedral mesh ensures effective surface development on the point cloud data. The cloud data after removing the noise is subjected to feature based segmentation. It re-ensures surface edges, boundary and areas of the scanned surface. Further, surfaces are divided based on their geometry like a conical shape, dome shape, and the transition shape and each of them is to be fitted with a clean surface, loft surface and bounded surface segments. This helps to reconstruct the complete part profile compensate for missing definition. Then, surface optimization is performed on the socket data and this process is known as decimation. The point cloud surfaces of the socket are then tessellated and saved as STL file.

As the resultant mesh size was large, it is better to represent it accurately with less number of triangles. The process of lowering the number of triangle meshes which makes it suitable for processing and handling of the data is known as decimation. It can be executed on the whole mesh or on any selected area of the mesh file. There are two types of decimation available, first is a chordal deviation

method and second is edge length criteria. However, this study does not consider the decimation process as it can lead to a reduction in accuracy in regions with high curvature, also it may infuence the outcome of the results. Next step is to optimize the triangle meshes as this process re-allocates the triangle meshes. The usefulness of this process is to obtain homogeneity in meshes. This process performs edge split and collapses depending on whether the edge is too long or too short.

3.3 RE tools application

The objective of RE system is to transform unorganized 3D point clouds into a surface replica with desired precision and accuracy. There are two segments available in these systems: one module converts the raw data into a triangle mesh and the second module reconstructs a digital surface model from a triangle mesh file. The present study employed two different CAD tools: CATIA V5R16 and SolidWorks 2010. For CATIA study, mesh file was formed using module Digitized Shape Editor and the surface model was reconstructed using the Quick Surface Reconstruction module and for Solid Works, Scan to 3D module was used. After data capturing three important steps include:

Step 1 - Processing of unorganized 3D point data. The outliers associated with point cloud data were removed, followed by the use of adaptive and homogeneous filtering techniques applied with different percentages. The initial point data captured comprises of all the geometric features of the object. The initial raw points consist of the higher amount of noise produced as a result of the 3D scanning process. Consequently, a huge amount of data size produced and for effective handling and processing of this data, a suitable filtering technique is applied which results in reducing the redundant points without losing object original geometry.

Step 2 –Development of triangle meshes and processing. The development of triangle meshes popularly known as tessellation. It is a process to build triangles by joining three neighboring points and replicates the same procedure until a network is formed to create a definite, lucid and consistent triangulated surface. In general, the initial raw mesh consists of sharp boundaries and non-manifold vertices; all these discrepancies need to be rectified to assurance accurate surface generation. Further,

it is essential that the meshes are cleaned and refined. The residual unwanted triangle meshes removed and created holes are filled. Occasionally, the triangle meshes are extremely dense which enhances the difficulty in handling and processing the file data. The solution to this problem is re-meshing and decimation of the mesh file. Smoothing the mesh moreover, helps in improving the accuracy of the generated surface model.

Step 3 – Generation of surface model and feature identification. The accuracy of the socket surface model was analyzed using the parameters including mean deviations (AD), maximum and standard deviation. Three different techniques were employed for the surface reconstruction from a triangular mesh file: feature recognition, surface fitting and NURBS surface patching. Subsequently, for regular features or prismatic profiles, not many software applications are available that allows semi or fully automated procedure for recognition of various features, highly depends on the intricacy of the profile. Several individual surfaces are linked resulting in an approximate global surface with automatic creation of arbitrary topology. The surface fitting technique was not applied in the current work. Since the development of each surface fits to characterize the whole surface of a part requires sufficient user expertise that will reflect on the outcome of the final result.

3.4 CATIA Methodology for Generating Free Form Surface from the Point Cloud Data

The first part of the current work was realized by means of CATIA software. It includes critical parameters of the filtering process, the mesh generation process and the settings applicable for smoothing process before surface reconstruction. For free-form geometry, it is important to carefully remove all outlier points manually after choosing initial point data of the concerned zone. The mesh file W signifies the default procedure employed without using any filtering or smoothing techniques prior to surface reconstruction.

3.4.1 Filtering technique effect

The Digitized Shape Editor module was used for the reduction of noise and redundant points by using two different types of filtering criteria. Use of the

adaptive filtering cause reduction in the point data based on a chord height deviation analysis criteria. This technique helps in removing points from flat zones, but preserves data close to the edges, boundaries and high curvature zones.

The use of homogeneous Fltering allows a uniform reduction in the point cloud data. Different point filtering percentages (15%, 22%, 30% and 45%) were applied to point data using both the filtering techniques. The default value taken by the software for filtering is 22%, which was used as the control for comparison purpose. The resultant files were studied and examined using reduced points (%), number of faces, reduction in mean and maximum deviation. The best result was provided by the homogeneous filtering technique for mesh (H) with 30% of reduced points with a reduction in a maximum deviation of 55.27% and mean deviation 25.67%. For the adaptive filter, mesh (A) with 15% of reduced points shows best results with a reduction in a maximum deviation of 72.31% and in mean deviation 35.76%.

3.4.2 Mesh smoothing process analysis

The process of mesh smoothing prime objective is to enhance the accuracy of the reconstructed surface, which can be used by operator input and shows global effects. There are two techniques available (single effect or the dual effect) for mesh smoothing from which the consumer can choose either of the ones. The importance of the single effect is that it will rub out the sharp edges present in the mesh resulting in the reduction of the volume of the object (shrinkage in the direction of the center of gravity of the object). The second technique lessens the distance between the surface and outliers; furthermore, it also reduces the deletion of the minor internal radius.

3.4.3 Decimation and Optimization mesh process

As the resultant mesh size was large, it is better to represent it accurately with less number of triangles. The process of lowering the number of triangle mesh which makes it suitable for processing and handling of the data is known as decimation. It can be executed on the whole mesh or any selected area of the mesh file. There are two types of decimation available, first is a chordal deviation method and second is an edge length criterion. However, this study does not consider the decimation

process as it can lead to a reduction in accuracy in regions with high curvature; also it may influence the outcome of the results. Next step is to optimize the triangle meshes as this process re-allocates the triangle meshes. The usefulness of this process is to obtain homogeneity in meshes. This process performs edge split and collapses depending on whether the edge is too long or too short.

3.4.4　Surface generation

The process of surface generation begins with triangle meshes. The complexity of the free-form structure of socket peripheral can be duplicated through automated reconstruction commands. In this work, the generation of the free-form surface was accomplished by the automatic setting of Surface Reconstruction module. The parameters that were analyzed include output surfaces, the percentage of points within tolerance, maximum and average surface deviation. The key input factors include the average surface deviation and the surface detail.

One important input parameter set by the operator was an average surface deviation to achieve the desired accuracy of the surface generated. At a lesser value, it provides small surface deviation, but in contrast number of surfaces generated also increases, which in turn increases the size of data. With the increase in the surface details from 250 to 7500, a significant reduction is shown in the maximum and mean surface deviation. The variation shown was more evident up to a surface facet of 1250, and another noticeable result was observed in an increase in the number of surfaces beyond this value. The surface detail of 1250 appears to be the standard value as beyond which it seems that there was not any significant variation in the results. This means that after this reference value, there does not seem any additional benefit for increasing the refinement.

3.5　Importance of PoP socket scanning

To date, conventional prosthetic socket making depends on upon the skills and experiences of the prosthetic practitioner. The present work reduces the effort of the prosthetic practitioner by employing automation process so that he/she gets consistent outcome measures indicating successful rehabilitation.

In the proposed method, the patient's psychological fear of rays (ionizing radiation from MRI or CT scan) for the stump measurement is alleviated, as the direct scanning of the live limb is harmful to human health. Although many technical literatures are available for integration of rapid manufacturing and traditional manufacturing through reverse engineering, whereas no report was found for converting PoP socket to AM socket.

Scanning of the negative cast can help in providing the more clear condition of the residual stump, as the negative cast is prepared by generating appropriate pressure points on the cast based on the clinical condition of the residual stump. Hence, the scanner can easily capture those marked points for digitization. Moreover, the socket design related database can be available for storage and iterative redesign in the future. The individual patient database may provide a clinical record of the different changes (volume, shape, colour, etc.) in the stump and overall impact of the prosthetic devices.

It's a general observation of P&O practitioner that the volume of the positive mold gets increased by 5 to 7 % in comparison to manual tape measurement of the residual stump when the positive mold is prepared from the negative mold. The positive mold modification becomes laborious with the traditional method scanning. Therefore, PoP cast (negative mold) scanning simplified the processes.

The work includes the assessment of the accuracy of the PoP socket digital model developed by RE procedure and determination of the key factors which influences the free-form, dimension and geometric accuracy. The investigation of absolute accuracy is very problematic since the only reference available to the user is the original model. However, the digital and the actual model are used for comparing the dimensional deviations at each corresponding point.

Assessment of the accuracy of the PoP socket digital model developed by RE procedure and determination of the key factors which influences the free-form, dimensional and geometric accuracy. The investigation of absolute accuracy is very problematic since the only reference available for the user is the original model.

The methodology presented in this thesis shows that inexperienced users have an extra advantage in working on instinctive and automated tools like ScanTo3D and digitized shape editor. On the contrary, an expert technician can help in improving the quality and accuracy of prosthetic digital models generated using a vigilant selection of different point processing parameters using a variety of CAD tools. The software used in this study has better flexibility in selecting different point processing parameters. The accuracy obtained for the developed PoP socket model in this study is in accordance with published literature results (Lin et al. 2005), for the use in medical applications and FEM analysis.

Chapter Summary

This chapter has delivered:

- The descriptions of materials and methods used in the fabrication of traditional prosthesis socket manufacturing.
- The 3D scanning for the PoP socket of the stump is employed in the place of expensive CAD models obtained through CT/MRI.
- Propose the development of a semi-automated methodology which integrates traditional process and reverses engineering methodology for developing a CAD model of prosthesis socket.
- This chapter provides an optimum balance for the best accuracy obtainable with maximum allowable deviation to lesser computer handling and processing time.
- A step by step alternating RE process with emphasis on using commercial software tools is proposed in this study that can also develop accurate digital surface models compared to conventional one step point cloud processing. The result obtained for the developed digital model is by the prosthetic and orthotic practice and FEM analysis.

CHAPTER 4

FINITE ELEMENT ANALYSES OF CAD MODEL OF SOCKET OBTAINED USING REVERSE ENGINEERING

Introduction

This chapter is focused on performing nonlinear static analysis using a hyper-elastic material model for the soft tissue which was carried out to determine the pre-stresses due to the donning procedure as well as the stresses developed due to body weight application. The model created for this study utilizes high-density linear elements and the mesh was verified to converge. The results of this study are not specific to one particular individual, therefore applying the procedure developed herein to a specific individual's anatomical geometry and prosthesis leading to results which can guide the redesign of the prosthesis socket. This chapter proposed a new perspective in socket analysis and design. The chapter also provides a comfortable interface for the distribution of load and understanding interface pressure over the residual limb. The stress distributions of the prosthesis socket were analyzed using the finite element analysis (FEA) method.

The finite element analysis was performed using the following methodology; the model geometry was first obtained and refined, the pre-processing stage of the FE model was completed by creating a mesh, load and boundary conditions were applied followed by defining element types, contact and material models. Lastly, the analysis was run and the results were post-processed. This chapter is subdivided into sections describing each of these steps in more detail.

4.1 Geometry acquisition and digitization of PoP socket

The residual limb geometry was developed by surface fitting point cloud data generated by scanning a physical model of a person's transtibial stump obtained by scanning of the negative cast of the patient's stump. Three below-knee male amputees participated in this study. The patients selected for the study were two unilateral and one bilateral amputation with Patellar Tendon Bearing (PTB) sockets having a uniform thickness of 5 mm with cotton liner. General information about the patients is given in Table 4.1.

Table-4.1: General information of below Knee Amputees

Patient	Age (year)	Height (cm)	Weight (kg)	Prosthesis in use (year)	Type of Amputee	Causes of Amputation	Side and Stump length (cm)
P1	36	161	61	11	Unilateral	Traumatic	Left 11.1 (±2. 0)
P2	48	176	70	24	Unilateral	Trauma-vascular disease	Right 6.3 (±2. 0)
P3	50	153	56	28	Bilateral	Trauma-diabetic	Right 18 (±2. 0) Left 15 (±2. 0)

P1 patient1, P2 patient2, P3 patient3

The prosthetic socket is made up of a typical stiff material, such as polypropylene or polyester having approximately 3 to 6 mm thickness (Steege et al., 1996). In practice, the socket thickness is decided by an empirical formula derived from the weight of the patients, i.e., (kg/20) (Duchemin et al., 2008).

The external volumetric geometry of the prosthesis socket of the residual limb surface was obtained from Bhagwan Mahaveer Viklang Sahayata Samiti (BMVSS) in Jaipur, India. Socket model is totally based on patient's actual geometry and dimension. Four PoP sockets were cast for each patient in the sequence shown in Figure 4.1 (a-d).

Figure-4.1: (a) Preparing PoP bandage (b) Cover the stump wit click film (c) Marking the pressure relief area at the patellar tendon (d) PoP cast is removed from the Patient residual limb

Initially, the external geometries of the lower limb surface of the patient are precisely reproduced using PoP cast slurry. Then, the PoP cast was scanned using

Steinbichler 3Dscanner COMET L3D as shown in Figure 4.2. It was difficult to capture the inside profile points due to the tubular segment of the cast. Due to large socket size, it was not possible to perform full scanning in a single field of view. Hence, the surface point clouds were captured in thirty equal steps. This non-contact 3D scanner is best suited for digitizing nonrigid (green state) objects having complex geometry like PoP cast socket mold. After capturing of Point cloud data, Geomagic software was used for constructing comparable CAD models of a socket. Owing to the complex geometry, precise meshing software, i.e. Hypermesh was used for creating a volume mesh of the CAD model followed by mesh refining. Final analysis of the socket was performed using HyperWorks.
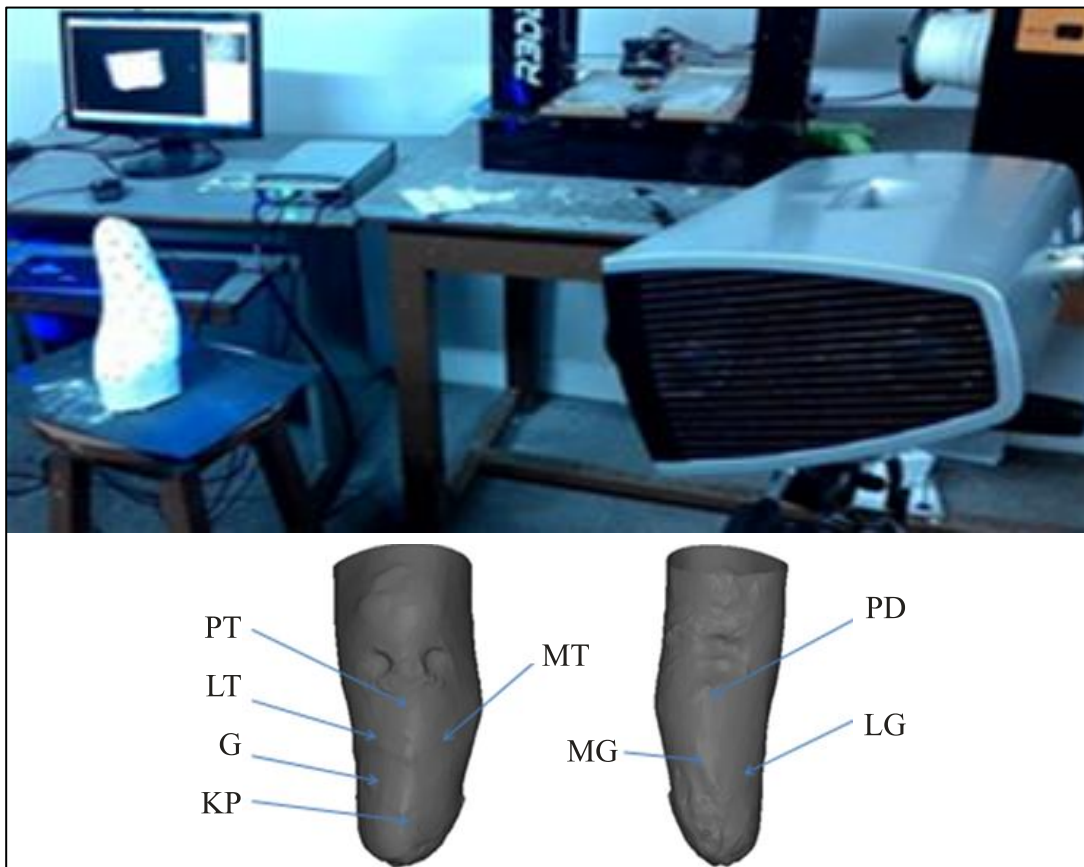
Figure-4.2: Digitization of PoP cast, and then scans view of anterior and posterior

4.2   Creating CAD Model

Utilize the method of reverse engineering involves the use of a non-intrusive 3D scanner to get the digitized data of the lower limb. Design system which is used to construct the CAD model of that residual limb based on the scanned points. CAD is the final stage of reverse engineering to design the socket, but the main challenge is to create the model itself. Before starting of the scan, a number of points marked on the surface of the model give all the attributes like humps, depressions, rounding's, etc. Once the model is created, the further process is to analyze it. The process of creating a model is to scans the socket using a blue light steinbichler scanner to create point cloud data. For the present study, a total of 26 scans were taken from different angles and with different model positions to scan the whole socket. After each scan, the previous scan meshed with the help of automatic meshing of a point to point (tie points) on the COMETPLUS mesh software.

The final model of prosthesis socket is created as a surface on COMET Plus Software. This is then followed by the post processing process which is done on the prosthetics socket model and involves processes such as removal of the associated area/noise, filling holes, segmentation of cloud, surface fitting, and analysis.

4.3   Generation of Finite Element model

The finite element technique is frequently used for the numerical analysis technique in biomechanics. FEM analysis is a computational approach for calculating the state of stress and deformation in the specific field. It is a useful method to understand the load transfer mechanics between the residual limb and its prosthetic socket. FEA is achieved by dividing a complex problem into a finite number of smaller elements, which is not solved by the analytical method. The accuracy of solution mostly depends on the number of elements of the model.
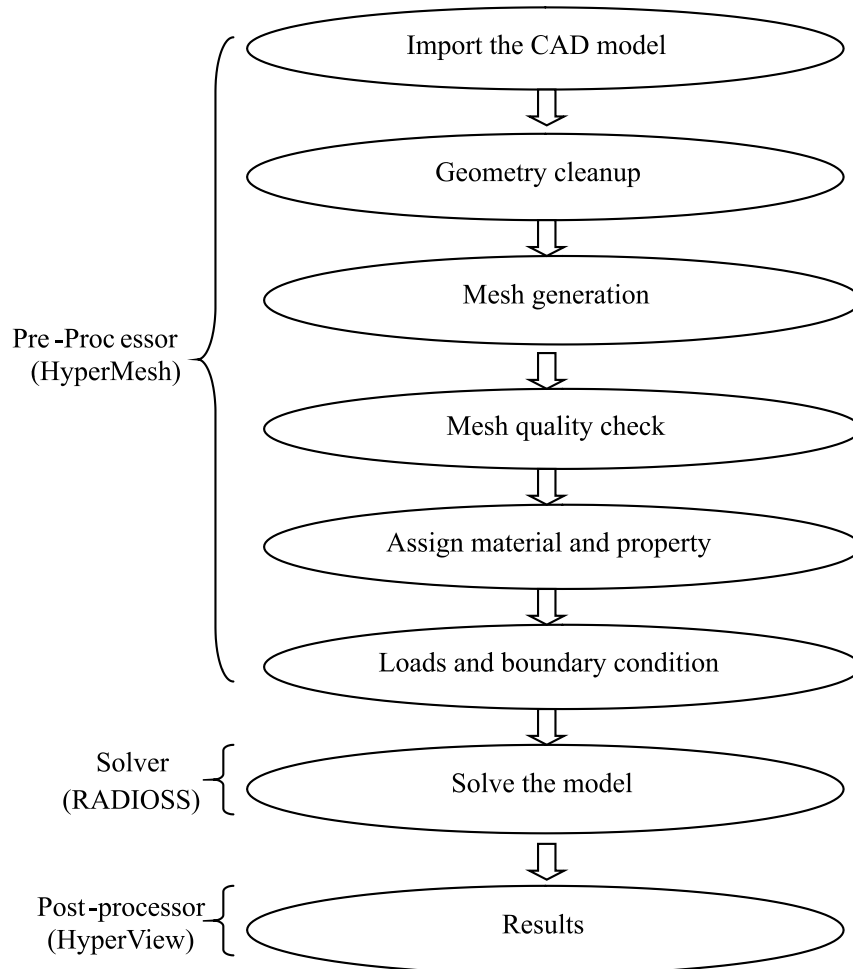
Figure-4.3: Flow chart of steps for FEM analysis on Altair Hyper Works

In developing the finite element model, first obtained the socket model geometry then refined. In the pre-processing stage, FE model was then accomplished by generating a mesh, applying load and boundary conditions, defining element types and material models. Finally, the analysis was run and the results were post-processed (Figure 4.3).

4.3.1 Mid-surfaces

There were no geometric irregularities, particularly free edges when the model was imported in HyperMesh. The geometry is a thin walled 3D structure and it contains outer and inner surfaces, and its two of the dimensions are very large in comparison to the third dimension. Therefore shell elements are chosen. So after visualizing, the mid-surface was extracted as shown in Figure 4.4 and thickness of

the geometry is virtually assigned to the 2D elements. Mathematically, the element thickness (specified by the user) is assigned to half in the $+Z$ direction (element top) and the other half in the $-Z$ direction (element bottom).
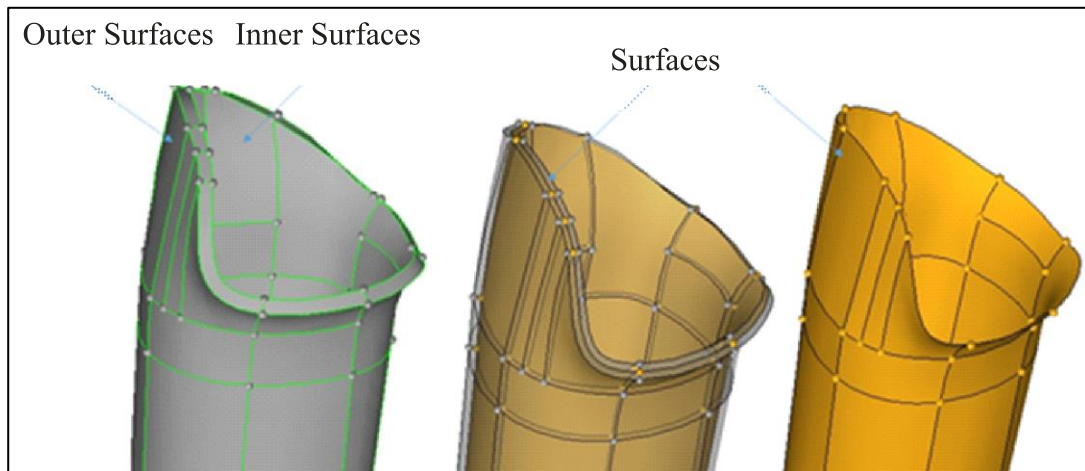
Figure-4.4: Extracting the mid-surfaces from outer and inner surfaces in HyperMesh

4.3.2 Mesh Generation:

2D elements are used for prosthetic socket design for mesh generation and divided into three basic element shapes e.g. tria, quad and mixed.

- **Tria:** There are two types of tria elements: Equilateral (trias) and Right Angled tria (R-trias) elements. R-trias are used only for specific applications such as mold flow analysis.

- **Quad:** Quadrilateral elements have been proved to be useful for finite element and finite volume methods, and for some applications, they are preferred to triangles or tetrahedra. Therefore quadrilateral and hexahedral mesh generation have become a topic of intense research. By connecting polygon nodes to their respective nodes on the object boundary, one gets a quadrilateral element mesh in the boundary region.

- **Mixed:** The mixed mode, the element type is the most common element type used due to better mesh pattern that it produces.

Meshed models with different mesh types are as shown in Figure 4.5. Note the more homogeneous mesh pattern resulting from "mixed" meshing.

(a) Tria   (b) Quad   (c) Mixed
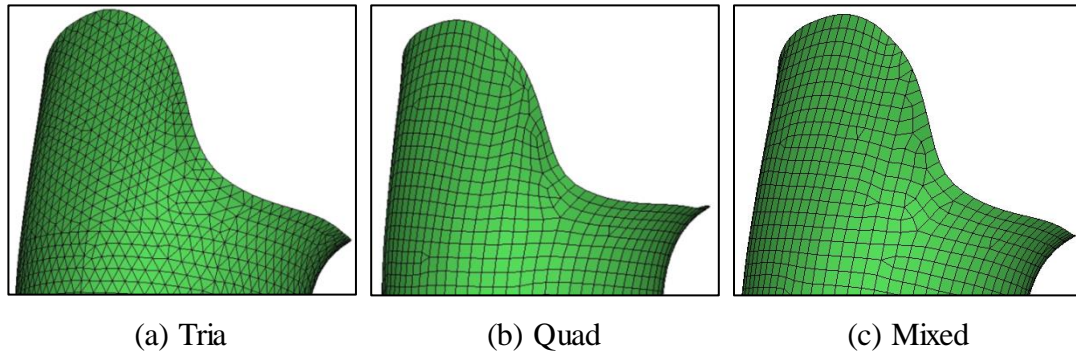
Figure-4.5: Meshed models with different element types

The STP model of the PoP socket was imported into HyperMesh 14.0 for FEA modeling. In the present work, generating the tria element contains 3-noded shell with six degrees of freedom at each node and appropriate element size of 5 mm was selected for meshing. To achieve faster convergence, mesh quality was reviewed to detect distorted or stretched elements, and further such defected elements were refined individually. The nodal distance at the outer surface for all sockets was uniform and steady. However, the element sizes in the inner volumes of the parts were non-uniform. As shown in Figure 4.6, the meshed model was established based on the actual shapes of the socket, and the number of elements with nodes is displayed in Table 4.2.
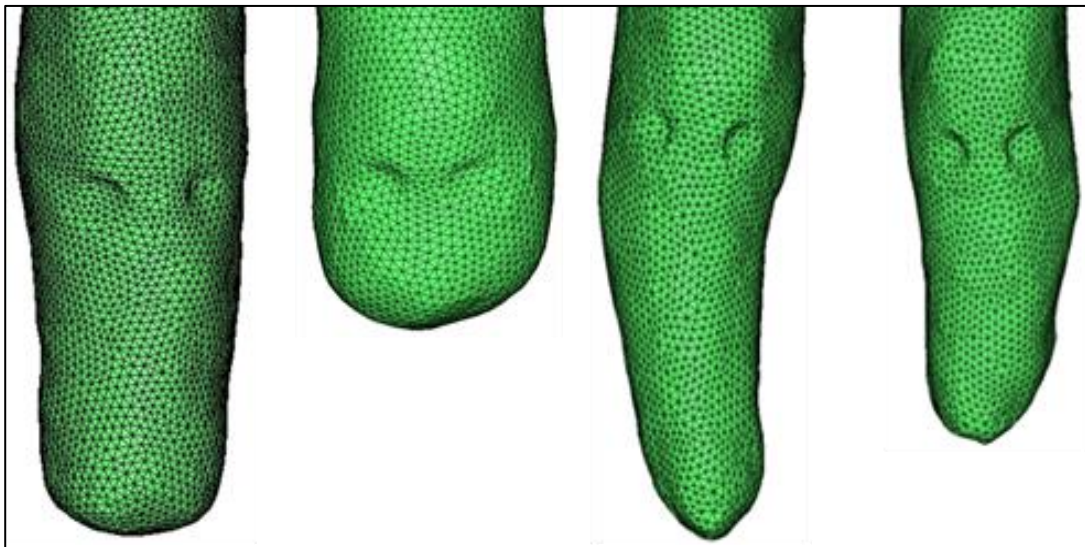
Figure-4.6: Mesh model of PoP socket of P1, P2 and P3 (right and left Limb)

Table-4.2: Finite element model properties

Parameters	P1	P2	P3	
Amputee side	Left	Right	Right	Left
Mesh Type	3D Shell Tria Elements	3D Shell Tria Elements	3D Shell Tria Elements	3D Shell Tria Elements
Element size	5 mm	5 mm	5 mm	5 mm
Number of mesh elements	8467	5010	6487	5950
Number of nodes	4269	2540	3278	3009

4.3.3 Element Quality Check

In FEA modeling, element quality greatly affects the accuracy of the analysis results. The FEA modeler must take into consideration element quality, and thereby judge whether the analysis results are meaningful. There are many important quality parameters that need to be checked that affect the accuracy of the analysis results. Some of them are as follows:

- *The Warpage* is the amount by which an element deviates from being planar. Since three points define a plane, this check only applies to quads, while tria elements do not have such problems. In this socket model warpage of up to five degrees is acceptable.

- *Aspect Ratio* is the ratio of the longest edge of an element to either its shortest edge or the shortest distance from a corner node to the opposing edge. Aspect ratios should rarely exceed 5:1.

- *The skew* of triangular elements is calculated by finding the minimum angle between the vector from each node to the opposing mid-side, and the vector between the two adjacent mid-sides at each node of the element. The minimum angle found is subtracted from ninety degrees and reported as the element's skew.

- *Chordal Deviation* of curved surfaces can be approximated by using many short lines instead of a true curve. The chordal deviation is the perpendicular distance between the actual curve and the approximating line segments.

- *Jacobian* measures the deviation of an element from its ideal or "perfect" shape, such as a triangle's deviation from equilateral. The Jacobian value ranges from 0.0 to 1.0, where 1.0 represents a perfect shaped element. In this case of Jacobian evaluation at the Gauss points, values of 0.7 and above are acceptable.

In all three types of meshed models were inspected and compared based on the various quality parameters using check elements. As in mixed type mesh, there were less no. of distorted elements, and mesh generation is smoother, so it is chosen for further modeling. After a number of iterations and inspections, an element size of 5 mm is chosen. The distorted/failed elements are corrected using various tools available in HyperMesh.

4.3.4   Material Properties

To perform static analysis, the mechanical properties of the liner, bones, and socket were assumed linear, elastic, isotropic and homogeneous (Zachariah et al. 2000, Zhang et al. 2000, Lee et al. 2004). From the literature, it was found that these non-linearities were disregarded in socket analysis. For soft tissues, young's modulus and the Poisson's ratio of 200 kPa and 0.49 was considered as material properties (Jia et al. 2004). For this study, HDPE material is used, for which the physical properties are enlisted in Table 4.3.

Table-4.3: Properties of different socket materials (Wu et al. 2003)

Material	Young's modulus (Mpa)	Ultimate stress (Mpa)	Density (Kg/m^3)	Poisson's ratio
Polypropylene	1500	80	910	0.3
High-density polyethylene (HDPE)	800	37	950	0.39
Low-density polyethylene (LDPE)	280	25	920	0.41
Polyurethane	1500	39	830	0.3

4.3.5   Loads and Boundary Conditions

The bottom of the socket was spatially restrained (a degree of freedom constrained) and the distal end of prosthesis socket base attached to pylon as shown in Figure 4.7. A shaft, along with the artificial foot is attached to the bottom end of the socket which is flat. The stiffness of the shaft is of a higher order as compared to the socket. Therefore, predetermined boundary condition up to 3 cm distance from the tip of the socket's distal end was applied. Loading was based on the weights of the patients in the range of (56-70) Kg and an approximate height of the patients is in the range of (153-176) cm. However, from a study point of view, a generalized weight of 80 kg is assumed. Thus, the total load due to gravity, i.e. 800 N vertical downward load was applied under the static condition and the load is evenly distributed on the patellar tendon (PT), medial tibia (MT), lateral tibia (LT), popliteal depression (PD) and kick point (KP) stance phase of the gait during the cycle. This load is applied at the top end of the socket. To distribute this force equally on all the nodes of the top end, an independent node at the center is created, and it was connected to all the nodes on edge through the rigid 1D element. From the previous literature, it was observed that most researchers analyzed transfemoral and transtibial prosthesis applied load equivalent to half (400 N) or full body weight (800 N) at the femoral head, or they applied forces equivalent to the reaction forces extracted from larger FE models (Jaime et al. 2012, Jia et al. 2004, lee et al. 2008).

Force=8.00e-02
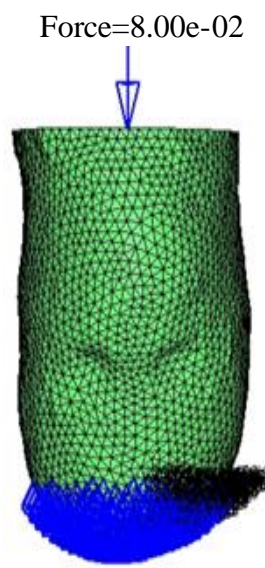
Figure-4.7: Loads and boundary conditions of patient P2

4.3.6   Stress Distribution

The deflection and stress distribution for the socket are shown in Figure (4.8 to 4.11). The von Mises stress distributions and displacements (in the y-direction) at the stump-socket interface are essential for socket design. For 800 N downward vertical load, the maximum stress of 1681 kPa, 2101 kPa, 1831 (L) kPa and 2782 (R) kPa respectively was observed in three patients as given in Table 4.4. Peaks of stress arise on the anterior side in all cases except P3 (left). However, the same P3 patient has developed extremely stress (2782 kPa) on his right leg anterior side (at kick point).
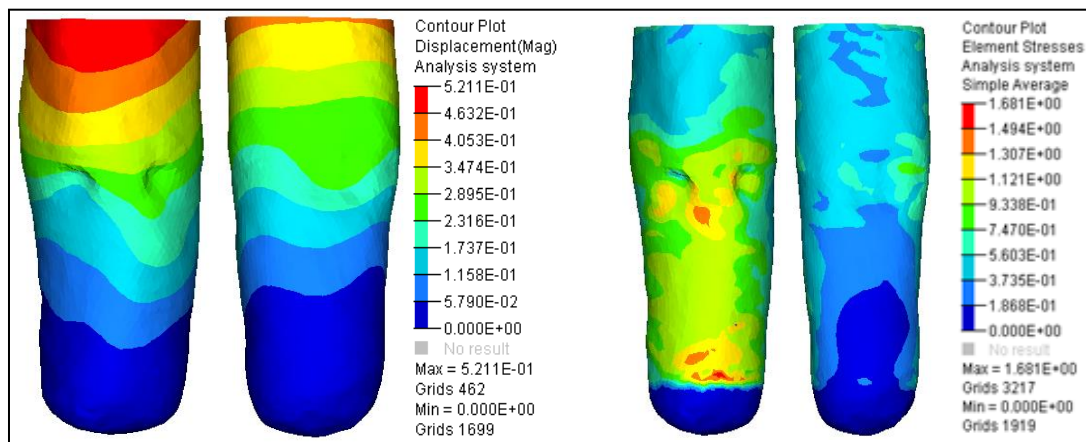
Figure-4.8: Anterior and Posterior deflection pattern and Von Mises stress distribution of P1
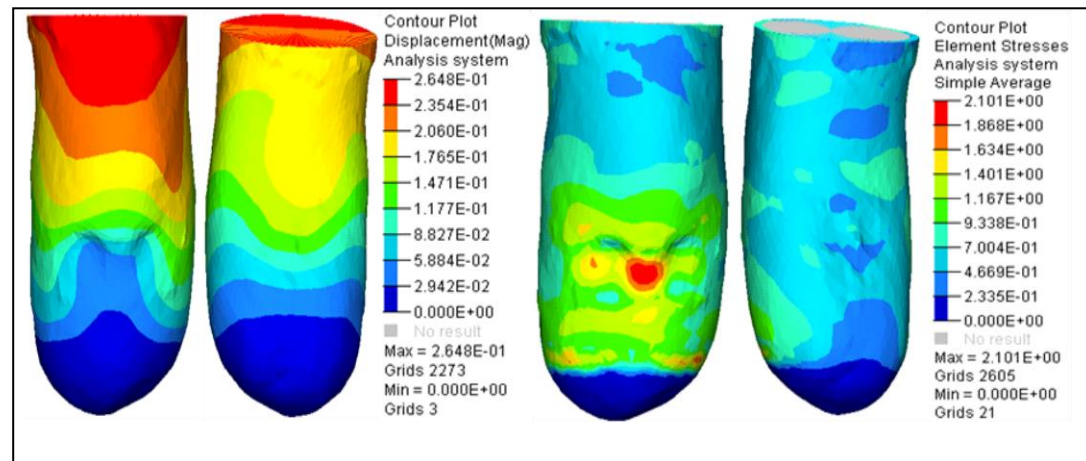
Figure-4.9: Anterior and Posterior deflection pattern and Von Mises stress distribution of P2
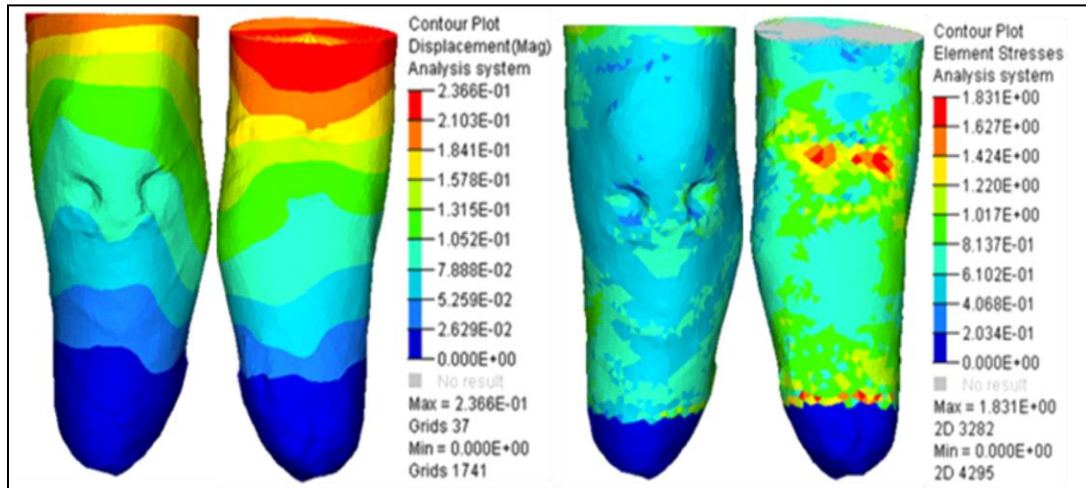
Figure-4.10: **Anterior and Posterior deflection pattern and Von Mises stress distribution of P3 left limb**
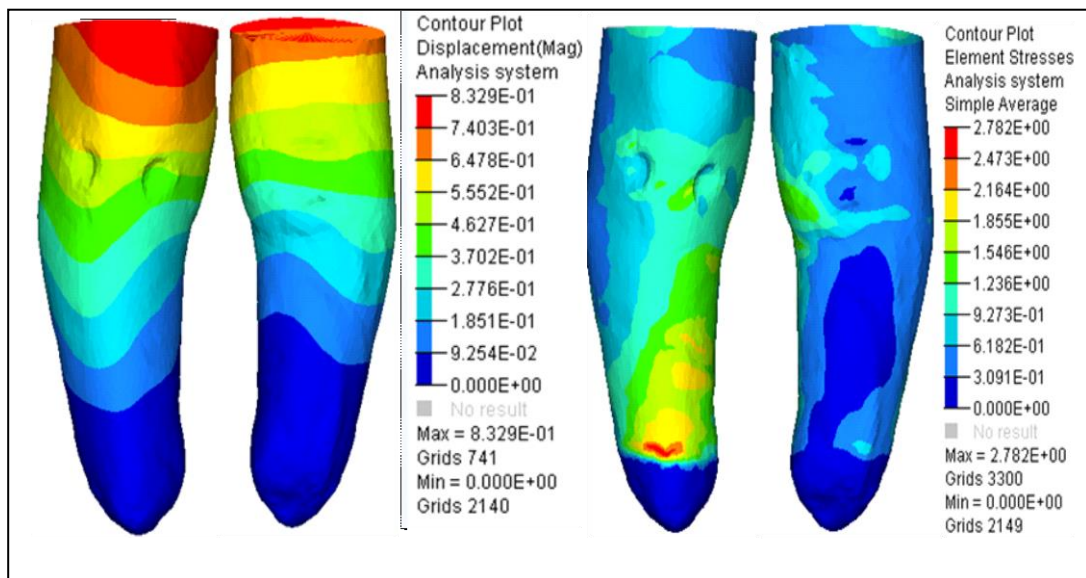
Figure-4.11: **Anterior and Posterior deflection pattern and Von Mises stress distribution of P3 right limb**

The deformations (displacements) obtained in various sockets are detailed in Table 4.5 and the maximum deformation (2.895E-1) was observed on the socket of patient P1. In all cases, maximum displacement occurred on popliteal depression except for patient P3 right leg. Further, the peak value of stress and displacement for different patients and regions of the PoP socket are given in Table 4.6.

Table-4.4: Von Mises stress distribution at different regions for PoP socket

Regions	Stress		P3 (kPa)	
	P1 (kPa)	P2 (kPa)	Left	Right
Lateral Tibia (LT)	1121	1401	1017	927
Gastrocnemius (G)	1121	1634	813	1236
Patellar Tendon (PT)	1681	2101	1222	1855
Kick Point (KP)	1681	1634	1017	2782
Medial Tibia (MT)	933	1167	610	2164
Medial Gastrocnemius (MG)	744	700	813	618
Popliteal Depression (PD)	933	466	1831	1546
Lateral Gastrocnemius (LG)	560	700	1222	618

Table-4.5: Displacement at different regions for PoP socket

Regions	Displacement		P3 (mm)	
	P1 (mm)	P2 (mm)	Left	Right
Lateral Tibia (LT)	1.737E-1	8.827E-2	7.888E-2	3.702E-1
Gastrocnemius (G)	1.158 E-1	5.884E-2	5.259E-2	2.776E-1
Patellar Tendon (PT)	2.895E-1	5.884E-2	1.052E-1	5.552E-1
Kick Point (KP)	1.158 E-1	2.942E-2	5.259E-2	9.254E-2
Medial Tibia (MT)	1.737E-1	1.177E-1	7.888E-2	1.851E-1
Medial Gastrocnemius (MG)	1.737E-1	8.827E-2	1.052E-1	9.254E-2
Popliteal Depression (PD)	2.895E-1	1.471E-1	1.578E-1	4.627E-1
Lateral Gastrocnemius (LG)	1.737E-1	8.827E-2	7.888E-2	1.851E-1

Table-4.6: Peak values of stresses and displacement at different regions for PoP socket

	P1	P2	P3	
			Left	Right
Maximum stress (kPa)	1681 (PT) (KP)	2101 (PT)	1831 (PD)	2782 (KP)
Maximum deflection (mm)	2.895E-1 (PD) (PT)	1.471E-1 (PD)	1.578E-1 (PD)	5.552E-1 (PT)

Four factors express the consistency of FE analysis: geometry, mesh, material properties and boundary conditions. This study presents a systematic framework for producing the pragmatic geometry acquisition of the lower limb profile using laser scanning. It also includes a procedure for socket design and structural response using FEM to establish structural consistency under given load. As a result, the proposed method offers a significant improvement in the analysis of different socket designs which improves comfort and quality of life for amputees.

In traumatic patient P1, patellar and kick point area have a more stress generation as compared to other areas. In trauma-vascular disease, patient P2 has more stress at patellar areas than another area. Similarly, for the third patient P3, diagnosed with diabetes, more stress has been observed at popliteal depression (left) and kick point area (right) of the residual limb. It is found in that the maximum pressure is at the patella tendon area and the lowest pressure is achieved on the lateral tibia area.

To the best of our knowledge, no literature has been found in different clinical significant cases which are considered in this study. The 3D scanning for the PoP socket of the stump is employed as a replacement for expensive CAD models obtained through CT/MRI. In future studies, the model will be validated experimentally using strain gauges placed in different regions and tested on a patient's residual limb. The limitation of the present study depends on the accuracy of the scanner. A new approach is to developing deflection and stress distribution directly from PoP scan data having adequate accuracy with less computational time. As a practical clinical implication of the current study, the low-cost prosthesis is obtained through material reduction using PoP socket will be can affordable in developing countries.

The classical theory of PTB total contact socket requires hand-casting for generating negative cast with pressure distributed at pressure tolerant areas (where the dynamic load can easily be tolerated). In contrast to the conventional approach, there is no need to apply any external pressure to the sensitive areas. So that the software model of the socket can be made thicker on pressure tolerant areas and vice

versa. Practically as this approach utilizes prosthetist skill, it gives a pre-assessment of the socket fit which decreases hit and trial of the socket. The advantages of using this approach that gets a simulation model of the PoP cast for analysis and less time-consuming in the modification of the prosthetic socket. By involving the expert personnel in the automation of prosthesis the human-touch intact, it increases the sustainability of the engineered product.

4.4 Socket thickness design based on aspect ratio criteria

Meshed model of the Prosthesis socket with a commonly used aspect ratio are analyzed for stress distribution using finite element method. An optimum socket thickness was arriving for a given socket. Thickness is an important parameter as too less thickness leads to the failure of socket and greater thickness leads to discomfort to patients. Geometry information about the short and long below-knee stump is shown in Figure 4.12. The transfer of power via the stump-prosthesis interface is almost impossible with short stumps when conventional fitting techniques are used.

Figure-4.12: Geometry of the short and long below-knee stump
L-stump length, D- stump diameter, e- eccentricity of the force

The design of the conventional patella tendon bearing (PTB) prosthesis is based on specialized regions of load transfer. The vertical load is carried mainly on the impression of the socket in the region of the patellar tendon. The regions on both sides of the tibial crest, the distal posterior surface, and the poplitea provide additional support in standing and ambulation. When the stump is short, it becomes spherical and the moment's transfer mechanism becomes quite inefficient.

The below-knee amputation provides a stump which is short in length. The resulting stump is cylindrical in shape, well-padded, comfortable, and easy to fit with modern below-knee prostheses of the total-contact-type. However, the loading area of the stump has repeated breakdown, and the stump became extremely sensitive and painful. Anterior and posterior view of short and long stump socket (HDPE), deflection (see Figure 4.13, a-d) and element stress distribution (see Figure 4.14, a-d) at different thickness 3mm, 4mm, 5mm, and 6mm.
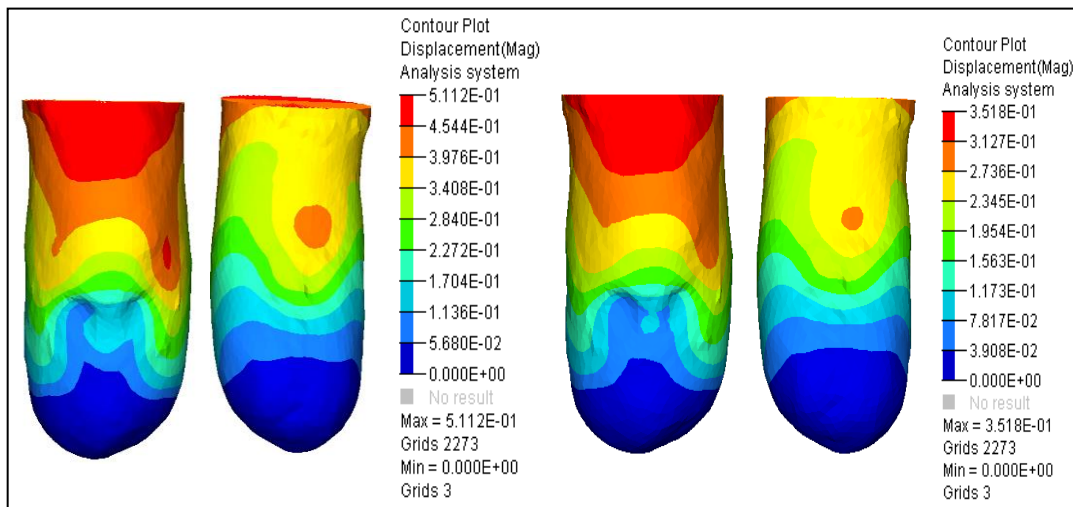
Figure-4.13 (a): Anterior and posterior view of the short stump socket (HDPE) deflection for 3mm and 4mm
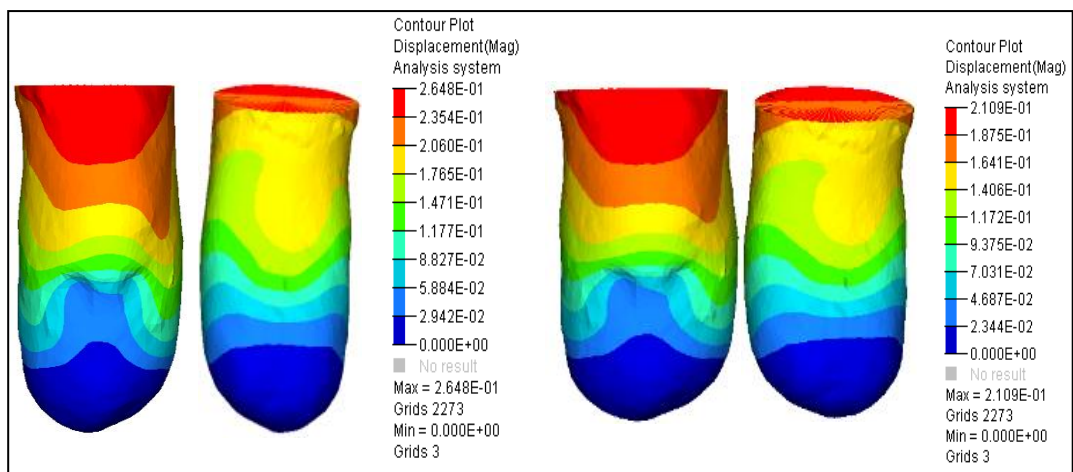
Figure-4.13 (b): Anterior and posterior view of the short stump socket (HDPE) deflection for 5 mm and 6mm
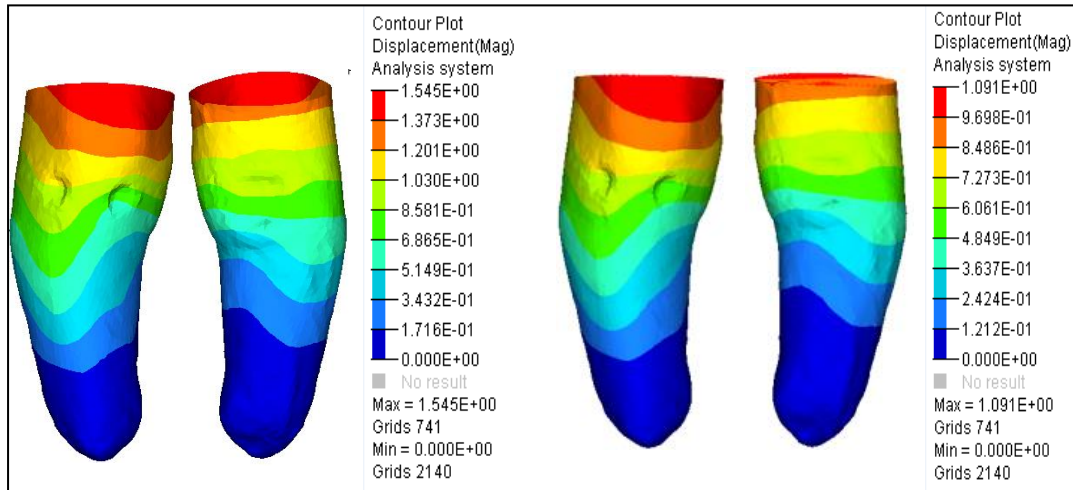
Figure-4.13 (c): Anterior and posterior view of the long stump socket (HDPE) deflection for 3mm and 4mm
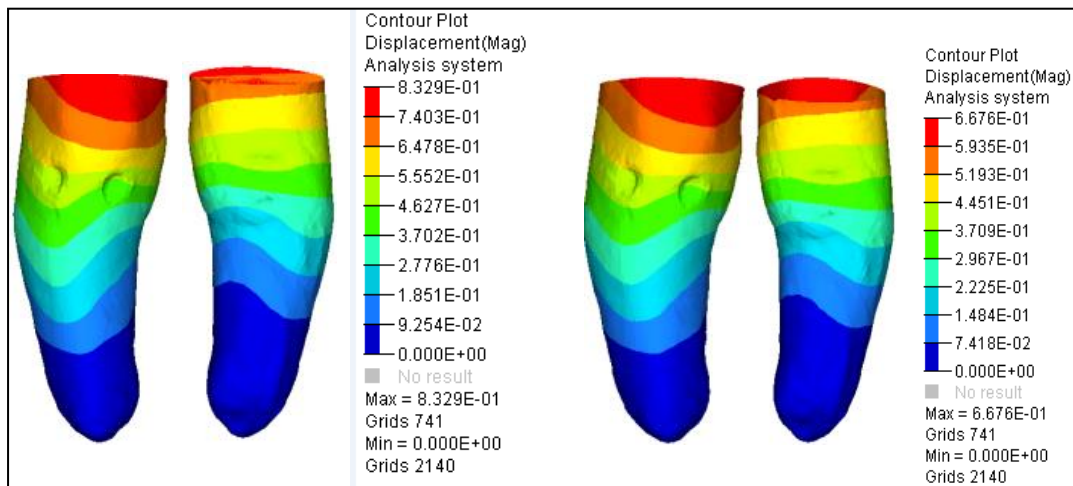
Figure-4.13 (d): Anterior and posterior view of the long stump socket (HDPE) deflection for thickness 5mm and 6mm
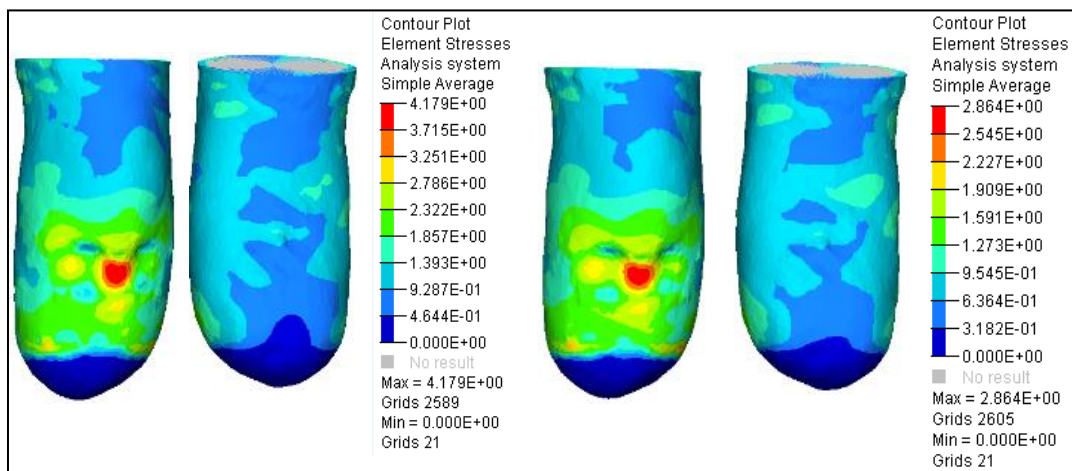
Figure 4.14 (a): Anterior and posterior view of short stump socket (HDPE) Maximum Von-Misses Stress for thickness 3mm and 4mm
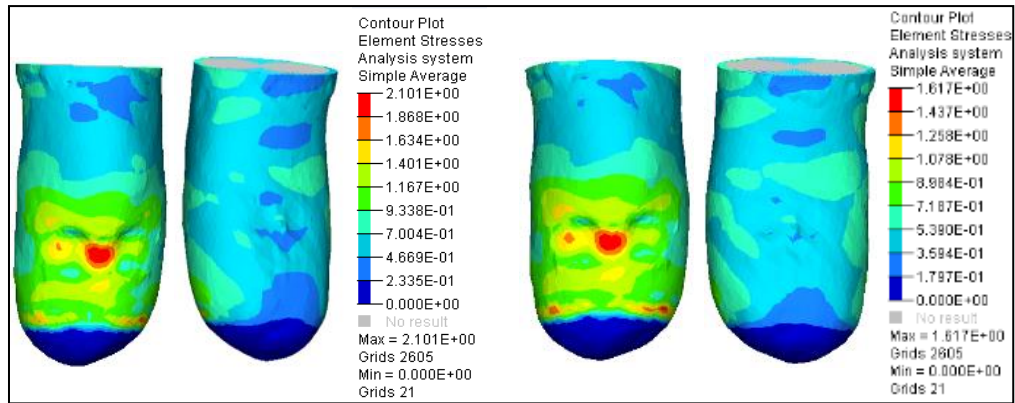
Figure 4.14 (b): Anterior and posterior view of short stump socket (HDPE) Maximum Von-Misses Stress for thickness 5mm and 6mm
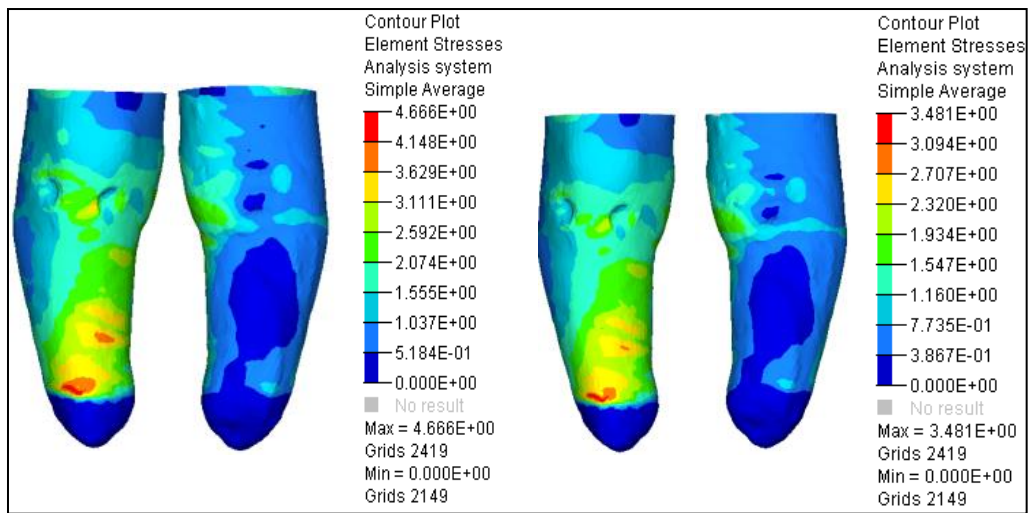
Figure 4.14 (c): Anterior and posterior view of long stump socket (HDPE) Maximum Von-Misses Stress for thickness 3mm and 4mm
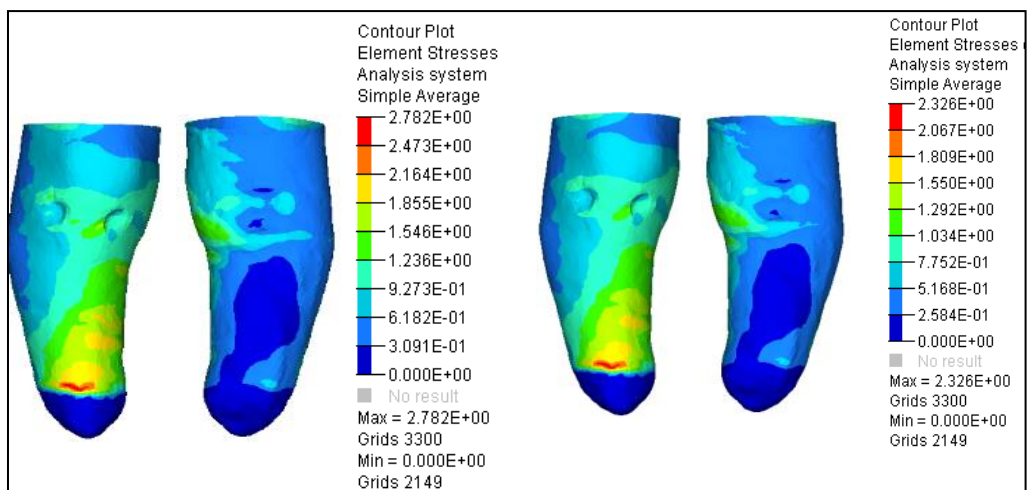
Figure 4.14: Anterior and posterior view of long stump socket (HDPE) Maximum Von-Misses Stress for thickness 5mm and 6mm

In the graphical representation Figure 4.15 between displacement and thickness, the initial stage of result shows that difference between the two parts of the short and long stump is large as compared to the final stage of the part. This result reveals that the short stump displacement remains approx constant (small change) however, displacement for long stump varies for a long part. For the part between stress and thickness, the short stump stress variation is considerably more as compared to long stump stress.

Displacement verses thickness

	3	4	5	6
Patient 2	0.51	0.35	0.26	0.21
Patient 3	1.5	1.1	0.83	0.66

Thickness (mm)

Patient 2   Patient 3

Maximum Von Mises Stresses verses thickness

	3	4	5	6
Patient 2	4.17	2.86	2.1	1.61
Patient 3	4.66	3.48	2.78	2.32

Thickness (mm)

Patient 2   Patient 3
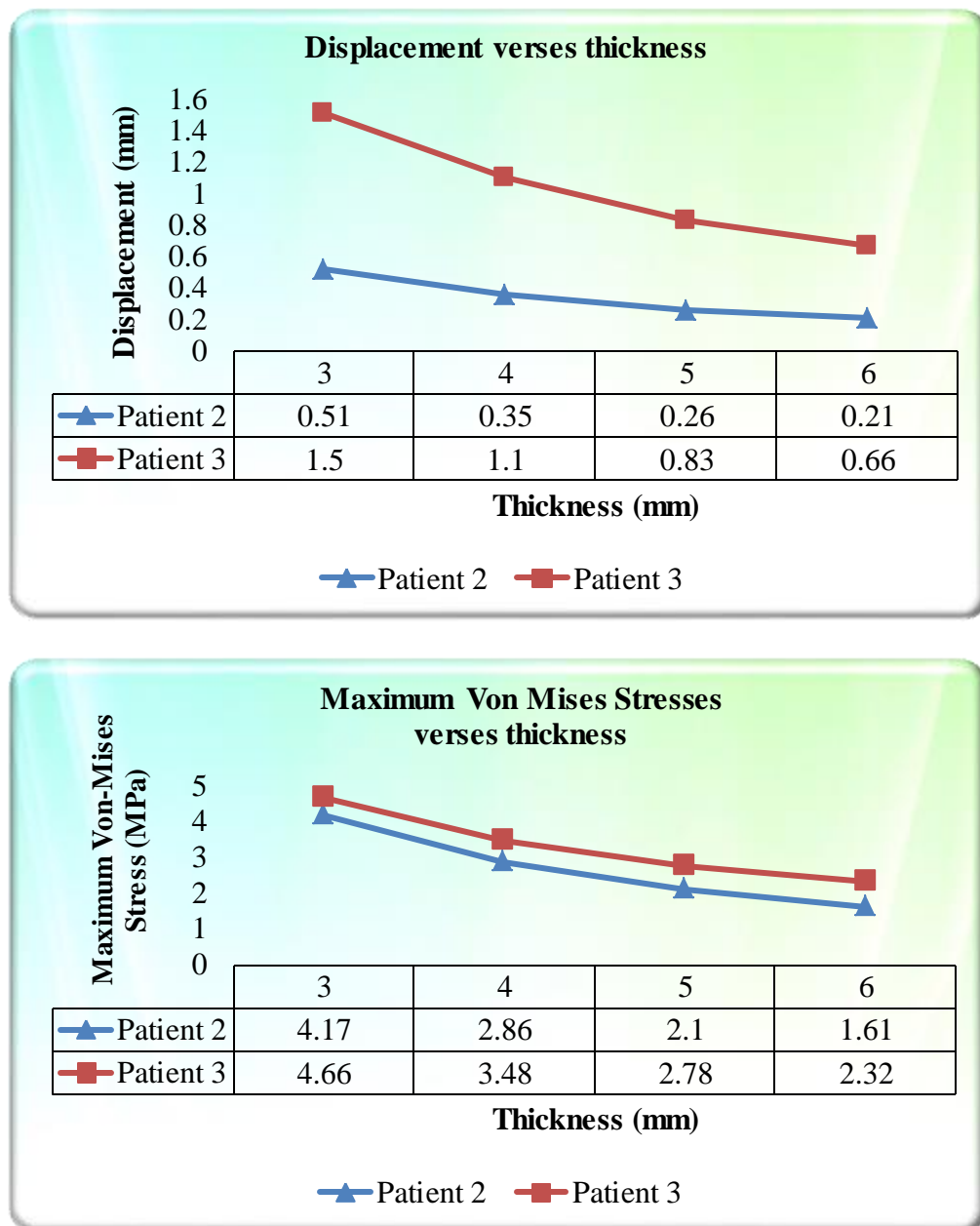
Figure-4.15: Displacement and von mises stress in pressure tolerant area verses thickness

Chapter Summary

This chapter presents a novel approach to improve the design of the BK prosthetic socket through FE analysis. A scientific understanding of pressure-displacement intensity at the socket-limb interface is essential for the improvement of prosthetic socket design.

The results provide significant insight into the socket design and a roadmap for customization of the sockets. Although stress–strain patterns and magnitudes have shown similar behavior for all the patients, however patient-specific solution is needed for comfortable socket design as the peak value of stress was found to vary.

CHAPTER 5
EXPERIMENTAL PRESSURE MEASUREMENT BETWEEN STUMP AND SOCKET

Introduction

This chapter discusses how to predict the pressure distribution around the residual limb under different loading conditions. The methodology for pressure measurement in the residual limb is to insert a pressure film in the prosthetic socket and record the pressure between stump-socket with the help of FUJIFILM. Further, these measurements are used to perform the pressure distribution to assist clinicians in designing ventilated sockets avoiding mechanical failures. Then, the focus is to evaluate the pressure distribution between the limb and socket at specific regions. Regression technique is used to develop analytical models for each of the loading conditions (half, full and walking). Subsequently, the population-based genetic algorithm has been utilized to predict the pressure regions (Min-Max) by optimizing the developed mathematical model. This methodology helps to correlate the simulation study results with the experimental results.

5.1 Measuring Interface Pressure using sensors

The distribution of pressure at the interface between the residual limb stump and the prosthetic socket has played a significant role in the rehabilitation of socket design. Biomechanics of stump-socket interface, especially the pressure and force distribution, have an effect on patient satisfaction and function. The information obtained has been used either to increase the understanding of socket load transfer, to evaluate the socket design, or to validate the computational modeling. Interface pressure measurements require a proper measurement technique, which includes the use of sensors, their placement at the prosthetic interface, as well as the related data acquisition and conditioning approach. An ideal system should be able to continually monitor real interfacial stresses; both pressure and shear, without significant interference to the original interface conditions. A variety of sensors were used to measure the socket pressure. They can be classified, based on their operation principle, sensor size, range, number of sensors and output device

5.2   FUJIFILM Pressure Film

The pressure measurements in the stump-socket interface prosthesis were carried out using the FUJIFILM (Japan). Pre-sensor is a measuring system developed by Fuji Photo Film Co., Ltd. and used in medical applications. One healthy male with right below-knee amputee 48-year-old, the unilateral subject was selected to participate in the study. The patient wears patellar tendon bearing (PTB) prosthesis socket with a uniform thickness of 5 mm with cotton liner.

Ultra super low pressure (LLLW) pressure film having pressure range (0.2-0.6 Mpa) was used in two sheet type A and C. Type A film is a base material coated with the colour forming material and film C is coated with a colour developing material. The coated sides of each film must face in front of each other and the flexible pressure sensing mats. During the application of normal operating pressure, the microcapsules are broken, and the colour-forming material transfers to the colour developing material and reacts, thereby generating a red colour. This sheet-based medium uses a chemical release mechanism to produce a pink stain on the sheet-surface and a greater pressure produces a darker stain.

In this experimental wok, pressure film (FUJIFILM) was placed at critical locations of stump (anterior, medial, posterior and lateral area) and pressure at this level is to refered as a continuous pressure which is detected by change in colour to red and the density change according to intensity of applied pressure. Pressure was applied for five seconds and further maintained for another five seconds. The density of red allows graphical evaluation of the strength of force. The colour intensity is directly proportional to the actual pressure. This pressure map was be visually inspected and compared to a colour calibration chart.

The patient did not report any pain throughout the employment of their transtibial prosthesis. In another word, stump soft tissue integrity was not disturbed, and they did not feel any significant pressure in the socket. The cutting of Fuji film into residual limb shape needs careful placement of film. The Film was sliced into strips according to limb dimension. The patient is made to stand, and a plumb line was dropped at the tip of the head of the fibula. The distance between the anterior

and posterior surface of the leg at the level of medial malleolus is measured and recorded. Figure 5.1(a) shows the measurement for the lower limb. Further film A is placed on the stump as illustrated in figure 5.1 (b). Then C-film is inserted into the socket as shown in Figure 5.1 (c), and the patient is made to stand in the standing frame in a relaxed posture. Finally, Figure 5.1 (d) predicts the pressure distribution on C-film colour by red.

(a)   (b)

(c)   (d)

Figure-5.1: Pressure measurement around the residual limb

5.3   Pressure measurement on stump

The FUJIFILM pressure sensor was used to identify, predict maximum pressure and the average compression loads in the selected areas of the stump. The

measurements using the FUJIFILM system were carried out in the room at a constant temperature (22-25°C), and humidity during the entire measuring is 65%. As it is a dynamic measuring with a pressure sensor, it is necessary to ensure the absenteeism of obstacles during the execution of the measurements walking by a subject with a pressure sensor. Figure 5.2 depicts the layout of the pressure sensing regions at Anterior, Lateral, Medial and Posterior sides of the lower limb of the stump.
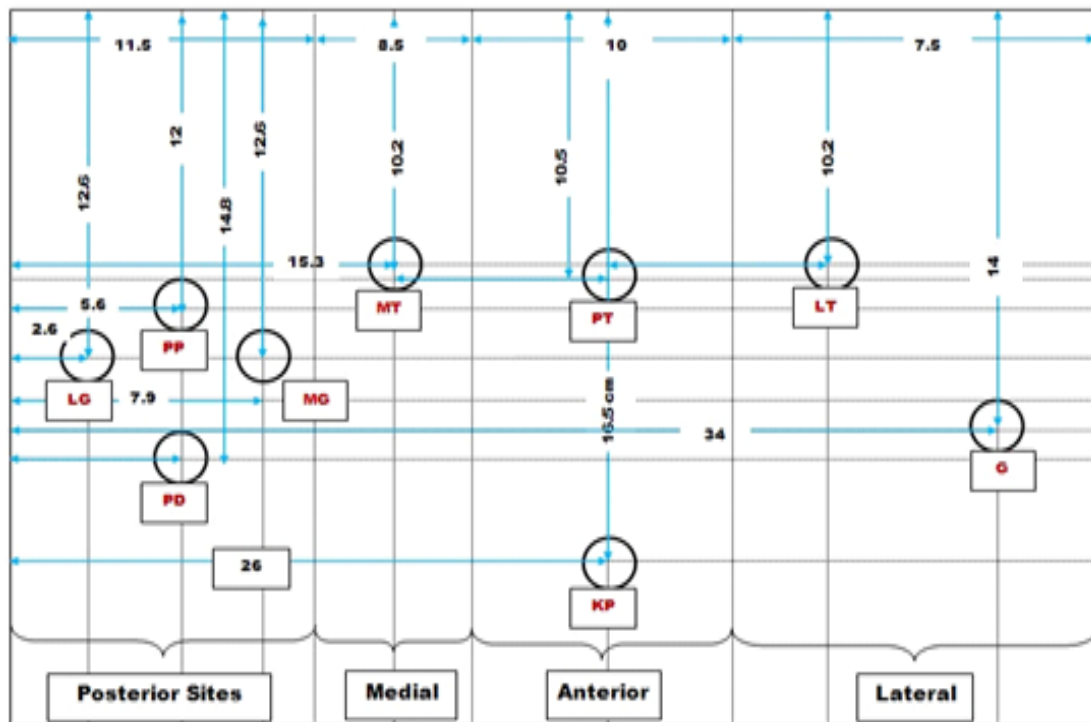
LG-Lateral Gastrocnemius, PP-Postero Proximal, MG-Medial Gastrocnemius, PD-Postero Distal, MT-Media; Tibia, PT-Patellar Tendon, KP-Kick Point, LT-Lateral Tibia, G - Gastrocnemius
* All dimensions in cm and overall dimension of socket is (37.5 x 18.5 x 0.4)

Figure 5.2: Layout of the pressure sensing regions

Figure 5.3 demonstrates how the pressure distribution resulted at posterior, medial, anterior and lateral display in a 2D configuration and varied during the stance phase of gait. This film has the advantage of being highly customizable and being adaptable enough to fit any stump size. The result shows that the pressures on the patellar tendon and lateral tibial condyle regions are similar and shows little change in pressure with alignment. The pressure distribution obtained through

FUJIFILM pressure sensor for the lower limb prosthesis socket is a suitable method for the quick diagnosis of peak pressure in the residual limb.

Figure 5.3: P**ressure distribution recorded around the residual limb during static load-bearing**

For all over stance, the pressure distribution of residual limb was investigated at nine sites. The peak pressures have been recorded at the Patellar tendon (PT) region of the anterior surface and low pressure at postero distal (PD) reason. The observed area of peak pressure agrees with previously published work.

The primary objective of the current study is to enable the real-time assessment and analysis of socket fit for a below-knee amputee during stance. Fitting between the socket and stump is an important factor for successful

ambulation because volume changes that occur throughout the day would also affect socket fitting. After placing on the prosthesis, half of the total body pressure is equally divided over forefoot and heel. The body weight of a person weighing say 120 pounds and standing relaxed in a naturally held position is distributed through the feet. The gait cycle is thus seen to consist of two phases. Stance, which comprises 60% of the entire reporting period, is followed by swing, the remaining 40% since the stance phase is longer, it follows that there is an overlap of periods when both lower limbs are weight bearing.

Zachariah and Sanders (2000) determined the differences in pressure between standing and walking and the results obtained in this study also presented a similar pattern. The ultra-super low pressure (LLLW) employed in the current research were fragile pressure film that allowed the placement of the stump and socket, which covered more than 80% of the stump for pressure map.

Fuji Pressure Film sensor captures high-resolution sensor placed between the stump-socket which offers full surface pressure profiles with a graphical representation for analysis. The sensor could facilitate the scanning of the pressure in the particular stump areas and thus optimize the prosthesis socket design, avoiding the soft skin damage, aching, and discomfort when using a prosthesis socket. The results and load distribution over the residual limb shows that the system is reliable for clinical application for measuring pressure measurement.

5.4 Flexi force pressure sensors

Sensor based amputee stump/socket structures for force/ pressure monitoring in amputee socket systems, which will bring about better-designed prosthetic sockets that ensure enhanced patient satisfaction. The aim is to monitor the force in the residual limb. In this investigation, divide the procedure to sensor selection criteria, sensor position selection, circuit design, data processing, and data analysis.

Six unilateral below-knee male amputees were selected for this investigation. The age of the amputees are between 30 and 70 years, height 161 and 176 cm, having a weight between 60 and 72 kg, respectively (See Table 5.1). This study

considered different clinically significant cases. The selected amputees regularly used prosthesis patella tendon bearing (PTB) socket with a uniform thickness of 5 mm with cotton liner. They had been using Exo-skeletal transtibial prosthesis from last 3 and 21 years with PTB socket in Jaipur foot. The measurements were carried out using the flexiforce sensor as shown in Figure 5.3. The flexiforce performed better when large slowly varying forces are applied for long durations.

Table-5.1: General information about patients

Patient	Age	Tall (cm)	Weight (kg)	Using Prosthesis (Year)	Type of Amputee	Clinically Significant cases	Stump length (cm)
P1	30	172	66	4	Unilateral	Accident	Right 18.1 ($\pm$2.0)
P2	42	173	70	3	Unilateral	Trauma-vascular disease	Left 15 ($\pm$2.0)
P3	36	174	72	3	Unilateral	Accident (Long)	Left 28 ($\pm$2.0)
P4	56	171	68	10	Unilateral	Infection (Short)	Left 16 ($\pm$2.0)
P5	70	168	63	9	Unilateral	Diabetic	Right 23 ($\pm$2.0)
P6	40	166	70	21	Unilateral	Conjugation	Right 22.8 ($\pm$2.0)
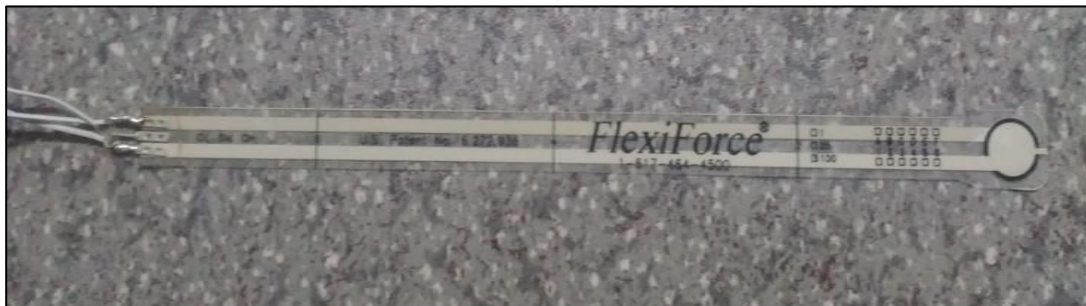
Figure-5.3: FlexiForce pressure sensor

The details of the FlexiForce sensor can be found below in Table 5.2. The sensor is of small thickness, flexible printed circuit, light weight custom shape, and size. It can measure the force between any two contacting surfaces and is durable enough to stand up in most environments with a force range (0 to 445N). These

sensors can be easily integrated between stump-socket interfaces. The sensor measures both static and dynamic forces between stump and socket. It is constructed from two layers of the substrate; substrate is composed of polyester film (or Polyimide in the case of the High-Temperature Sensors). On each layer, a conductive material (silver) is applied, followed by a layer of pressure-sensitive ink. The adhesive is then used to laminate the two layers of substrate together to form the sensor. The sensor acts as a variable resistor in an electrical circuit. When the sensor is unloaded, its resistance is very high (greater than 5 MΩ); when a force is applied to the sensor, the resistance decreases. Table.5.1 indicates the properties of this sensor.

Table-5.2: Physical Properties and performance FlexiForce Standard Model A201

S. No	Parameters	Value	Unit
1	Thickness	0.208	mm
2	Length	197	mm
3	Width	14	mm
4	Sensing Area	9.53	mm
5	Standard Force Ranges	0-445	N
6	Linearity (Error)	< ±3%	
7	Repeatability	< ± 2.5% of Full Scale	
8	Response Time	< 5	μsec
9	Operating Temperature	-9 to 60	°C

5.4.1 Genetic Algorithm

Genetic Algorithm (GA) is a population-based search and optimization techniques originally introduced by Holland, 1992. It is a heuristic tool, which is based on the Darwin principle of natural selection involving evolutionary processes such as selection, mutation, and crossover. The population means a group or a set of solutions. The design variables are encoded into the solution strings of a finite length, and the search starts with a population of the encoded solutions created at random instead of the single point in the solution space. Based on the solutions in the current population, it uses the genetic operators to replace the old population with the new population of solutions till the termination criteria are satisfied. Thus,

this algorithm assesses only the objective function, and genetic operators - selection, crossover, and mutation are used for exploring the search space. One can specify the bounds and constraints for the variables in this algorithm. GA begins with the initialization of randomly generated individuals of chromosomes. In each generation, it performs processes of fitness evaluation compared with the best value and modified. Here, modification means crossover and random mutation to form a new population. During crossover, parent chromosomes are selected to produce child chromosomes after possible recombination. The new population is then used in the next iteration of the algorithm. The algorithm is run until some stopping criterion is met such as a maximum number of generations of adequate fitness level.

The principal aim of using a genetic algorithm in this study is to predict maximum and minimum pressure at the specific region of a socket interface. This objective is achieved by optimizing the developed analytical model of pressure using sensor based measurements and regression analysis. Based on the constraint condition the parameters are optimized by the genetic algorithm. The genetic algorithm determines optimal pressure values and recommends the values of process parameters, height, weight, and stump length.

5.4.2 Experimental Setup

The experiments were carried out on amputees using an experimental setup as shown in Figure 3. One step down transformer is used to convert AC voltage of 220 V to 9-0-9V and also, analog to digital converter (ADC) in the form of an IC is used to convert AC to DC voltage. An analog-to-digital converter (ADC, A/D, or A to D) is a device that converts a continuous physical quantity (usually voltage) to a digital number that represents the quantity's amplitude. The conversion involves quantization of the input, so it necessarily introduces a small amount of error. Furthermore, instead of continuously performing the conversion, an ADC does the conversion periodically, sampling the input. The result is a sequence of digital values that have been converted from a continuous-time and continuous-amplitude analog signal to a discrete-time and discrete-amplitude digital signal.

Figure-5.5: Flexiforce set up with a National Instrument system

One capacitor is used to make DC voltage constant, and resistance is used to drop the voltage. Then experimental setup is connected to data acquisition block/card (DAQ-9171), four channels NI 9234 chases (National Instruments) by BNC probe cable to the virtual instrumentation software (Lab view) for data acquisition. Data acquisition (DAQ) is the process of measuring an electrical or physical phenomenon such as voltage, current, temperature, pressure, or sound with a computer. A DAQ system consists of sensors, DAQ measurement hardware, and a computer with programmable software. Compared to traditional measurement systems, PC-based DAQ systems exploit the processing power, productivity, display, and connectivity capabilities of industry-standard computers providing a more powerful, flexible, and cost-effective measurement solution. FlexiForce, force sensors can measure the force between almost any two surfaces and are durable enough to stand up to most environments. The sensors are available off-the-shelf for prototyping that can be customized to address the particular needs of your product design and application requirements.

5.4.3 Circuit Construction

There are many ways to integrate the FlexiForce sensor into an application. One way is to incorporate it into a force-to-voltage circuit. A means of calibration must then be established to convert the output into the appropriate engineering units. Depending on the setup, an adjustment could be made to adjust the sensitivity of the sensor.

In this case, as shown in Figure 5.6, it is driven with a -5 V DC excitation voltage. This circuit uses an inverting operational amplifier arrangement to produce an analog output based on the sensor resistance and a fixed reference resistance (RF). An analog-to-digital converter can be used to change this voltage to a digital output. In this circuit, the sensitivity of the sensor could be adjusted by changing the reference resistance (RF) and drive voltage (VT); a lower reference resistance and drive voltage will make the sensor less sensitive, and increase its active force range.
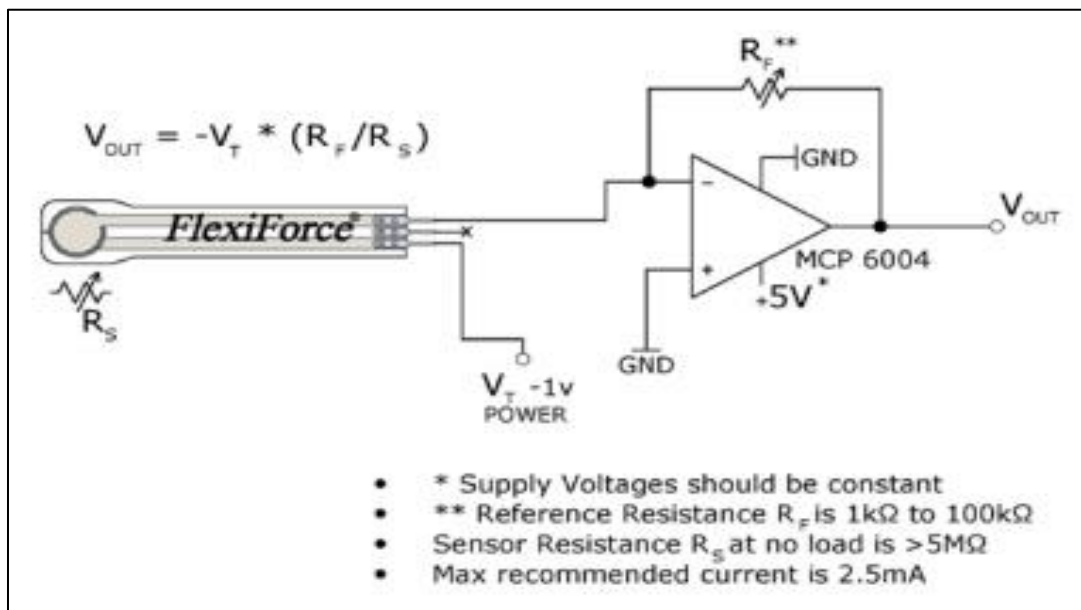
Figure-5.6: Circuit diagram

5.4.4 Data Acquisition

In the present study, eight specific regions are identified to measure pressure at different loading conditions (half, full and walking). Before initiating a measurement, all hardware components of the FFS system (socket, connecting the cable, converter) must be appropriately connected. The FFS is placed between the liner and socket at eight specific regions. After wearing the prosthesis, an amputee is

advised to take a half load on both legs, full load on amputation side and walk 10-12 meters for dynamic pressure measurement. Further, a pressure measurement at all eight regions can be viewed simultaneously in real-time using the software on laptop/PC screen and the measurement can be repeated, if required.

The Flexible Force Sensor is an ultra-thin force sensor that is ready to plug-n-play shown in Figure 5.7. The FFS works like any other bridge transducer, by converting non-linear resistance changes to a linear output voltage proportional to force. Paper-thin, the FlexiForce circuit is only 0.208 mm thick making it ideal to measure the force between virtually any two surfaces. The FFS is a complete sensing solution that is easy to use and accurate for a variety of applications.
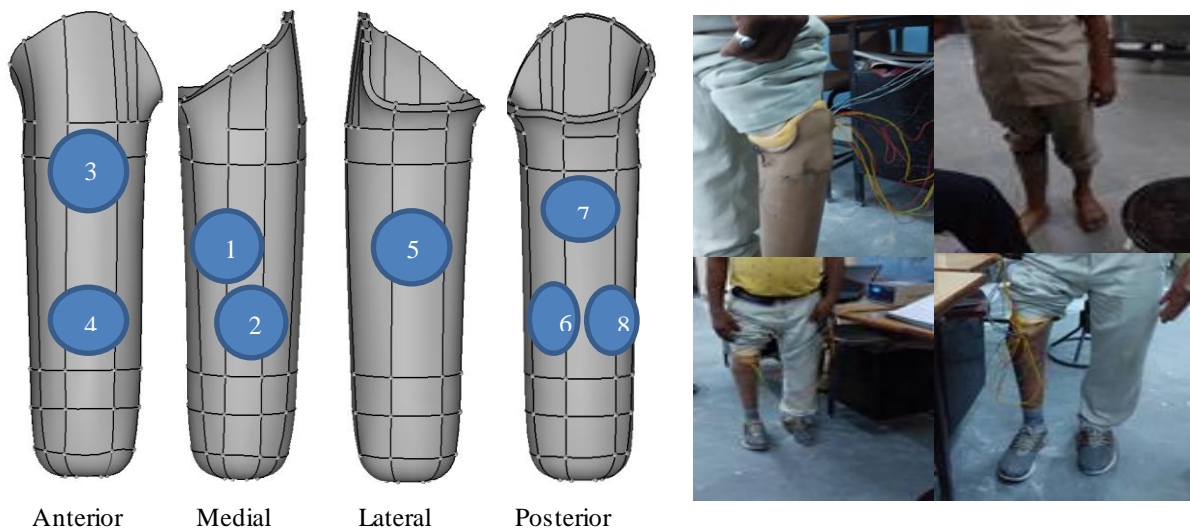
Figure-5.7: The pressure points (Left) and fitting of sensor (Right) on the limb

The measured pressure at the eight specific regions is presented in Table 5.3. For this study, three trials were performed and an average of the pressure data is selected and reported. The maximum pressure at all the three (half, full and walking) conditions are shown in bold. From Table 5.3, it was observed that the strongest impact of maximum pressure between stump-socket interfaces is on the patella tendon bearing (PTB).

Table-5.3: Static and dynamic pressure (kPa) data using Flexiforce sensor

S. No.	Patient 1			Patient 2			Patient 3			Patient 4			Patient 5			Patient 6		
	(H)	(F)	(W)	(H)	(F)	(W)	(H)	(F)	(W)	(H)	(F)	(W)	(H)	(F)	(W)	(H)	(F)	(W)
1	20	50.2	61.4	22	56	75.2	27	108.2	125.6	27.2	135.2	108	21	98.4	102	36.2	51.2	72.2
2	35	124.81	206.5	41.8	98.8	180.2	21.2	65.8	111.4	40.4	171.4	167.4	26	132	127	41.3	93.3	130.2
3	**40**	**230**	**250**	44	128	**220**	**30**	**155**	**275.2**	43	**220**	**235**	32	147.6	**262**	**43**	151.2	**241**
4	38	112.8	142	**45**	196	127.6	29.6	120	148.8	**44**	156	229.6	36	110.8	176	37.6	138	226.4
5	34	122.23	193.4	39.2	121.6	146.4	24	63	166.4	41	108	136	**39**	**196**	243	38	120	165.6
6	31	151.12	165.12	32	**200.2**	210	25	72	79.6	36	116	204	36	81.06	100	34	**167**	196
7	30	116	219.6	35.2	156	204.4	26	95.6	153.6	27	176	220.6	36	129.6	184	32	150.4	234
8	27	146.6	224	31.2	164.6	210.6	20	150.4	122	28	210.8	224.4	27	100.2	169	29	146	222.2

5.4.5   Optimization problem formulation

In the present study, the pressure at different loading condition is mathematically formulated using regression analysis technique. The developed mathematical model is optimized to predict the optimum values of weight (WT), stump length (SL) and height (HT). Regression analysis is carried out using statistical tools of Minitab 16 software, on the experimental data collected from the patients (Table 5.3). The pressure for three loading conditions was expressed as a function of WT, SL, and HT as shown in equations (1-3).

$$P \text{ (Half)} = 115.297 - 1.674(SL) - 0.761(HT) + 1.315(WT) \tag{1}$$

ANOVA table for the half load response model is tabulated in Table 5.4. The results were obtained using Minitab 16 software. The model F-value of 151.998 implies that the model is significant. There is only 0.01 % chance that such higher model F-value may have occurred due to noise. From Table 5.4, the higher value of the determination coefficient (R^2=97. 33 %) and adjusted determination coefficient (adj. R^2=94.73 %) signifies that only less than 2.67 % of the total variation is not clarified by the model. Hence this model can be used to navigate the design space.

Table-5.4: ANOVA Table for half load

Source	Degree of freedom	Sum of squares	Mean squares	F-value	P-value
Regression	3	442.893	147.631	151.998	<0.0001
Residual	2	1.939	0.969		
Total	5	444.833			
R^2 = 97.33 %			Adjusted R^2= 94.73%		

The ANOVA table for the full load response model is given in Table 5.5. The model F-value of 163.846 implies that the model is significant. There is only 0.01 % chance that such higher model F-value may have occurred due to noise. From Table 5, the higher value of the determination coefficient (R^2=99. 79 %) and adjusted determination coefficient (adj. R^2=98.98 %) signifies that only less than

0.21 % of the total variation is not clarified by the model. Hence this model can be used to navigate the design space.

P (Full) = 471.323 -1.271(SL)+1. 0265(HT)-6.361(WT)   (2)

Table-5.5: ANOVA table for full load

Source	Degree of freedom	Sum of squares	Mean squares	F-value	P-value
Regression	3	4244.231	1414.744	163.846	<0.0001
Residual	2	17.26919	8.634595		
Total	5	4261.5			
$R^2 = 99.79$			Adjusted $R^2 = 98.98$		

The ANOVA table for the walking load response model is given in Table 5.6. The model F-value of 361.573 suggests that the model is significant. There is only 0.01 % chance that such higher model F-value may have happened due to noise. From Table 6, the higher value of the determination coefficient (R^2=99. 90 %) and adjusted determination coefficient (adj. R^2=98.53 %) signifies that only less than 0.1 % of the total variation is not clarified by the model. Hence this model can be used to navigate the design space.

P(Walking) = 162.266 +5.933(SL)+1.543(HT)- 4.462(WT)   (3)

Table-5.6: ANOVA table for walking load

Source	Degree of freedom	Sum of squares	Mean squares	F-value	P-value
Regression	3	1934.433	644.8111	361.573	<0.0001
Residual	2	3.566694	1.783347		
Total	5	1938			
$R^2 = 99.90$			Adjusted $R^2 = 98.53$		

All the patients were satisfied; there were no reports on the subject, sensing abnormal pressure or any discomfort to their residual while using a prosthesis. The

stroke of the subject, measured from the data acquired while walking on the flat floor and average speed is 6.23 Sec/gait cycle.

The current study employed MATLAB R2014a optimal tool box to obtain GA result. The GA program was run using a different setting of genetic parameters to predict the value of height, stump length and weight for minimized value of the maximum and minimum pressure at eight specific regions. The parameters of GA algorithm are a number of iteration 100 population size 20. A uniform crossover scheme is used with mutation having adaptive feasibility.
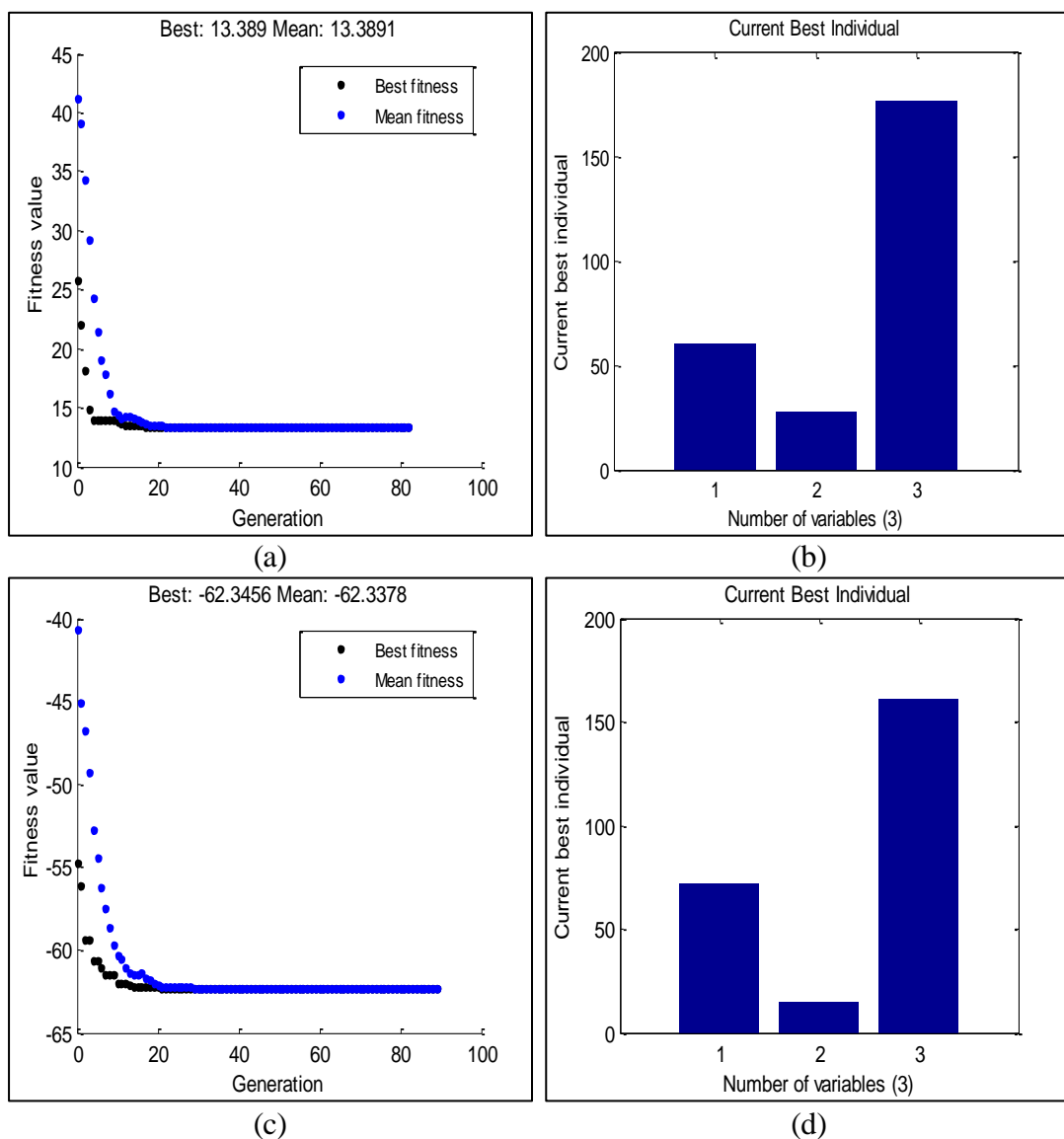
Figure 5.8: Half load condition (a) convergence plot for minimum pressure (b) best individual parameters for minimum pressure (c) Convergence plot for maximum pressure (d) best individual parameters for maximum pressure

The convergence graph of a GA algorithm for maximum and minimum pressure for half load is shown in Figure 5 (a) & (c). From the convergence plot, GA could find the minimum and maximum pressure 13.39 kpa and 62.34 kpa respectively for the half load condition. The negative sign in Figure 5 (c) shows the pressure maximization case in GA. The GA obtained a result and best individual parameters influence is presented in Figure 5 (b) & (d). From the graph, it was observed that the patient's weight plays a significant role in pressure evaluation, followed by stump length and height. The results of GA algorithm for half load are in full agreement with the experimental result performing with flexiforce pressure sensor.

(a)   (b)

(c)   (d)
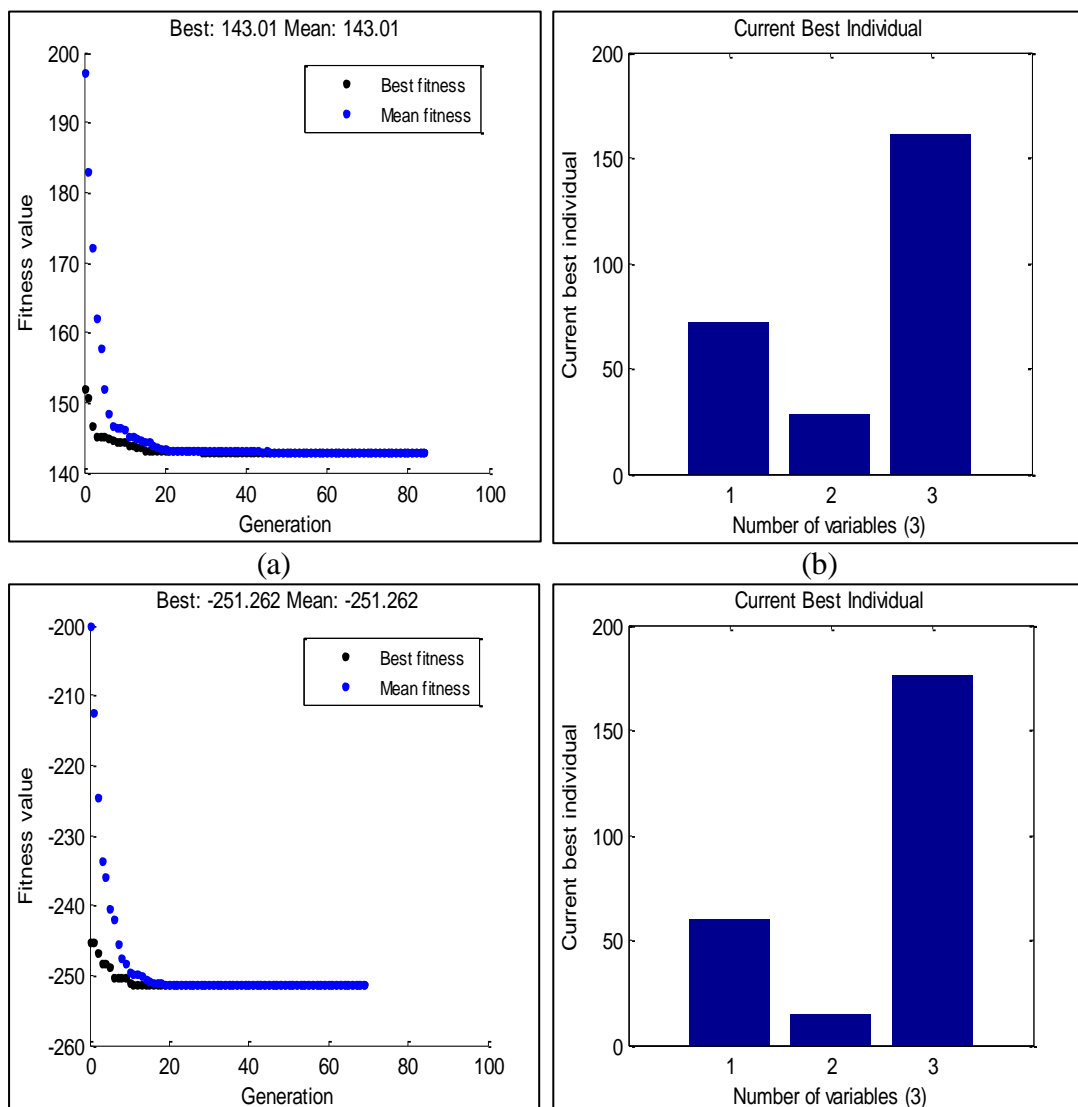
Figure 5.9: Full load condition (a) convergence plot for minimum pressure (b) best individual parameters for minimum pressure (c) Convergence plot for maximum pressure (d) best individual parameters for maximum pressure

An investigation was performed to study the effect on measured pressure for varying load conditions. The convergence plot for full loading condition using a GA algorithm for maximum and minimum pressure for full load is shown in Figure 6 (a) & (c). From the results, GA could find the minimum and maximum pressure value 143.01 kpa and 251.262 kpa respectively for the full load condition. The GA obtained a result and best individual parameters influence is presented in Figure 6 (b) & (d). The result depicted the same trend as for the half load condition and it was found that the patient's weight plays a major role in pressure evaluation, followed by stump length and height. The results of GA algorithm for full load are in full agreement with the experimental result perform with flexiforce pressure sensor.

(a)

(b)

(c)

(d)
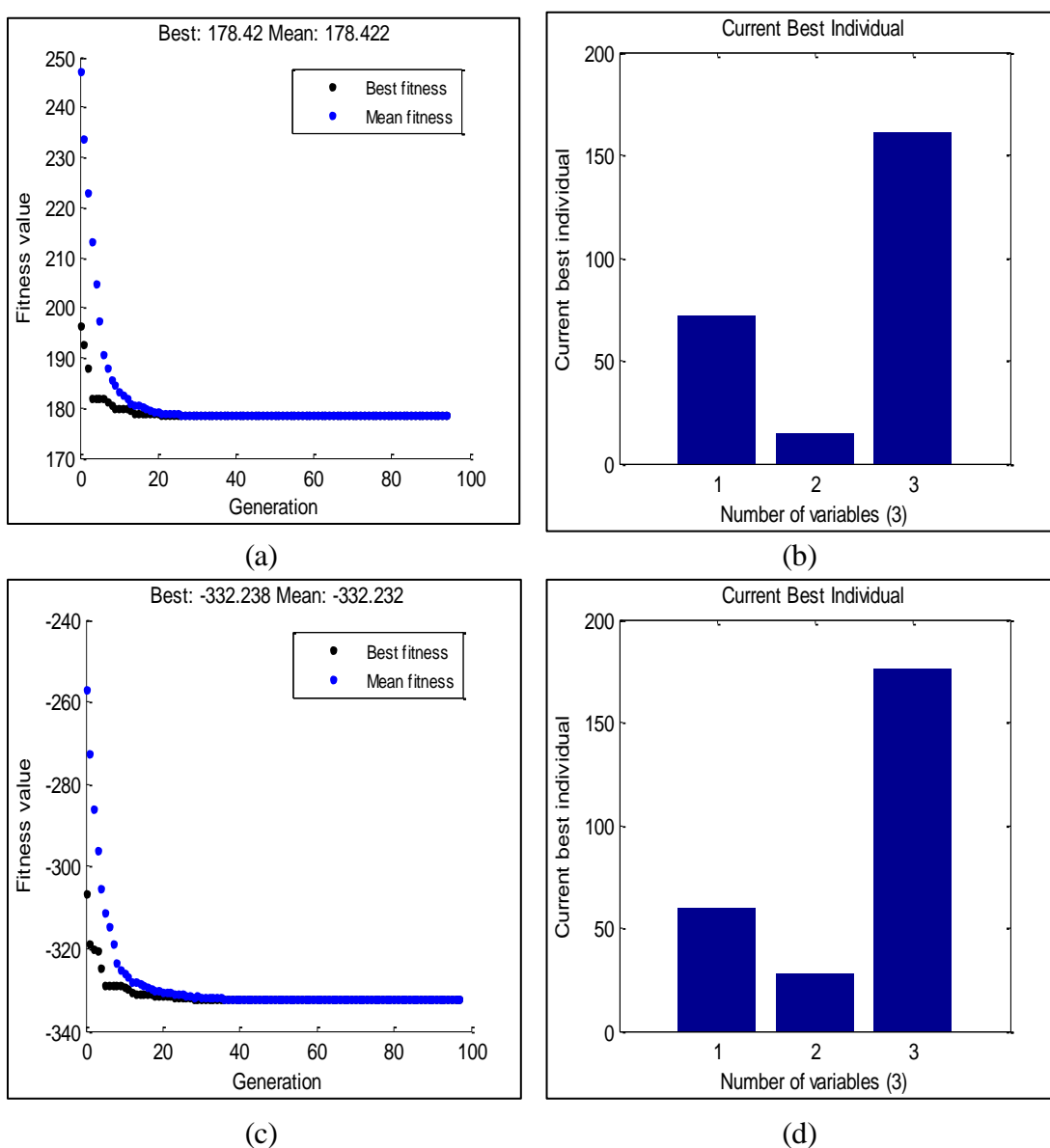
Figure 5.10: Walking load condition (a) convergence plot for minimum pressure (b) best individual parameters for minimum pressure (c) Convergence plot for maximum pressure (d) best individual parameters for maximum pressure

The last investigation was performed for the walking condition to study the effect on measured pressure. The convergence plot for walking condition using GA algorithm for maximum and minimum pressure for walking is shown in Figure 7 (a) & (c). From the graph, GA could find the minimum and maximum pressure 173.422 kpa and 332.232 kpa respectively for the full load condition. The GA obtained a result and best individual parameters influence is presented in Figure 7 (b) & (d). The result depicted same trend as for the half load condition and it was found that the patient's weight plays a major role in pressure evaluation, followed by stump length and height. The results of GA algorithm for walking load are in full agreement with the experimental result performing with flexiforce pressure sensor.

Chapter summary

Fuji film was determined to be an exact and reliable method for determining contact areas and stresses within stump socket can also be applied in the testing and modification of the lower limb prosthesis socket.

A new methodology was developed using the low-cost piezo-resistive flexiforce sensor for quantitatively analyzing the pressure distribution at eight specific regions. Six clinically significant cases were considered for pressure prediction under different loading conditions. It was found that a patient's weight plays a major role in pressure evaluation followed by stump length. The present approach significantly evaluates the pressure variation for different loading condition. The adopted methodology helps in providing pressure monitoring system for socket fitting which will help in better-designed prosthetic sockets that ensure enhanced patient satisfaction.

<div align="center">

CHAPTER 6

INVESTIGATIONS INTO EFFECT OF PHYSIOLOGICAL PARAMETERS ON SOCKET DESIGN USING ARTIFICIAL NEURAL NETWORK ANALYSIS

</div>

Introduction

       This chapter discusses a ANN based methodology to forecast the interface pressure between limb and socket under different critical region of the socket. The purpose of this chapter is to evaluate the effects of Patient-specific physiological parameters viz. height, weight, and stump length on pressure development at the transtibial prosthetic limb/socket interface. In addition, the Taguchi approach for evaluating the statistical significance of amputee's physiological parameters on the maximum pressure developed at limb/socket. The pressure data were collected by measuring the micro-strains developed at limb/socket interface for nine Patients during stance and ambulation conditions using strain gauges placed in different regions of the socket. Then, the ANN model was used to predict the maximum pressure values for Taguchi based parametric design of physiological parameters.

6.1   Evaluation Methodology

       Amali et al. (2006) developed an ANN model to evaluate the pressure distribution between the residual limb/socket for below-knee amputees. Also, for understanding the complex relation between the surface strain measured at limb/socket interface and the internal pressure exerted owing to the Patient's physiologic properties. Sewell et al. (2012) had developed an inverse problem approach for static and dynamic pressure predictions for prosthetic socket fitting assessment. They designed backpropagation ANN, which forecasts the pressure at the residual limb/socket interface utilizing the strain measurements from the socket surface.

       These studies described the pressure measurement at limb/socket interfaces, which will be help in the realization of the intricate problems confronted during a socket fitting or a new socket design. However, these studies, could not deliver

convenient clinical tools which could aid the assessment of the prosthetic socket. In addition, no prior studies available reported the relation between Patient's physiological parameters and the pressure measured at the limb/socket interface. Psychological factors are among an essential aspect, which should be taken into account while investigating lower limb prosthesis (Horgan et al. 2004). The pressure developed on the limb/socket interface during ambulation condition may be either constructive or destructive to the amputee (Neumann et al. 2004). The excess pressure at limb/socket interface can lead to soft tissue damage, skin breakdown leading to painful sores. Therefore, it is vital to understand the relation between Patient's physiological parameters and the maximum value of the pressure measured at the limb/socket interface.

Numerous studies have been reported to evaluate the pressure distribution aiming for best quality of the socket fit. The acquisition of accurate data from the pressure measurements at limb/sockets interface requires a precise measuring technology, including a suitable sensor, the positioning of sensor and data collection. To collect strain data in different condition such as "half load, full load and walking condition", nine volunteer trans-tibial amputees were investigated. The Patients (P) are selected using following clinically significant criteria: amputation due to vascular disease, trauma (P2), diabetes (P7), infection (P4), short stump (P2) and long stump (P3), conjugation (P6) and accidental causes (P1, P5, and P8). All Patients were unilateral, below-knee amputees aged between 26 to 70. They often used patellar tendon bearing (PTB) sockets with a uniform thickness of 5 mm with cotton liner. The youngest Patient (P8) was 26 years old and has been using a prosthesis 12 years, therefore walked a little quicker than others. It represents the replacement of the lost function of the ankle joint and the foot, which is essential for smooth and natural walking. Table 6.1 describes the general physiological information about the Patients.

Strain Gauges have a small patch of silicone, a metal that shows a change in their electrical resistance in response to any applied mechanical load (See Figure 6.1) (Tiwana et al. 2012 and Poeggel et al. 2015). Strain gauges are very sensitive and susceptible to moisture and variations of heat; consequently, they are over and

over again used in Wheatstone bridge configurations to overcome these issues (Stefanescu at al. 2011).
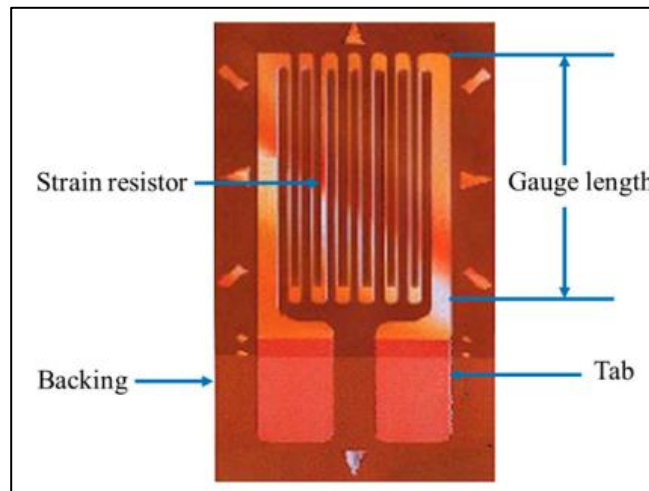
Figure-6.1: Strain gauge

Table-6.1: Physiolgical characteristics of nine male test Patients

Patient	Age (years)	Height (cm)	Weight (kg)	Time using prosthesis (years)	Type of amputee	Reason for amputation	Amputated side	Stump length (cm)
P1	30	172	66	4	Unilateral	Accident	Right	18.1 (±2. 0)
P2	42	173	70	3	Unilateral	Trauma vascular disease (Short)	Left	15 (±2. 0)
P3	36	174	72	3	Unilateral	Accident (Long)	Left	28 (±2. 0)
P4	56	171	68	10	Unilateral	Infection	Left	16 (±2. 0)
P5	70	168	63	9	Unilateral	Accident	Right	23 (±2. 0)
P6	40	166	70	21	Unilateral	Conjugation	Right	22.8 (±2. 0)
P7	46	162	63	8	Unilateral	Diabetic	Right	20.3 (±2. 0)
P8	26	168	52	12	Unilateral	Accident	Left	25 (±2. 0)
P9	50	167	64	15	Unilateral	Accident	Left	19.1 (±2. 0)

One of the major aspects in socket design is to identify the crucial locations for strain measurement. Moreover, the anatomical physiognomies of the limb play a major role in deciding the proper pressure at specific zones to cause the accurate fit

and avoid pain. In this study, eight regions that produce minimal surface distortion were considered as shown in Figure 6.2.
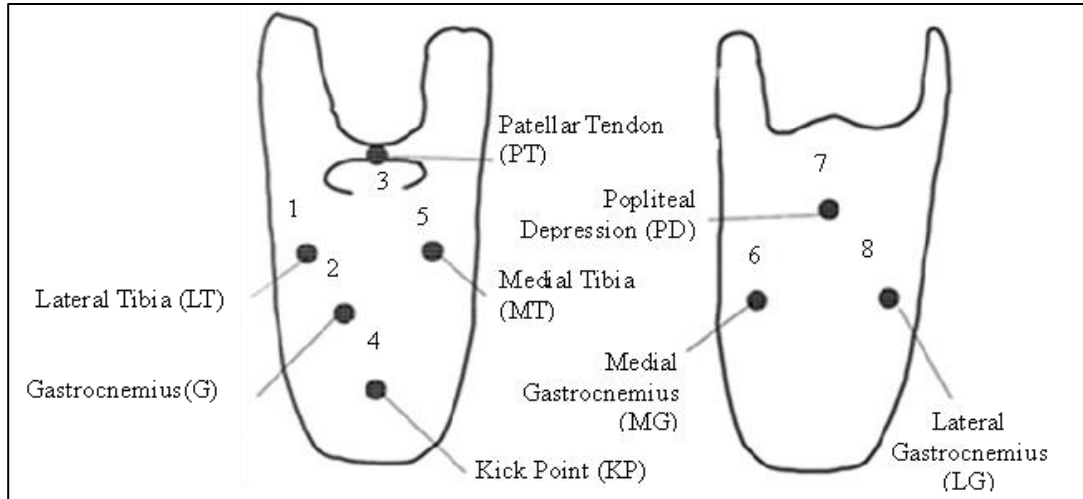
Figure-6.2: Anatomical physiognomies of the limb

To measure surface strains, a transducer is used. The transducer can measure the strain response due to internal pressure exerted owing to the Patient's physiological properties at different conditions. The accuracy and repeatability of the transducer are vital to collect reliable data. The strain measurement through the strain gauges is frequently used to monitor structures to get accurate and repeatable responses due to the loading of the component. The strain gauges offer various benefits such as generous response for a small load and do not slip when these are bonded. The output of the gauges can be caught quickly in electronic format. Therefore, the strain gauges are more suitable for this application. The specifications of the strain gauges used in this work are given in Table 6.2.

Table-6.2: Strain gauge specifications

Type	Metallic foil type strain gauge
Resistance	120 Ω
Gauge factor ranges	± 2.13
Gauge length	7 mm
Gauge width	3 mm
Reading	Displays strain as microstrain

The strain gauges are placed at eight locations which are bounded outside the socket using a glue gun. The actual instrumented photograph of the socket along with glued strain gauge in different views viz. anterior, lateral, medial, and posterior are shown in Figure 6.3. The strain gauges are then attached to the data logger to measure microstrain during stance and ambulation conditions.

| (a) Anterior | (b) Lateral |
| (c) Medial | (d) Posterior |
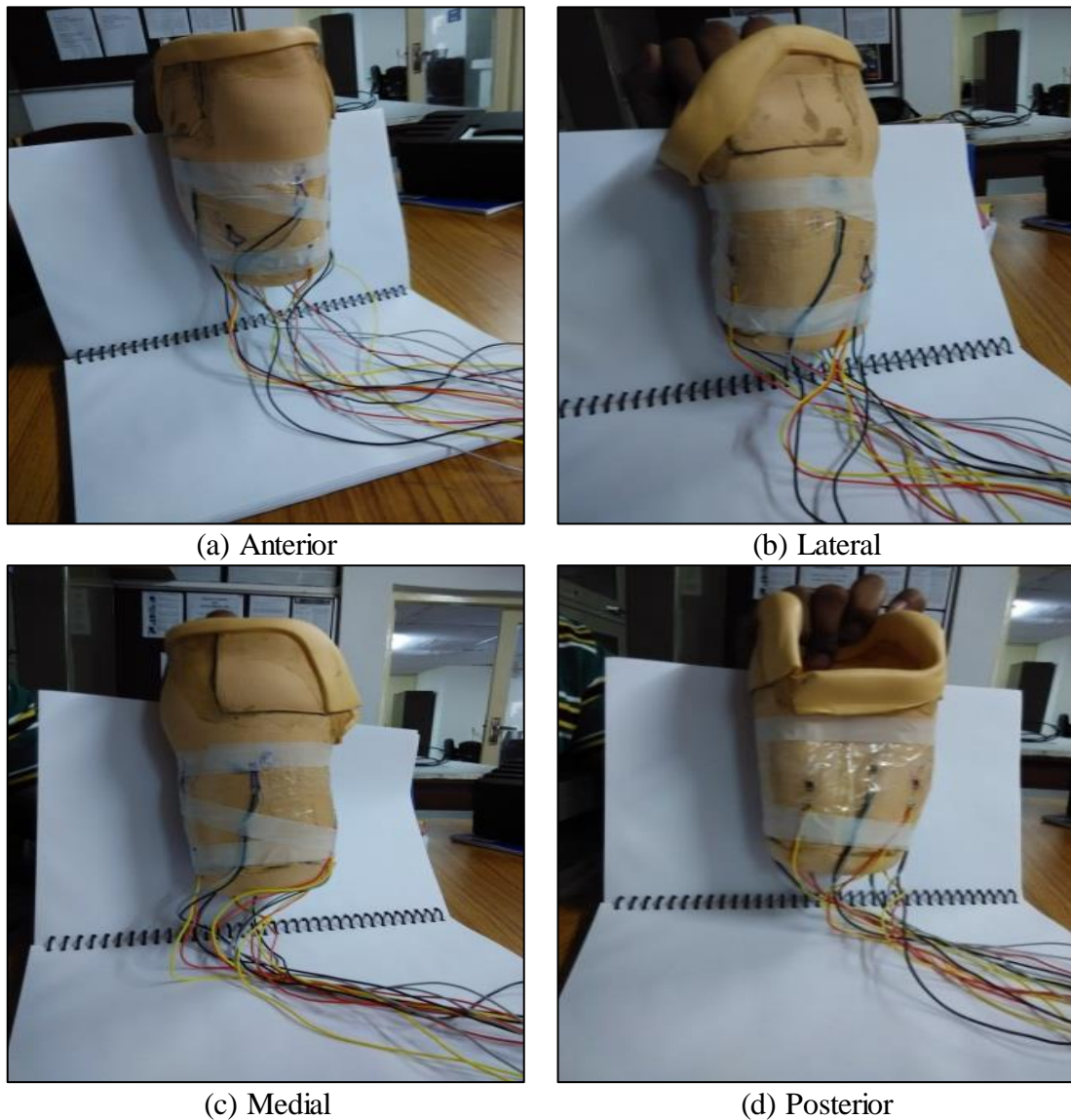
Figure-6.3: Different views of prosthesis mounted with strain gauges

6.2 Experimental Details

An eight channel strain gauge data logger is utilized to collect microstrain values at the stump/socket interface. To gather strain data at different condition, the load on the socket was varied by changing the body weight of the Patient under

different load conditions to the walking condition as shown in Figure 6.4. Figure 6.5 represents the patient with a prosthesis, instrumented strain gauges, data logger and software process readings.

| 50% | 100% Load | Walking |
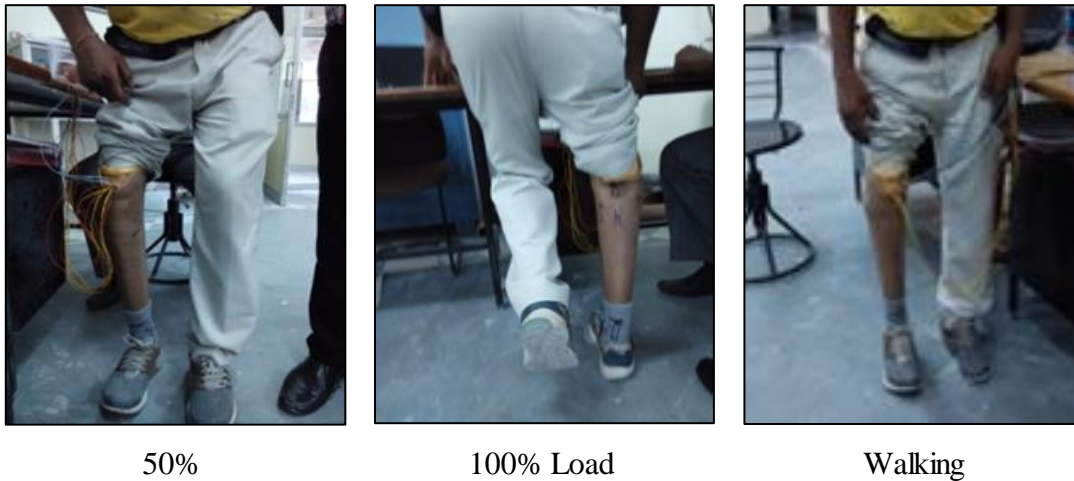
Figure-6.4: Loads to the prosthesis

Figure-6.5: Photograph of instrumentation with patient

Table-6.3: Pressure at different condition at different regions

S. No.	Patient 1				Patient 2				Patient 3			
	50% (Half)	100% (Full)	Walking	Average	50% (Half)	100% (Full)	Walking	Average	50% (Half)	100% (Full)	Walking	Average
1	24.8	58.26	73.04	52.033	52.6	110.4	92	85	43.2	47.2	43.2	44.533
2	64.8	303.08	247.1	204.993	79.2	128	135	114.067	77.6	117.6	159.2	118.133
3	205.44	324.91	346.5	292.283	142.4	197.6	220	186.667	372.8	571.2	763.2	569.067
4	177	112.8	132	140.6	126.4	160.8	176	154.4	237.6	338	526.4	367.33
5	102.5	122.23	193.4	139.4	68.8	97.6	103	21.133	48	120	145.6	104.53
6	87.34	161.15	155.72	134.737	65.6	81.04	90	78.88	116.8	233.6	296	215.467
7	118.6	216	229.8	188.13	116.8	169.6	184	156.8	124.8	210.4	264	199.73
8	55.25	186.89	233.59	158.577	47.2	68	89	68.0667	72	156	262.4	163.467
	Patient 4				Patient5				Patient 6			
1	20	68	85.6	57.867	78	128.8	37.6	81.47	35.2	147.2	108	96.8
2	48.8	104.8	199.2	117.6	27.2	56.8	102.4	62.133	106.4	198.4	198.4	167.733
3	134.4	228	223.2	195.2	178.4	195.2	375.2	249.6	216	456	529.6	400.533
4	193.6	296	157.6	86.667	69.6	120	128.8	106.1	166.4	340	259.2	255.2
5	159.2	121.6	126.4	51.467	44	63	66.4	57.8	51.2	108	136	98.4
6	120	210.4	220	183.467	32	72	73.6	59.2	101.6	216	304	207.2
7	95.2	176	234.4	168.53	42.4	85.6	93.6	73.87	77.6	176	220.8	10.933
8	87.2	169.6	221.6	159.467	103.2	150.4	112	121.87	108.8	260.8	294.4	221.333
	Patient 7				Patient 8				Patient 9			
1	31.2	58.4	25.6	38.4	25.6	32	32	29.867	35.3	50.6	98.1	61.33
2	68	110.4	44.8	74.4	84	98.4	67.2	83.2	65	116	146	109
3	144	197.6	160.8	167.467	111.2	167.2	112.8	130.4	143	196.2	265.1	201.45
4	153	184.8	57.6	131.8	90.4	121.6	60	90.667	120	163	240.1	174.33
5	43.2	72.8	40.8	52.267	41.6	35.2	38.4	38.4	77.5	159.6	199	145.33
6	47.2	77.6	111.2	78.6667	84	68.8	56	69.6	68	131	182	127
7	55.2	100	42.4	65.867	58.4	61.6	41.68	26.107	79	137	197	137.67
8	134.4	161.6	106.4	134.133	95.2	109.6	77.72	94.1733	61	114	173	116
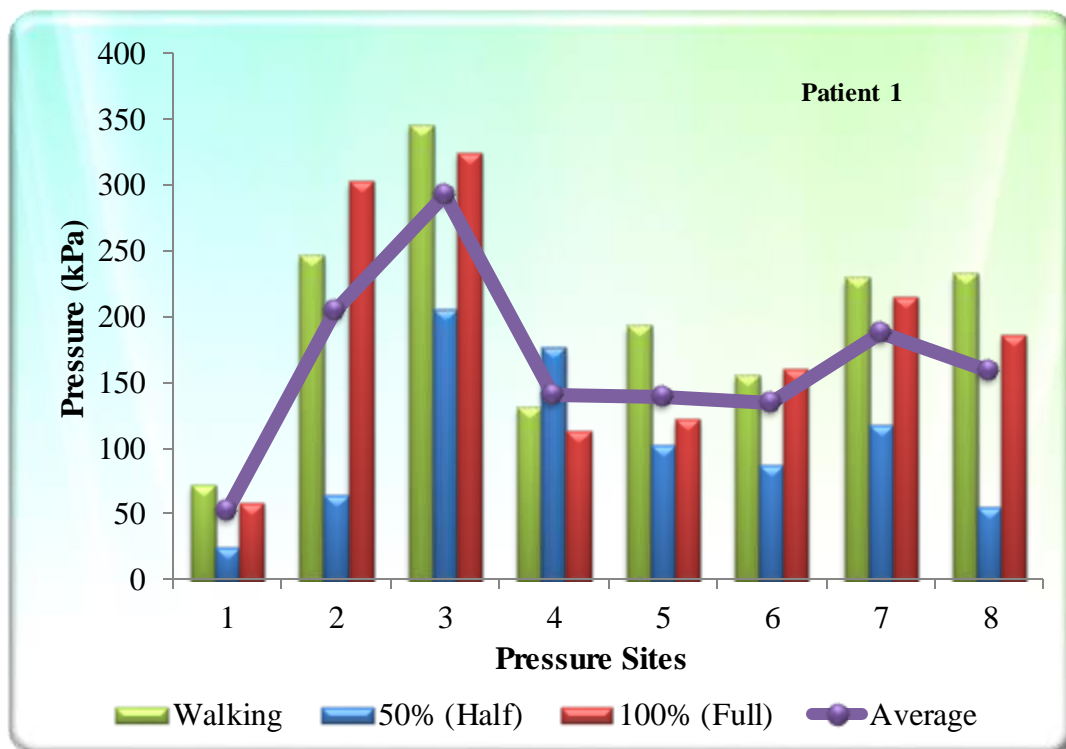
Figure-6.6 (a): Graphical representation of pressure measurement at critical region for patient 1
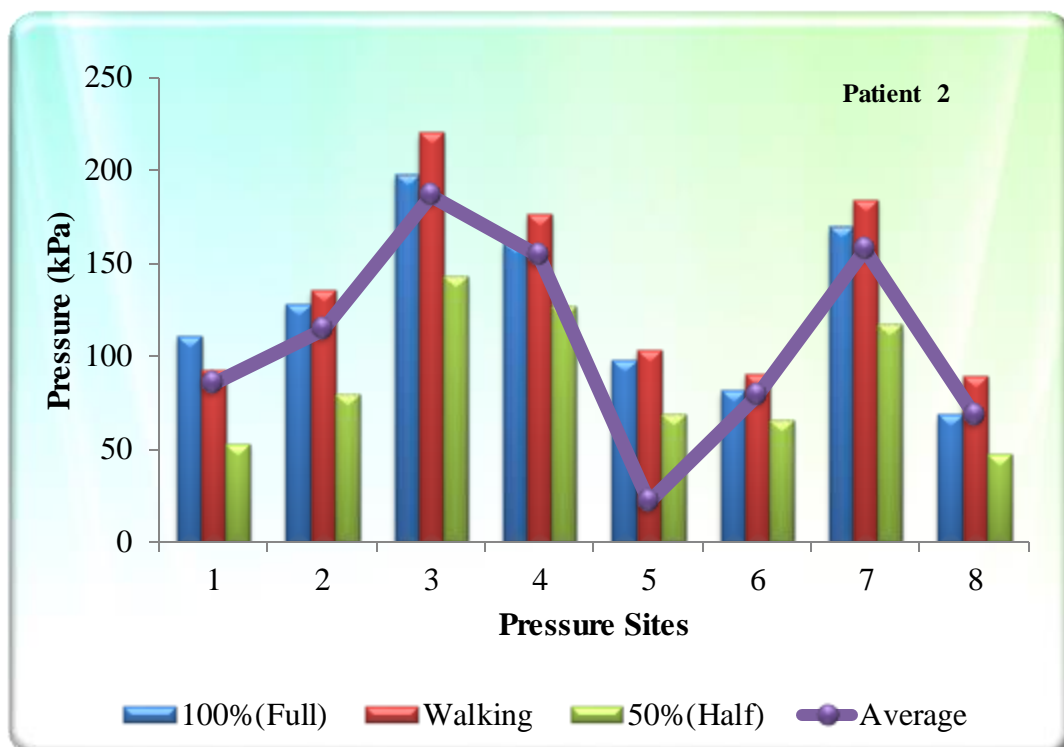
Figure-6.6 (b): Graphical representation of pressure measurement at critical region for patient 2
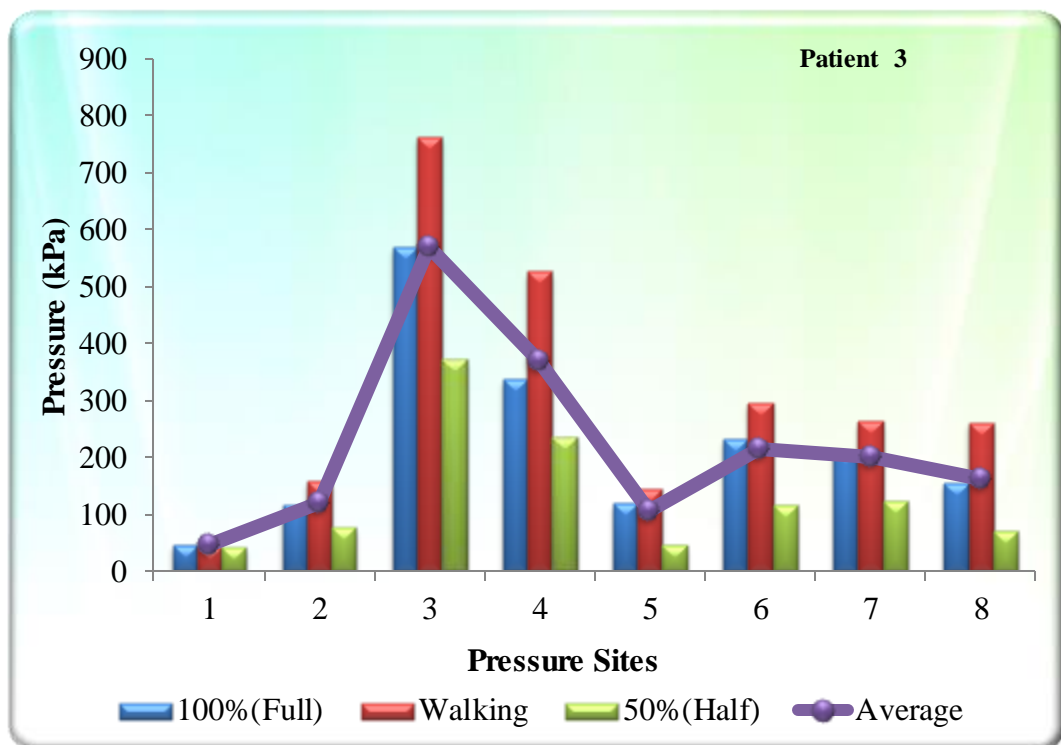
Figure-6.6 (c): Graphical representation of pressure measurement at critical region for patient 3
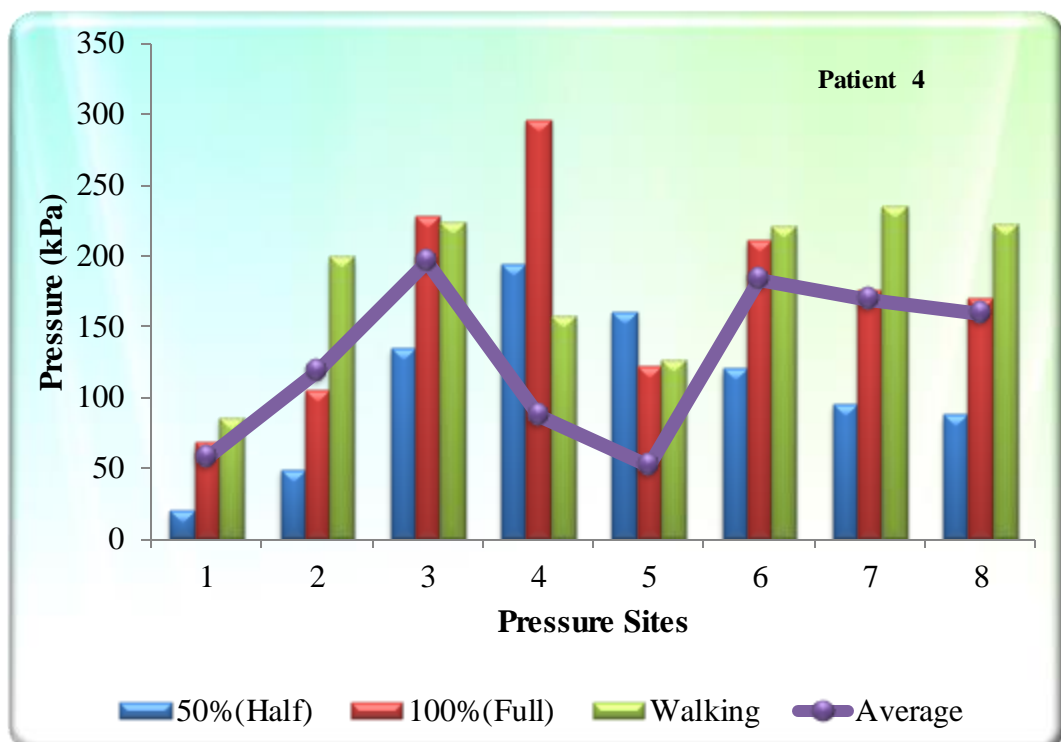
Figure-6.6 (d): Graphical representation of pressure measurement at critical region for patient 4
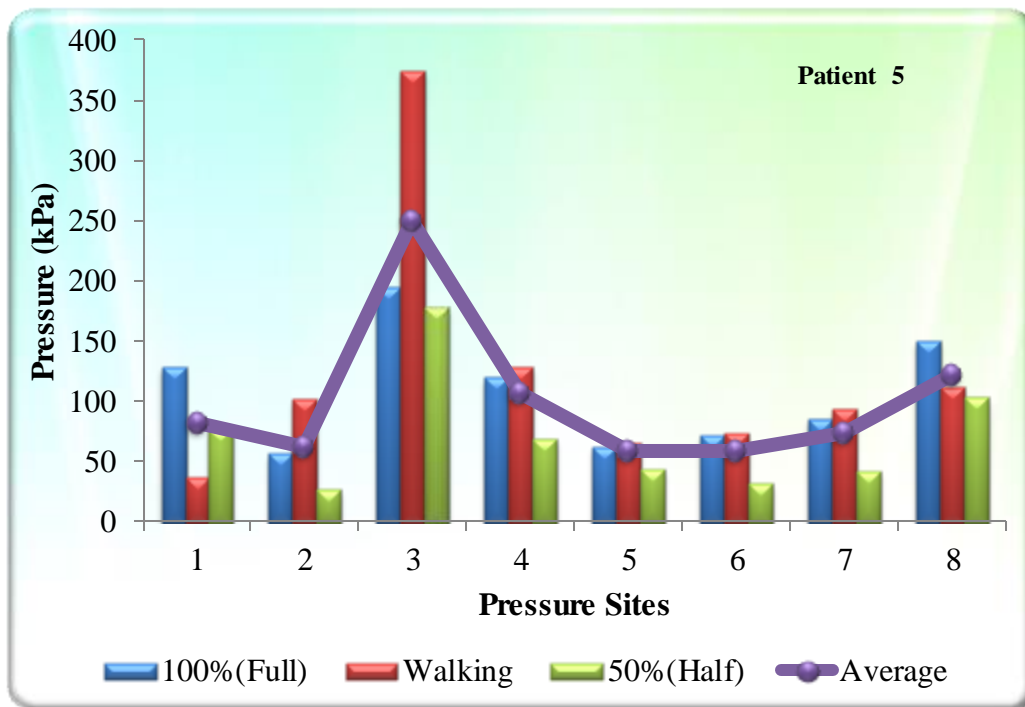
Figure-6.6 (e): Graphical representation of pressure measurement at critical region for patient 5
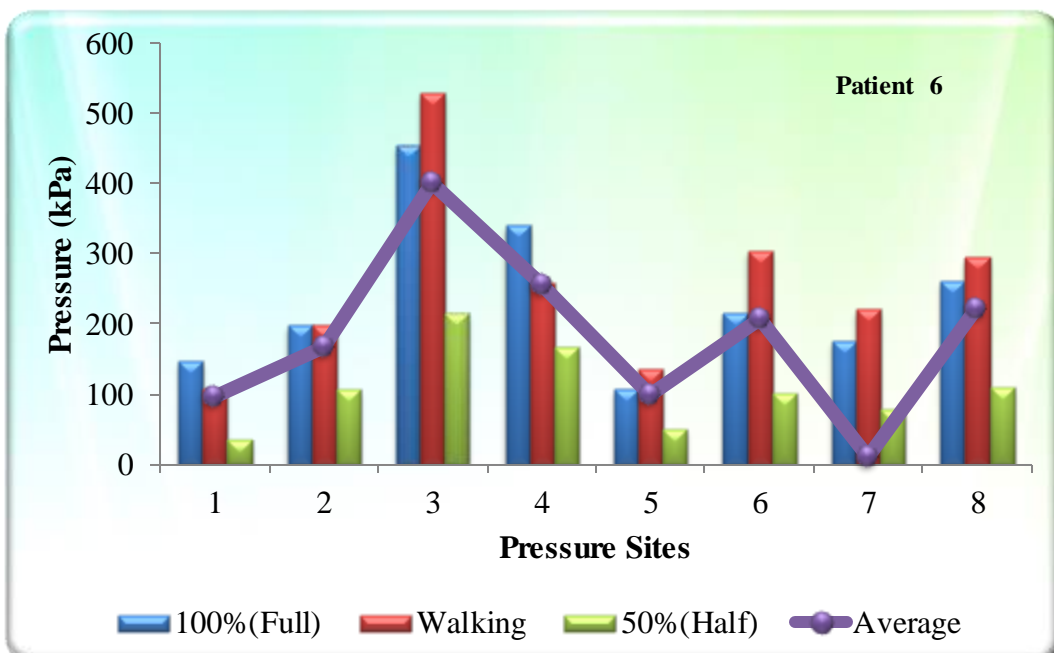
Figure-6.6 (f): Graphical representation of pressure measurement at critical region for patient 6
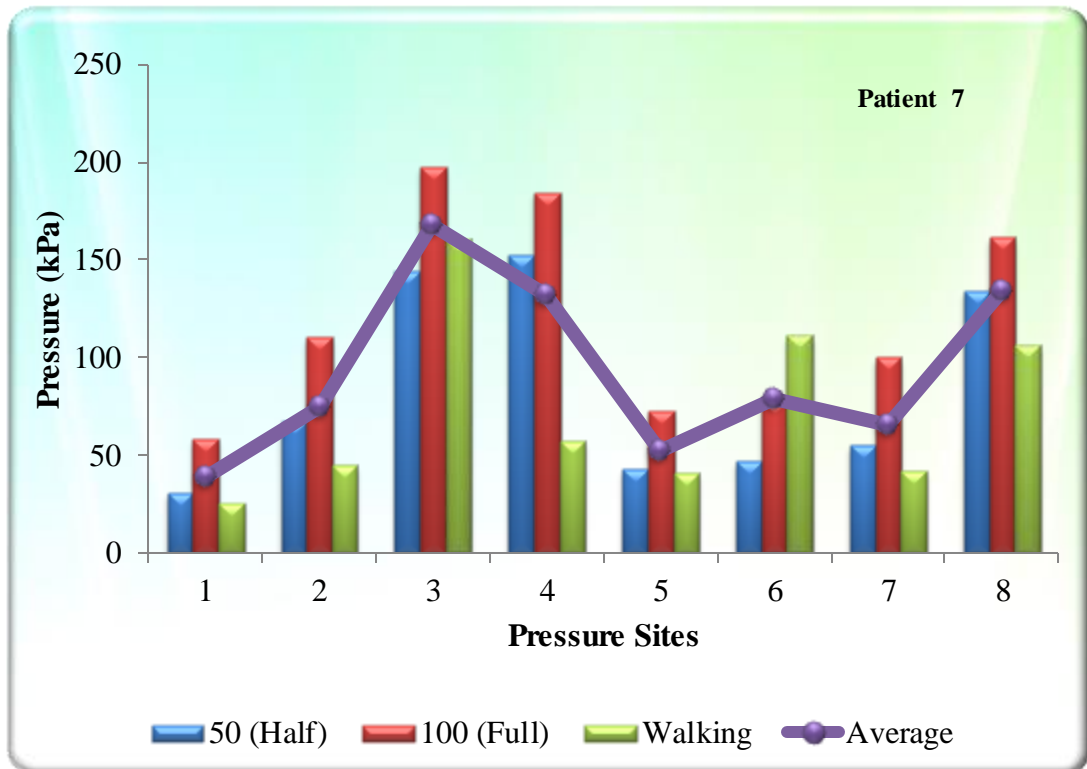
Figure-6.6 (g): Graphical representation of pressure measurement at critical region for patient 7
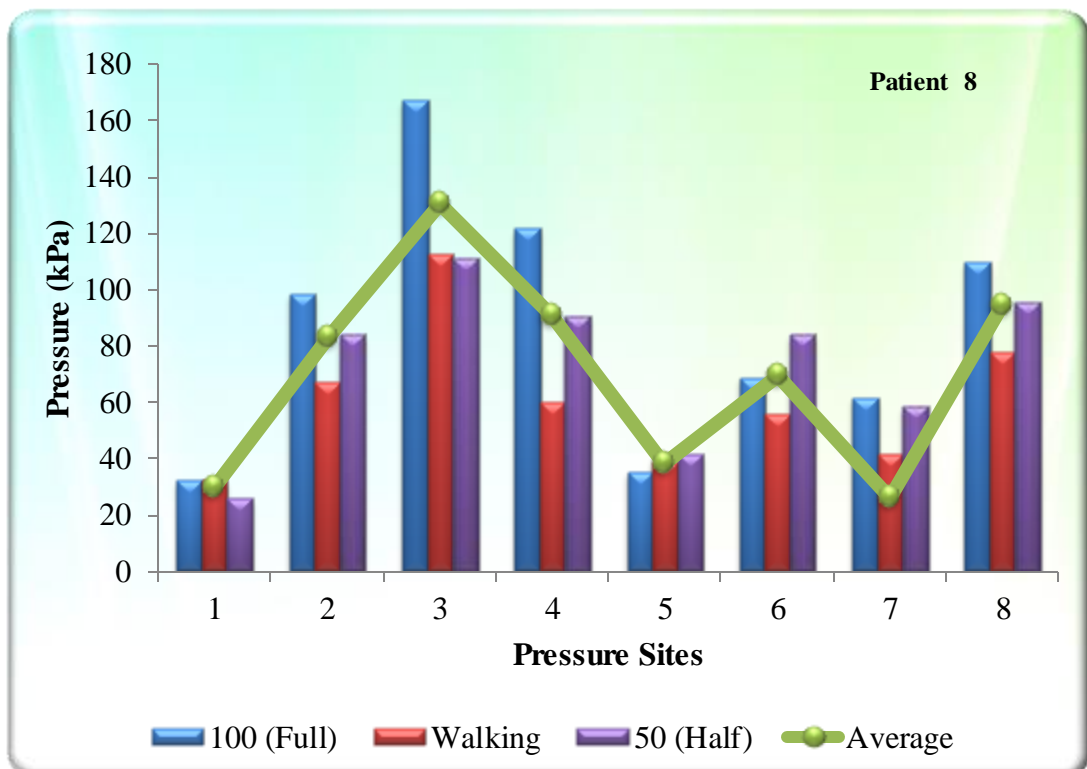
Figure-6.6 (h): Graphical representation of pressure measurement at critical region for patient 8
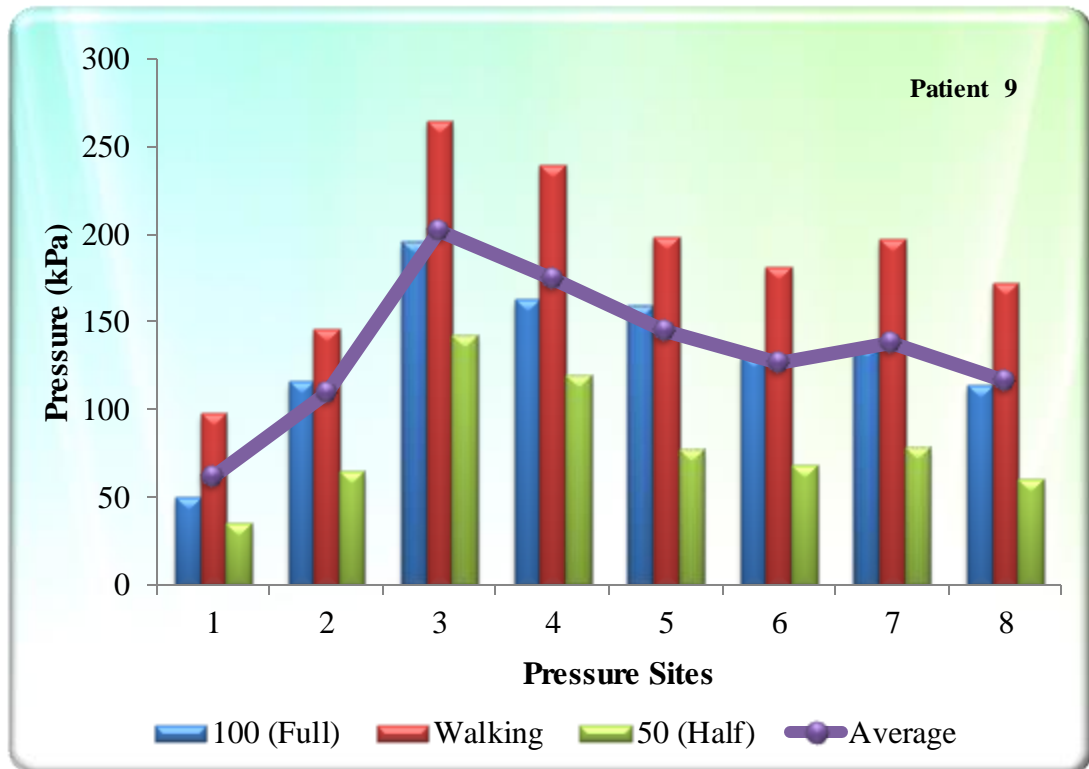
Figure-6.6 (i): Graphical representation of pressure measurement at critical region for patient 9

The zero load condition is defined at which Patient lifts his prosthesis above the ground. Then, the Patient was requested to introduce different load conditions of prosthesis viz. 50% load, full load and walking load as shown in Table 6.3 with pictorial representation in Figure 6.6 (a-i). The strain was measured at different conditions and stated above and subsequently processed to calculate the pressure values using the following formula.

$$E = \frac{\sigma}{\varepsilon}$$

Where,

E= Young modulus of material (Silicon rubber)

σ= stress

ε=Strain

The pressure values at 50%, 100%, walking load conditions were calculated using equation (1) and the average value of pressure is listed in Table 6.4. It has been noted that the zone three i.e. patellar tendon had maximum pressure developed

out of considered eight regions due to interfacial load produced during different conditions. The previous studies also found the similar observation regarding the pressure generated at limb/socket interface is maximum at patella tendon region.

Table-6.4: Pressure values computed from strain-data logger system at different regions

S. No.	Maximum Pressure value for different Patients								
	P1	**P2**	**P3**	**P4**	**P5**	**P6**	**P7**	**P8**	**P9**
1	52.03	85.00	44.53	57.87	81.47	96.80	38.40	29.87	61.33
2	204.99	114.07	118.13	117.60	62.13	167.73	74.40	83.20	109.00
3	242.28*	246.67*	569.07*	215.73*	249.60*	400.53*	167.47*	130.40*	201.45*
4	140.60	154.40	367.33	86.67	106.10	255.20	131.80	90.67	174.33
5	139.40	21.13	104.53	51.47	57.80	98.40	52.27	38.40	145.33
6	134.74	78.88	215.47	183.47	59.20	207.20	78.67	69.60	127.00
7	188.13	156.80	199.73	168.53	73.87	10.93	65.87	26.11	137.67
8	158.58	68.07	163.47	159.47	121.87	221.33	134.13	94.17	116.00

6.3   Artificial Neural Networks

Artificial neural network (ANN) is an advanced simulation method that involves a database training to predict response exactly from a set of inputs. This technique is an iterative process and used to solve complex, non-linear problems because it can emulate the learning ability of human beings. The main benefit of the ANN approach over conventional regression analysis is that the network makes a solution without the need to designate the relations between variables. The artificial neural network is constructed of numerous cross-linked simple processing units called neurons. A neuron collects various input signals, but it delivers only one output signal at a time.

The neural network is an excellent parallel distributed processing technique involving prominently interrelated neural computing elements which have the ability to learn, acquire information, and make it available for use. ANN has been extensively used to describe complex functions in various applications. It effectively

implemented in biomedical engineering and applications, explaining numerous problems in areas of lower limb prosthetic, clinical outcomes, signal processing, medical diagnosis and health care. ANN has been a widely used modeling tool for unknown or semi-unknown processes.

In the present analysis, height, weight, and stump length are taken as the three input parameters. Each of these parameters is categorized by one neuron and therefore the input layer in the ANN structure has three neurons. The database is constructed considering experiments at the limit ranges of each parameter. Experimental result sets are used to train the ANN to understand the input-output correlations. The database is then divided into three types, namely: (i) a training category, which is exclusively used to adjust the network weights and (ii) a test category, which corresponds to the set that validates the results of the training protocol. Generally, seventy-five percent data (patterns) is used for training and twenty-five percent for testing

Table-6.5: Data for ANN training

Patient	Height (cm)	Weight (Kg)	Stump Length (cm)	Max. Pressure (unit)
P1	172	66	18.1	242.28
P2	173	70	15	246.67
P3	174	72	28	569.07
P4	171	68	16	215.73
P5	168	63	23	249.60
P6	166	70	22.8	400.53
P7	162	63	20.3	167.47
P8	168	52	25	130.40
P9	167	64	19	201.45

The actual measured pressure data on transtibial prosthetic sockets was used to develop the ANN model. ANN model is established, which is used for interpolation of the incomplete pressure data set that was available for the analysis.

The experimentally measured maximum pressure values on transtibial prosthetic sockets for different Patients based on their physiological parameters (Table 6.5) were used in ANN modeling. The developed ANN model can be used to predict the maximum pressure in relevance to Patient's physiological parameters useful for the statistical analysis.

The data shown in Table 6.5 was used to train the back propagation feed forward ANN model. The feed forward neural network is built on various interconnected artificial neurons, classified into the input, hidden, and output layers. The information is accessible by the interconnected weights that can be altered in learning phase. The output of neuron at any layer is calculated by

$$Y_j = f \sum_{i=1}^{n} w_{ij} x_i + \Theta_j \quad \dots (2)$$

Where,

Y_j = final output from j^{th} neuron

f = tansig activation function

n = number of neurons in the previous layer

w_{ij} = synaptic weight between i^{th} and j^{th} neuron

x_i = output from i^{th} neuron

Θ_j = bias at j^{th} neuron

In back-propagation technique, an input is generated by the neural networks to compute the output of individual neurons. The output was calculated as an error between the anticipated output, T_j, and the actual output, Y_j. By the least squares method, the quadratic error function (E_j) among the actual output and the network output is computed by the following equation.

$$E_j = 0.5 \sum_j (T_j - Y_j)^2 \quad \dots (3)$$

The gradient search algorithm was used for minimizing the mean square error of network output. The mean square is computed using the formula

$$MSE = \frac{1}{n}\frac{1}{m} \sum_{i=1}^{n} \sum_{j=1}^{m} 0.5(T_j - Y_j)^2 \quad \dots (4)$$

Where, T_j is the target output of the jth neuron, Y_j is the predicted value of the jth neuron, n is the total number of training pattern, and m is the number of output nodes.

In the developed ANN architecture, the height, weight, and stump length are selected as input neurons, while the maximum pressure is selected as output neuron. The training of the network was done using Levenberg–Marquardt (LM) backpropagation neural network (BPNN) algorithm for fast supervised learning and 70% of data have been used for training, whereas 15% of data were used for testing and 15% for validating each. The other parameters used while training the network where the learning rate μ=0. 0001, Marquardt adjustment parameter Mu=0. 05, eopse to train=1000, goal= 0.0001. The ANN architecture was selected based on the performance of the ANN model by changing the number of neurons in the single hidden layer from 1 to 10 and performance of the network is plotted in Figure 6.7. It was observed from Figure 5.6 that the lowermost MSE (0.0325) is achieved with eight neurons in a hidden layer. Therefore, three-layer neural network architecture with back propagation algorithm was chosen have an input layer (I) with three input nodes, a hidden layer (H) with eight neurons and an output layer (O) with one output node hired for this study is shown in Figure 6.8.
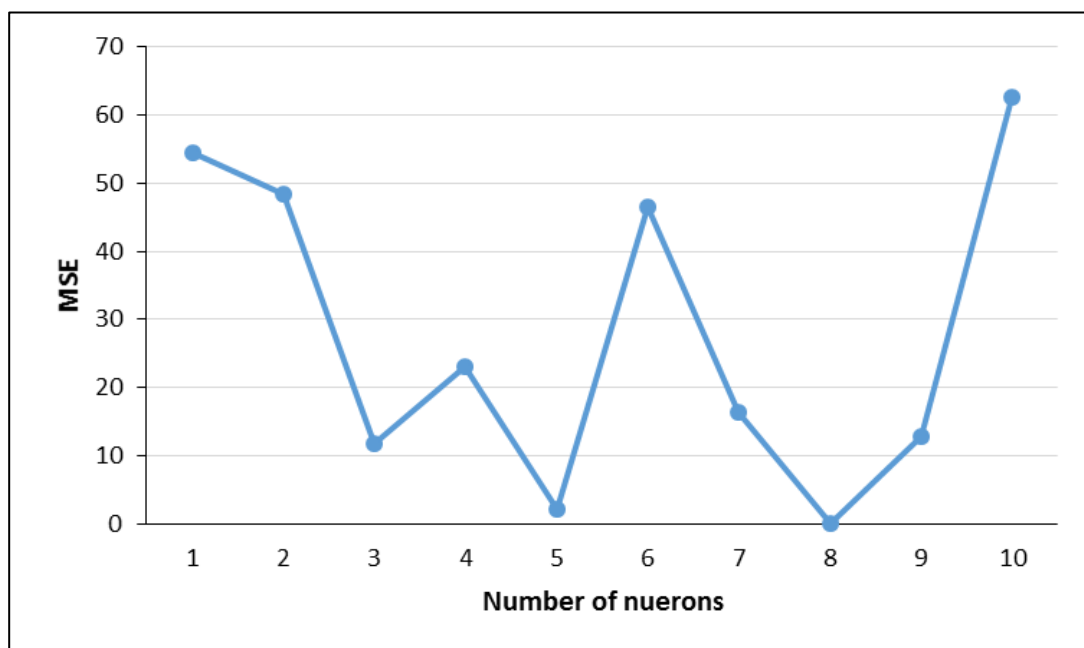
Figure-6.7: Performance of network with varying number of neurons
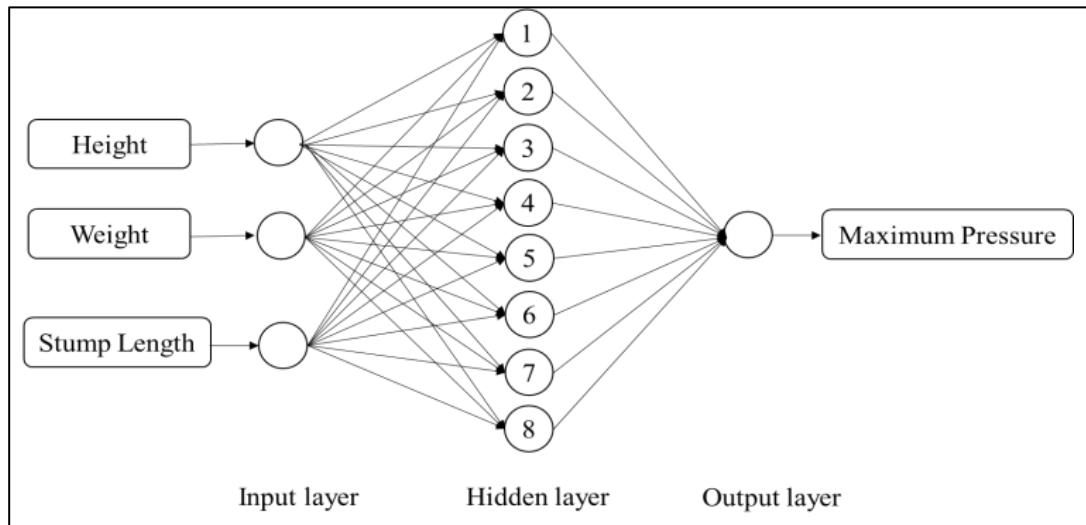
Figure-6.8: ANN 3-8-1 architecture

To check the prediction capability of the developed ANN model, the maximum pressure data for three different Patients were collected and compared with the ANN predicted pressure values. The comparison of ANN predicted and actual measured values as shown in Table 6.6. It was perceived that the established ANN model has a superb ability to forecast maximum pressure developed at a limb/socket interface. The average absolute percentage error of 4.62% and maximum absolute error 6.00% found in ANN prediction as compared to actual measured values, both of which are well within the tolerable limits. Therefore, the developed ANN model is reliable enough to use for the prediction of maximum pressure values based on physiological parameters.

Table-6.6: Comparison of actual measured and ANN predicted values

Patient's Physiological parameters				Maximum pressure at limb-socket interface		
Sr. No	Patient No.	Height	Weight	Stump length	Actual measured	ANN predicted	Absolute % error
1	S10	163	65	19	186.65	175.44	6.00
2	S11	165	66	18.2	279.54	265.30	5.09
3	S12	170	69	23	351.69	361.51	2.79

Table-6.7: Physiological parametric design and predicted pressure values

Trial	Height (cm)	Weight (Kg)	Stump Length (cm)	Max. Pressure (unit)	Calculated S/N ratio
1	162	50	15	242.28	42.30
2	162	62	21	246.67	42.85
3	162	74	27	569.07	55.07
4	168	50	21	215.73	42.30
5	168	62	27	249.60	47.16
6	168	74	15	400.53	54.23
7	172	50	27	167.47	43.25
8	172	62	15	130.40	44.27
9	172	74	21	201.45	55.10

6.4   Taguchi Experimental Analysis

The Taguchi technique is a powerful tool for modeling and analyzing the impact of control factors on performance output which works on the orthogonal array. It is commonly adopted as a method for optimizing design parameters because it is simple, efficient, and systematic. The method is initially projected as a means of refining the quality of products through the application of statistical and engineering concepts. Since experimental techniques are usually costly, complex, time-consuming, and difficult to accomplish real experiments with entire accuracy.

An orthogonal array was obtained by using Taguchi method to consider the effect of various factors on the target value and defines the plan of experiments. The Taguchi design of experiments techniques has been used to evaluate the effects of Patient's physiological parameters like height, weight and stump length on the maximum pressure at transtibial prosthetic limb/socket interface. The Taguchi L9 orthogonal array has been used to design the experiments. The Taguchi technique employs orthogonal arrays in experimental design to analyze a large number of parameters using a small number of experiments. Moreover, the deductions withdrawn based on a small number of experiments are valid through the complete experimental region covered by the parameters and their levels.

Therefore, the Taguchi L9 orthogonal array was nominated to investigate the effects of Patient's physiological parameters on the amount of pressure developed at transtibial prosthetic limb/socket interface. The developed ANN model was used to predict the maximum pressure values for different parametric settings based on Taguchi L9 matrices. Table 6.7 shows the trials along with corresponding parametric settings and ANN predicted maximum pressure values for the corresponding trial. The S/N ratio considers both the mean and the variability into account. It is the ratio of the mean (signal) to the standard deviation (noise). The ratio depends on the quality characteristics of the product/process to be optimized.

The Taguchi method can be classified as three types of S/N ratios are used for different characteristic: lower-the-better (LB), higher-the-better (HB) and nominal-the-best (NB). The experimental observations are transformed into a signal-to-noise (S/N) ratio. There are several S/N ratios available depending on the type of characteristics. Since the lowest maximum pressure developed on the transtibial prosthetic socket signifies the better conditions, the smaller, the better S/N ratio is used and can be calculated as logarithmic transformation with the following equation:

$$\eta = -10 \, \mathrm{Log}\left(\sum \frac{y^2}{n}\right) \dots \dots (5)$$

Where y is the value of the maximum pressure predicted by ANN, and n is the number of the trials.
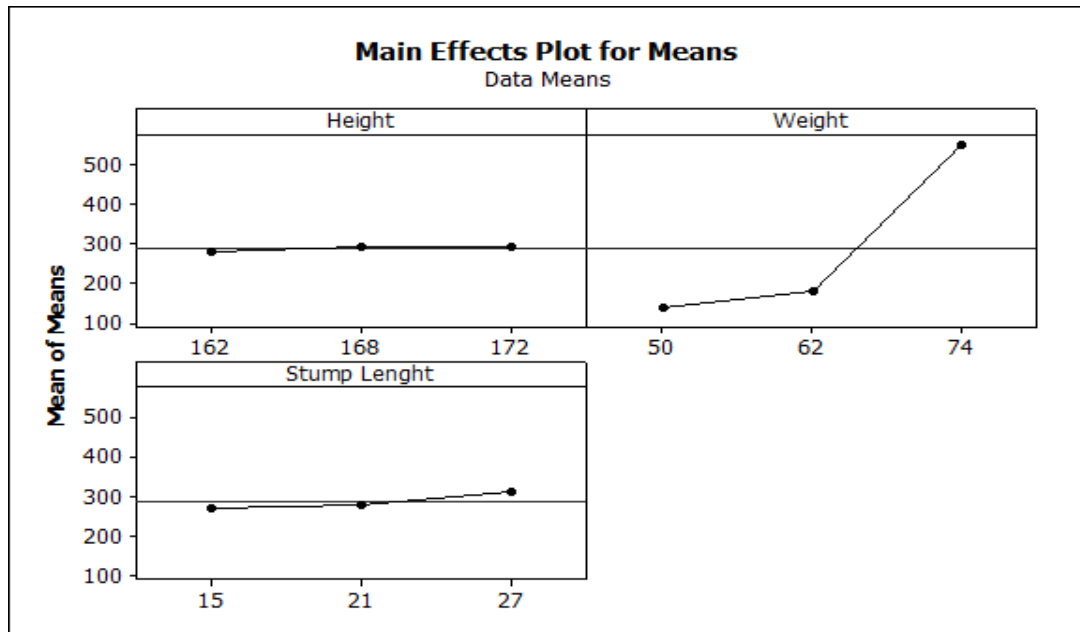
Figure-6.9: Effect of physiological parameters on maximum pressure at limb/socket interface

Figure 6.9 shows, the effects of Patient's physiological parameters on the maximum pressure developed at transtibial prosthetic limb/socket interface. It can be clearly observed that the weight of the Patient is a vital parameter that decides the amount of pressure at transtibial prosthetic limb/socket interface. The pressure has been generated at a limb/socket interface with the increases of weight. The stump length also observed to be an important parameter deciding the maximum pressure value. The pressure has developed at transtibial prosthetic limb/socket interface increases linearly with increase in stump length. However, the height of patient observed to be having the nonsignificant effect of pressure.

Table-6.8: The results of ANOVA performed at the 95% confidence level

Parameter	DOF	Sum of Squares	Mean Square	F-value	P-value	Percentage contribution
Height	2	348	174	0.13	0.887	0.108
Weight	2	313101	156551	114.22	0.009	98.035
Stump Length	2	3187	1593	1.16	0.462	1.00
Error	2	2741	1371			
Total	8	319377				
Standard Deviation=37.022		R^2=99. 14		$R^2_{adjusted}$= 96.57		

The relative significance of Patient's physiological parameters on the maximum pressure at limb/socket interface was examined by ANOVA. The results of ANOVA at 95% confidence level for Patient's physiological parameters are presented in Table 6.8. The p-value less than 0.5 directs the parameters which have a significant effect on response and therefore, the weight and stump length are found to be significant parameters. From ANOVA, the Patient's weight was seen to be most important parameters which play a vital role in deciding the amount of pressure developed at transtibial prosthetic limb/socket interface. The weight contributes 98.035% on pressure generated followed by stump length, which contributes 1.00%. The stump height was observed to be a not significant parameter for pressure distribution. The large value of the determination coefficient (R^2=99. 14%) indicates that only less than 0.86 % of the total variations in pressure experienced by the transtibial prosthetic socket are not clarified by model. The large value of the adjusted determination coefficient ($R^2_{adjusted}$=96. 57%) promises significance of the model.

6.6   Chapter summary

The following vital conclusions were drawn:

- For all Patients, it was observed that the patellar tendon region experiences maximum pressure.

- The ANN model with 3-8-1 architecture was observed to be the best model to predict the maximum pressure value with the mean square error 0.0325.

- The ANN model was found to be reliable in predicting maximum pressure values with an average absolute percentage error of 4.62% and maximum absolute percentage error of 6.00%.

- The Taguchi analysis indicates that the maximum pressure value increases with an increase in the weight of the Patient significantly.

- The results of ANOVA suggest that the weight, and stump length affects significantly on deciding the maximum pressure values each contributing 98.035% and 1.0% significantly.

CHAPTER 7
ADDITIVE MANUFACTURING OF SOCKET BASED ON TOPOLOGY OPTIMIZATION

Introduction

This chapter presents the topology optimization based additive manufacturing of prosthetic socket to minimize the structural weight to the compliance of the prosthetic socket. In the first part CAD model of the socket obtained through reverse engineering procedures explained in chapter 3 is used for generating the meshed model of the socket. Further, based on the inputs from the ANN and optimization model discussed in chapter 6, Topology optimization was performed on the meshed model to generate the compliant socket. Finally, the resulting topology optimized socket was fabricated using an FDM-based Additive Manufacturing machine. The steps and procedure and discussed in this chapter.

7.1   Design optimization

For successful rehabilitation of lower limb amputees, a well-designed, flexible and better fit prosthetic socket is mandatory. The socket is an important part of below knee prosthesis which defines the comfort level in the patients. The socket provides the interface between the prosthesis and residual limb, and its design influences the prosthetic fit affecting cost, comfort, energy expenditure, and eventually helps during patient ambulation period. Several studies have been reported which suggests that the attainment of these goals presents a challenge to the prosthesis practitioners. The primary concern for the patient discomfort and pain is the presence of high contact pressure at different specific regions of the residual limb. The contact pressure at these regions can be as high as 1000 KPa (Sewell et al., 2012), adversely affecting patient recovery and poses serious health issues like cancer. Therefore, it becomes primarily important to relieving such high pressure from sensitive regions, providing patient satisfaction and comfort. One promising solution to this problem is by reducing the stiffness of the socket and redistribution of pressure by making a socket walls complaint at these high-pressure areas. Some of the previous

approaches provided local compliance (concentric spiral slots) by realizing a socket wall thickness reduction. However, it was found that the results are not good enough for relieving high pressure from sensitive areas.

The present work deals with introducing the concept of topology optimization (TO) in the field of the prosthetic socket for effective pressure reduction, better socket fitting and patient comfort. TO method can produce an optimum material distribution that optimizes some specific performance criteria specified by the part designer, even when an initial design concept is lacking. TO can be referred to as structural technique which combines with a numerical solution method (i.e. the finite element method) for optimal mass distribution in a given domain. It helps in describing the regions where the material is needed and where voids are needed. This method has the capability to direct and elucidate in which places skeletal materials are required to endure the expected loads (e.g., for mastication) and also for soft tissue support structures. Due to this, TO allows for greater design freedom than only shape and size optimization (see Figure 7.1).
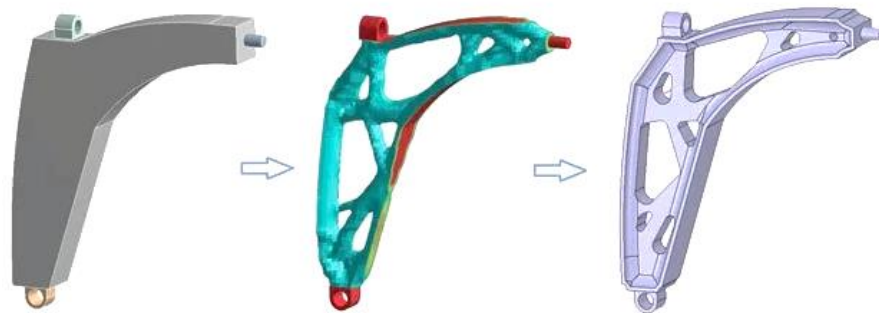
Figure-7.1: Topology optimization of automobile upper control arm

Since its inception in the late 1980s, TO is widely used in designing industrial components and has become an area of active research. The first solutions to a topology optimization problem were provided by Michell. For cases of simple loading and boundary conditions, he provided optimal topologies for truss-like structures. Earlier, this concept was used only for mechanical structural problems, but now it has gained wide acceptance among other disciplines as well. The application areas in which TO have been used includes automobile, aircraft,

implants, fluid flow and acoustics. Such development is due to the evolution of some conventional topology optimization techniques and new advanced promising methods.

There are different methods available for topology optimization: (1) density based methods (2) Hard kill methods (3) Boundary-variation methods (4) biologically inspired methods. However, the present work takes into account the first method for topology optimization. As for continuum structures, density based methods are most popular material parameterization techniques. The density approach deals with associating only one design variable with each individual element. Solid Isotropic Material with Penalization (SIMP) is one of the popular density based methods. The density based methods work on a fixed area of finite elements having the main aim of minimizing an objective function by categorizing whether each component consists of solid material or void. In structural topology optimization, compliance is often referred as the objective, and constraints are placed on the volume of material and stiffness or deflection that may be utilized.

7.2   Transtibial socket model preparation

The original socket model of four different patients was taken for investigation. The PoP socket is scanned using contactless laser scanning and surface model is reconstructed. The four socket models are extracted from 3D scan using the software COMET PLUS (Steinbichler, Germany) as shown in Figure 7.2. Using measurement tools, the appropriate design domain is extracted and the dimensions details were recorded and reported in Table 7.1.

| (a) | **Anterior** | **Posterior** | (b) | **Anterior** | **Posterior** |

| (c) | **Anterior** | **Posterior** | (d) | **Anterior** | **Posterior** |
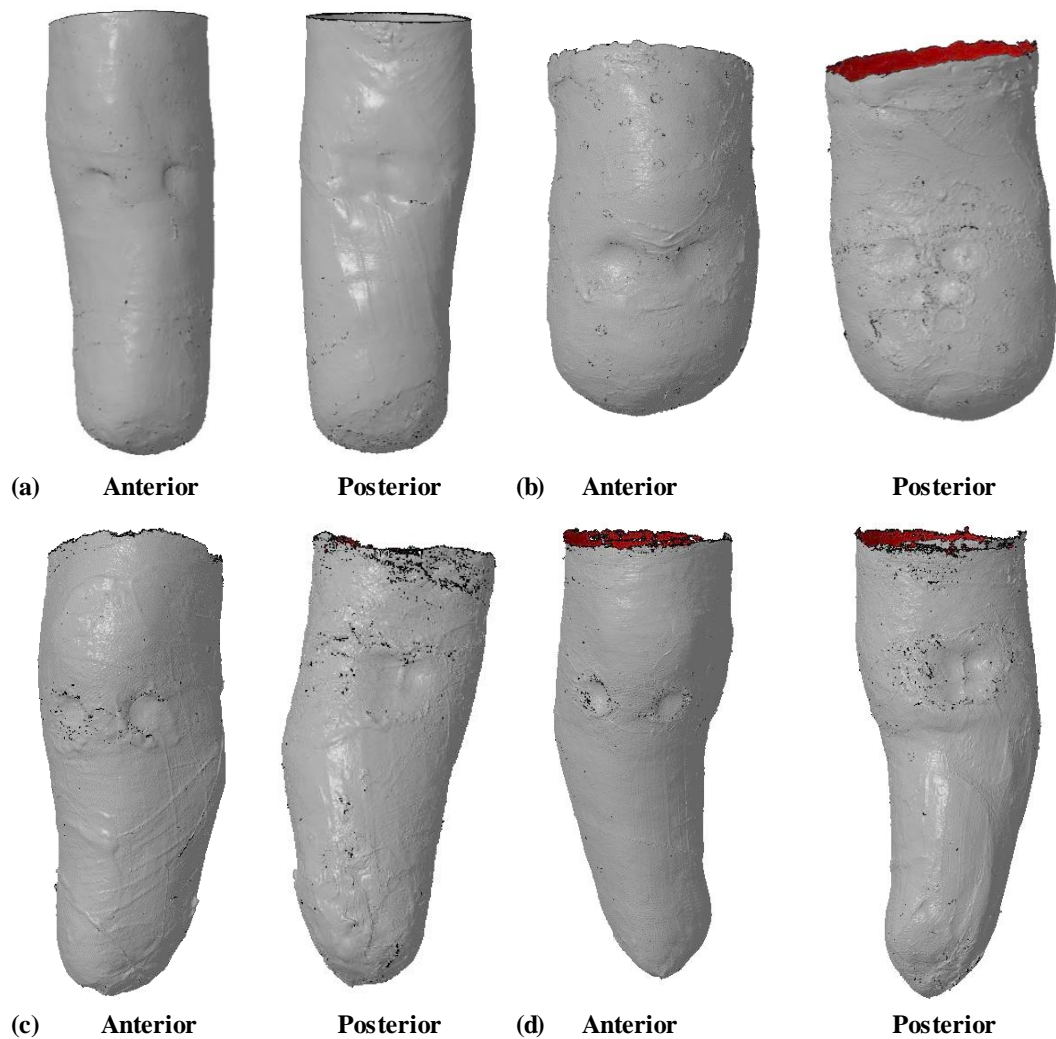
Figure-7.2: Scanned original socket model (a) Patient 1 (b) Patient 2 (c) Patient 3 [Left] (d) Patient 3 [Right]

Table-7.1: Dimensional specification of socket models

Parameter	Patient 1	Patient 2	Patient 3 (Right)	Patient 3 (Left)
Length (mm)	`355.36	167.72	251.92	248.89
Diameter (mm)	129.04	103.08	104.70	103.30
Area (mm^2)	98064.51	53185.56	68290.98	62893.46

For the final design using the SIMP technique, it is required to identify a suitable value for the transitional density material penalization factor. The most appropriate penalization factor to this specific problem was considered, as it was found that a factor of 3 is satisfactory. Before proceeding to the topology

optimization analysis, certain assumptions are made i.e. the material of socket is isotropic and homogeneous.

7.3 Topology Optimization of socket model

The topological optimization of socket is performed considering tetrahedral elements for mesh generation. Tetrahedral elements are used where high accuracy is desired in terms of geometry and stress solutions. The Altair's Opti Struct software was used for performing topology optimization. To be able to set up the problem and review the results, HyperMesh and HyperView are also used. HyperMesh is the pre-processor which is used to discretize (mesh) a CAD model, set boundary conditions, properties and options and to set up the problem to be solved (optimization, static analysis, model analysis etc.). From HyperMesh, a model which completely describes the problem is exported and then processed using Optistruct. Further, the results from Optistruct are evaluated using the post-processor HyperView. The socket needs to be flexible, but strong, to permit normal gait movement, but not twist/bend under pressure to improve amputee rehabilitation, care and reducing the weight with the cost of the prosthetic.
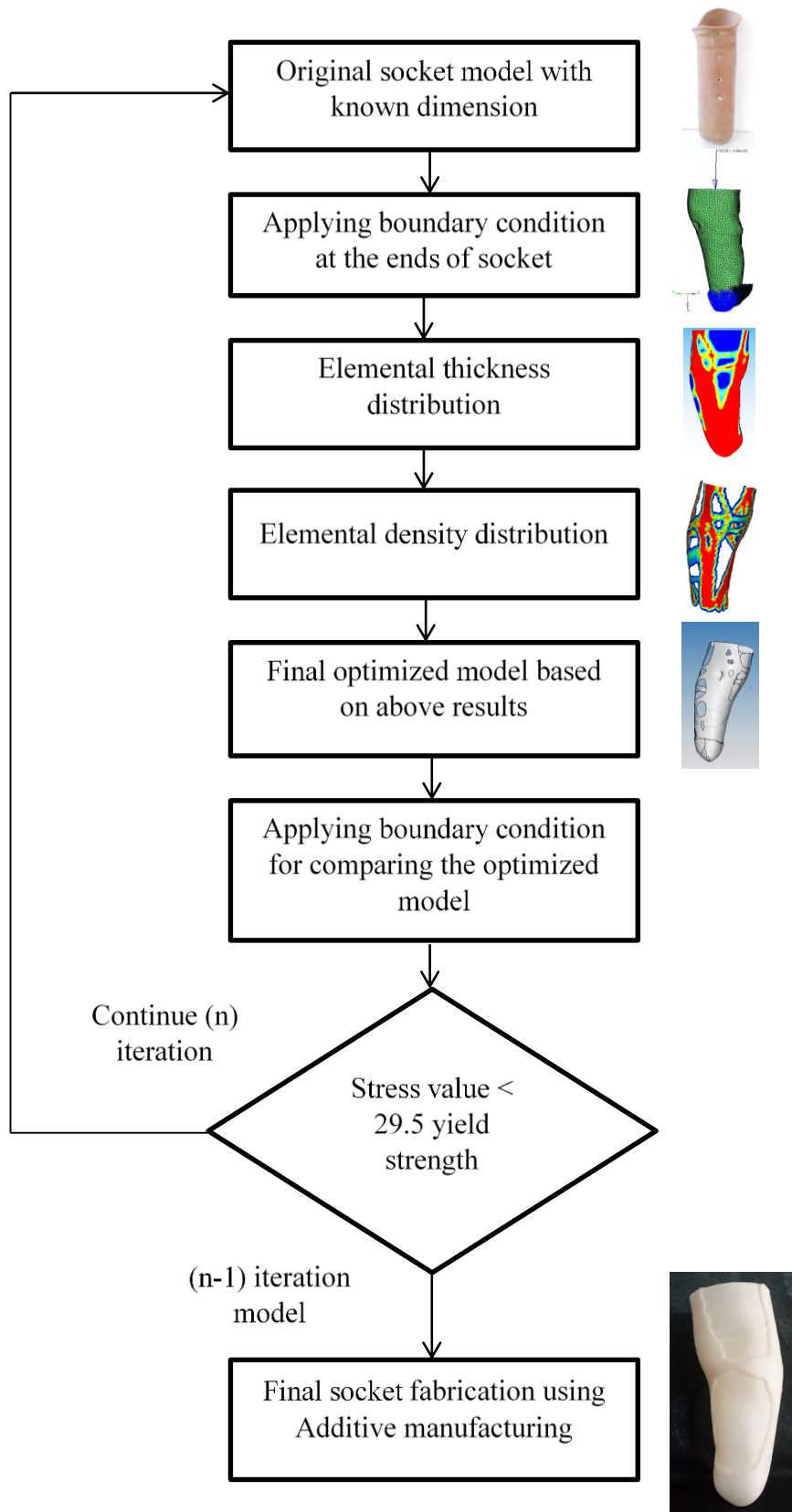
Figure 7.3: Flowchart of topology optimization of socket

The flow chart for topology optimization is shown in Figure 7.3, which describes various steps used to perform topology optimization. This assumes that an FE-model of the problem is available and different properties are used for the design and non-design elements. Altair Hyperworks and Optistruct interface is used for problem formulation and optimizing the boundary condition. The method attempted to replicate the compliance of the socket under vertical loading conditions at the top of the prosthetic socket keeping bottom surface fixed. The objective function is to minimize the volume of the socket keeping the strength intact. Table 7.2 shows the different parameters which were considered for minimizing the volume of the socket. Once, the optimized design is obtained, it is verified with the stress values of the socket keeping the same constraints when the values are within the yield strength.

Table-7.2: Topology optimization parameters

Objective	Minimize weight compliance (Increase Stiffness)
Constraints	1) Volume Fraction Upper Bound $= 0.50$ 2) Maximum Displacement of the centre node $= 2$ mm
Design Variables	The density at each element in the design space
Manufacturing Constraints	Minimum member size $= 15$ mm

The optimization attempted to replicate the compliance of the socket under vertical loading condition at the top of prosthetic socket and the bottom surface was fixed. Our objective function is to minimize the volume of the given socket. The topology optimization techniques used in this study reduced the volume of the original design by some value, so that socket strength is not reduced. Topology optimization produced reliable and satisfactory results within the yield strength of the material. The results of the topology optimization studies are shown in Figure 7.4 (a) and (b), in the form of elemental thickness distribution for patient P1, P2 and P3 (Left and Right) respectively. The red (light colour) zones indicate the solid material, whilst the blue (dark colour) zones indicate the recommended locations for void creation. The results of elemental thickness distribution are extremely vital as it suggests the need of varying thickness throughout the socket material. The regions

with high pressure require more material thickness in comparison to low-pressure regions.
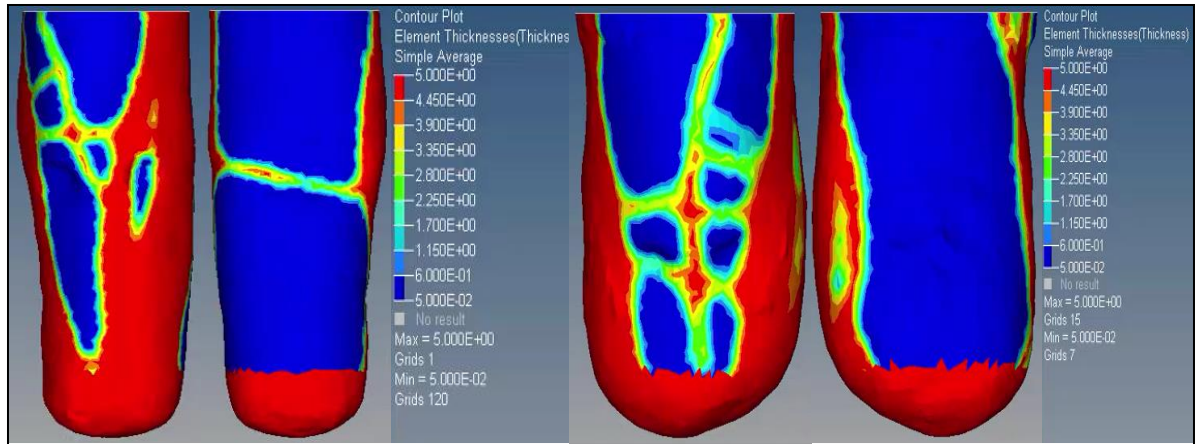
Figure-7.4 (a): Elemental thickness distribution of P1 (left) and P2 (right)
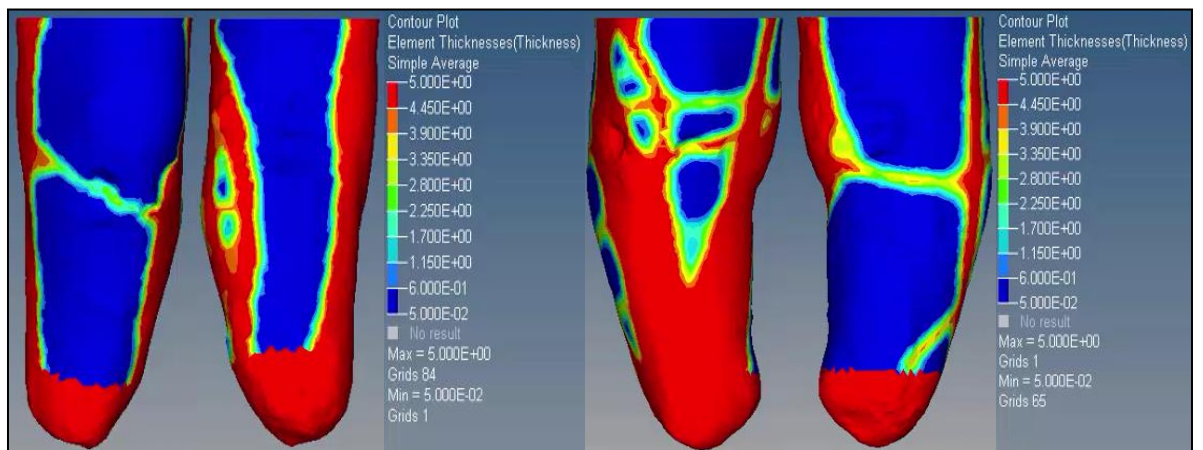
Figure-7.4 (b): Elemental thickness distribution of P3 (left) and P3 (right)

Furthermore, the result of elemental density distribution is depicted in Figure 7.5. It should be noted that the element density plots represent the optimal material distribution upon the convergence of the optimization. The red colour indicates that the material is critical for the loads and the blue colour indicates less elemental distribution which can be removed or redesigned. The transitional regions depict that density of the material as intermittent. It was clearly seen from Figure 7.5 that some irregular and strings like design are formed. It is also noted that more material is distributed towards the region of higher stress, which is in accordance with the above results. Thus, the regions with no load are shown as void and for specific

areas having higher loads are shown as solid. As the results suggested in below Figures, material removal inside the original prosthesis is not the only engineering interpretation of the socket elemental density distribution in output from the topological optimization analyses. Additionally, for high mass reduction percentages, the stress state in the prosthesis must never reach more than about 30% of the material yield strength, evading the probability to fear the effect of fatigue phenomena, at least in short-time predictions.

<div align="center">

(a)   **(b)**
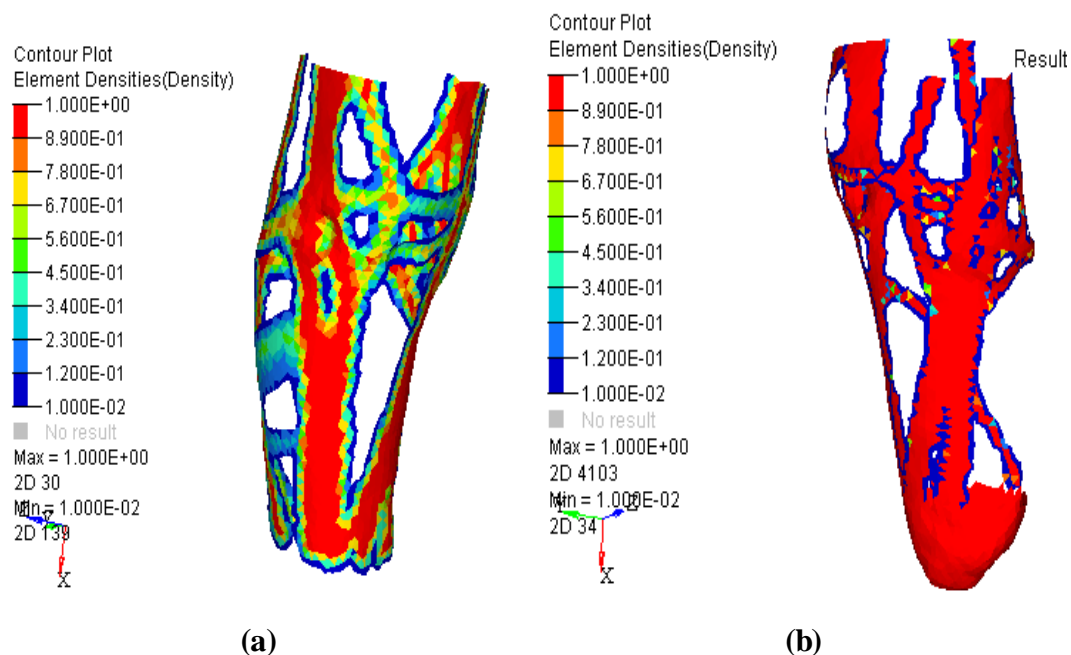
Figure-7.5: Elemental density distribution for (a) Patient 1 (b) Patient 2

</div>

7.4 Prosthetic socket fabrication using Additive Manufacturing

It is generally the case that structures designed using TO will have a more complex geometry than those developed from engineering intuition. This can limit the applicability of topology optimization derived designs in practice as it may not be possible to manufacture them. Some of the past research has shown that ability to simplify the problem by defining loads, boundary conditions, and design area results in an improved design that is never realized earlier. The resulted enhanced design structures are not only manufacturable but have optimum characteristics in comparison to the original design. Several such examples are available in the

literature showing the need of manufacturing optimized design structures and profiles.

Manufacturability of optimized design has been a big hurdle in the adoption of TO technology for research studies and industrial applications. The conventional manufacturing machines are inadequate to fabricate such complex profiles with intricate features. The additive manufacturing (AM) enables the fabrication of geometrically complex objects with intricate features which are the ideal requirement for TO, exploiting the design freedom offered by AM. These two technologies will fit well providing excellent optimum designs in reality to the outer world.

In light of additive manufacturing capability to manufacture any intricate design and topology, it unlocks the possibility to overcome the limitation imposed by traditional manufacturing techniques. There are a large variety of AM technologies that are available in the market based on different working principles. However, the high cost and large AM machine dimensions limit it to only research studies and bigger industries. In the past few years, there was a clamor to bring AM within reach of small industries, consumers and technology hobbyists (John et al., 2011). There are seven categories of AM technologies available as given by ASTM along with their terminology and definitions.

Recently, the truss ground structure has been specified by optimizing the cross-sectional area (Zegard et al., 2014). This study tested the applicability of AM by printing the part and examining it further. It was found that there are certain geometrical differences among the printed and original structures. This account for the need of including process is variability, uncertainty, issues and limitations before printing the part. Several other studies have reported about the general idea of combining AM and TO technologies and their interaction effects to take advantage of material removal (Emmelmann et al., 2011; Villalpando et al., 2014). Consequently, the final topologies would be restricted to overhang angles less than this experimentally determined angle.

Apart from this, researchers are just beginning to explore the medical application of these two technologies (i.e. AM and TO) mainly for tissue scaffolds. Recent literature has shown the studies related to tissue scaffold optimization for multi-functionality requirement (Almeida and Bartolo, 2013; Dias et al., 2014). The main criteria for optimization are maximum load handling with enough porosity to allow fluid to flow through the material. Several other studies have been reported in the same area of tissue scaffolds but with different optimization criteria (Challis et al., 2010; Chen et al., 2011; Guest and Prevost, 2006, 2007).

The AM technology mostly used in integration with TO is selective laser melting (SLM). In SLM, a laser completely melts metallic powder particles together forming a 3D component. As SLM is recognized for its choice of manufacturing constraints permitting difficult geometries and high material efficiency. Several researchers have integrated TO and SLM with the objective of enhanced design and making most of two technologies (Emmelmann et al. 2011; Tomlin et al. 2011; Muir 2013). However, SLM has certain specific issues related to it. Kruh et al., 2010 and Song et al., 2014 has discussed various challenges and issues related to SLM printing and emphasize on issues that need to tackle prior to its use.

7.5 FDM-based Additive Manufacturing for Generating Topology Optimised Sockets

For improved gait support and comfort, it is important to fabricate socket with high stiffness and flexibility, providing varying thickness wall. There are primarily two methods for fabrication of such a socket. The first one is a single wall approach that fulfills the need of high and low compliance in a series fashion. For rigid regions, material needs to be thicker than a nominal thickness, and area needs to be flexible are thinner. The second approach consists of printing socket using double wall thickness. The inner wall is thinner as compared to outer wall for enhancing the flexibility and maintaining the rigidity from inside. The present study concerns with only single wall approach.

7.5.1 Fabrication of 3D printed socket

RP is an emergent technology. Integration of Three-dimensional (3D) printing, 3D scanning, and reverse engineering are relatively novel technologies used for

fabrication of custom-made parts with complex shapes profiles. Additive Manufacturing (AM) technologies follow layer-by-layer material deposition technique allowing the fabrication of intricate and freeform shapes with simplicity. In the area of medical application, the real benefits become more extensively known and appreciated. The FDM-based 3D printer was chosen from several RP processes because it requires minimum post-processing with good mechanical properties.

The STL file has extensively used the format in rapid prototyping. The STL file model is obtained by tessellation of the original model from the scanner is loaded in a 3D printer for digital manufacturing. The complex freeform shape of a prosthetic socket results in a huge size of the file when tessellated. The process of printing the parts on the R3D2 ELAM system begins with the CAD model saved in STL format. The surface defining the design must not contain any discontinuity (non-manifold edge). The part could be reoriented and repaired for optimum print quality using Netfabb and MeshMixer. Slic3r was used to slice the part with suitable layer thickness and for adjusting other printing parameters before the G-code was generated. Initially, the extruder head and printer bed were heated to a predefined temperature and then extruder head begins to extrude molten plastic to build prototype taking shape from bottom to top layer by layer. Acetone–ABS mixture is used on the printer bed for effective part adherence. The acetone solution offers a satisfactory adhesion of the part on printer bed during the printing process.

The use of the low-cost entry-level 3D printer, R3D2 FDM-based printer consists of horizontal translating (x-y) heated bed platform with a usable build area of 200 x 220 mm and vertical translating (z-direction) extruder fitted with a nozzle. Also, the maximum build height of the machine is 200 mm as shown in Figure 7.6. It is a layer-by-layer extrusion-based rapid prototyping process. The extrusion process is directed by a stepper motor with a feed of 1.8 mm diameter Acrylonitrile Butadiene Styrene (ABS) filament into a heated 0.15 mm diameter nozzle. The R3D2 ELAM machine is used to fabricate parts with a layer thickness of 0.075 mm. AM Machine extrudes the filament through its heated nozzle to build a socket layer by layer. Extruder temperature was set at 220°C, then the filament enters at 210°C for first, and outer layer temperature with the bed temperature of the printer was 60°C. The AM socket may require mild sanding or sandpaper polish to remove seam or burr.
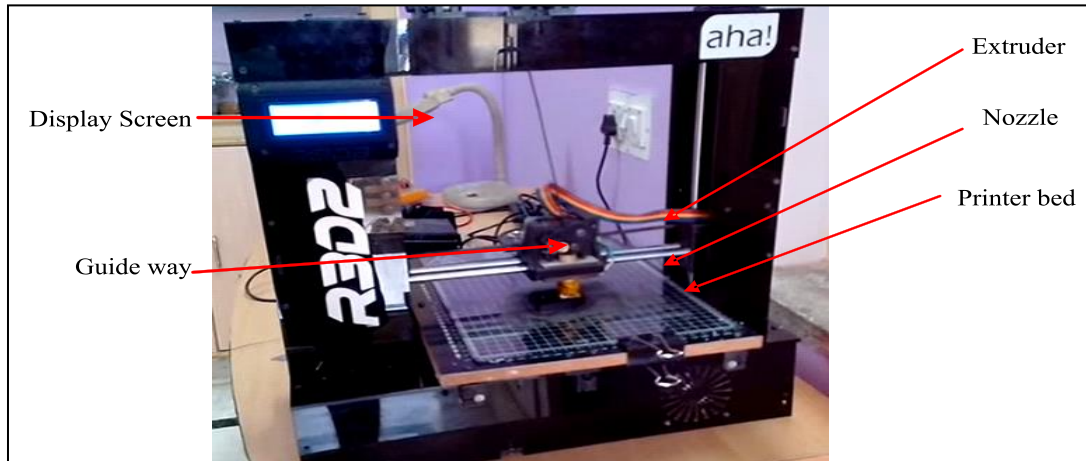
Figure-7.6: R3D2 FDM-based additive manufacturing machine

The time taken to form the prosthesis socket by 3D printer was 480 minutes and complete prosthesis. The weight of the prosthesis is 256 grams and the wall thickness of the prosthesis socket varied from 3.2 mm at the distal end to 4.5 mm at patella-tendon of the stump. The overall time of socket manufactured by the proposed method is 250 minutes. Therefore, the proposed RE and AM integrated digital manufacturing process of the socket overcomes all above hassles associated with traditional manufacturing. The finished AM socket is shown in the bottom of the (Figure 3.6). For the prosthetic socket, both traditional and proposed processes of manufacturing are schematically represented**.**

Based on the results of Topology Optimisation a test socket is fabricated using FDM-based additive manufacturing machine (see Figure 7.7). The Printed socket is then verified for dimensional accuracy. As geometric fidelity is one of the critical issues with AM technology. In the same context, the initially printed socket is compared with its CAD model for geometric deviation before the final printing of the socket. The procedure followed for geometric inspection is same as was used in Chapter 3. starting with the scanning of the socket and further inspecting it in the inspection software (Steinbichler).

| Anterior | Posterior | Lateral | Medial |
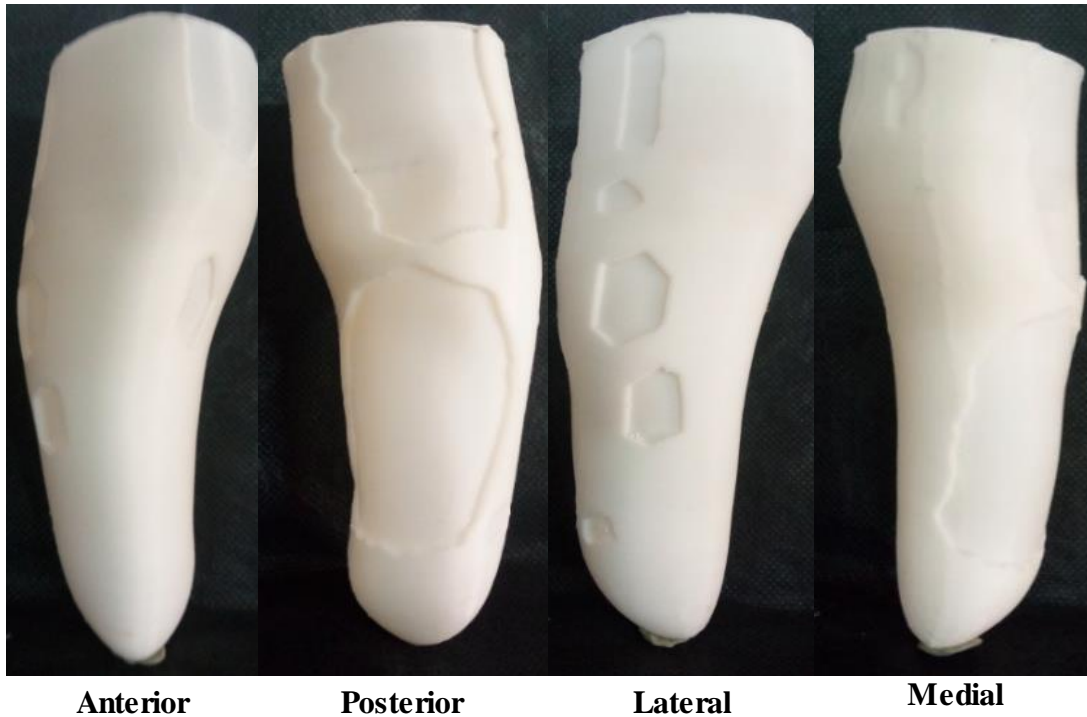
Figure-7.7: Optimized Prosthetic socket using AM

7.5.2   Dimensional evaluation

The performance of any system depends on inspection planning strategy. Thus an optimum inspection is required to accomplish more accurate and faster results. The dimensional evaluation of AM prosthesis socket and PoP socket was carried out using the Steinbichler INSPECTPLUS inspection software. Figure 7.8 gives the average deviation of STL data of both AM prosthesis socket and PoP socket, which were to be aligned electronically for accurate dimensional comparison. In the present case, best-fit alignment was chosen for dimensional comparison due to the presence of free-form surfaces. Once alignment is complete surface comparison is carried out between the two STL file and the results are shown in Figure 7.9. It is clear from the comparison chart that deviation is spread across the profile and the maximum deviation of the AM socket from PoP socket is approximately 2.2 mm. This deviation is near to the conventional values and hence gives hope for acceptance of the proposed approach.
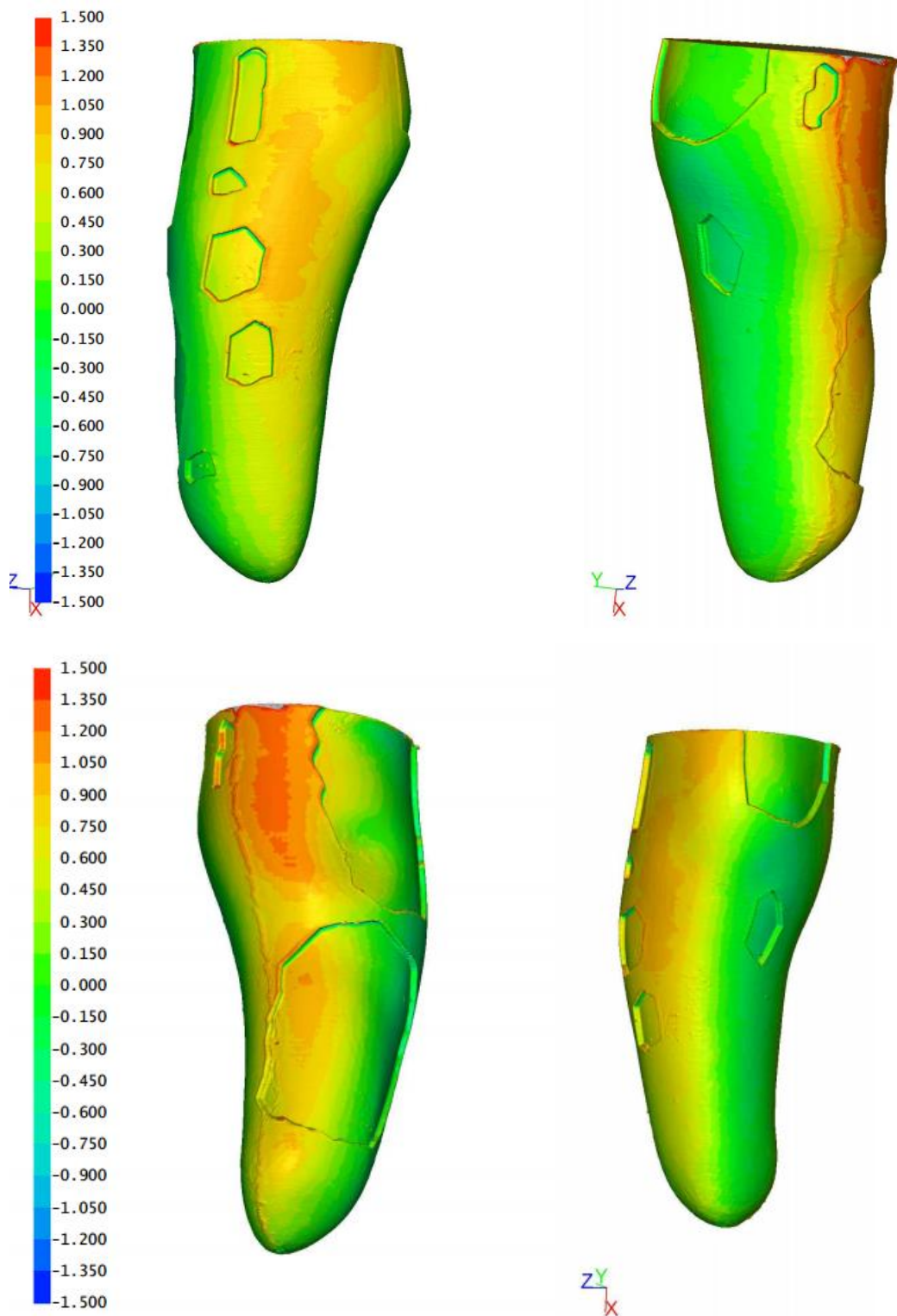
Figure-7.8: Average deviation showing (a) Lateral and Medial (b) Posterior and Anterior view
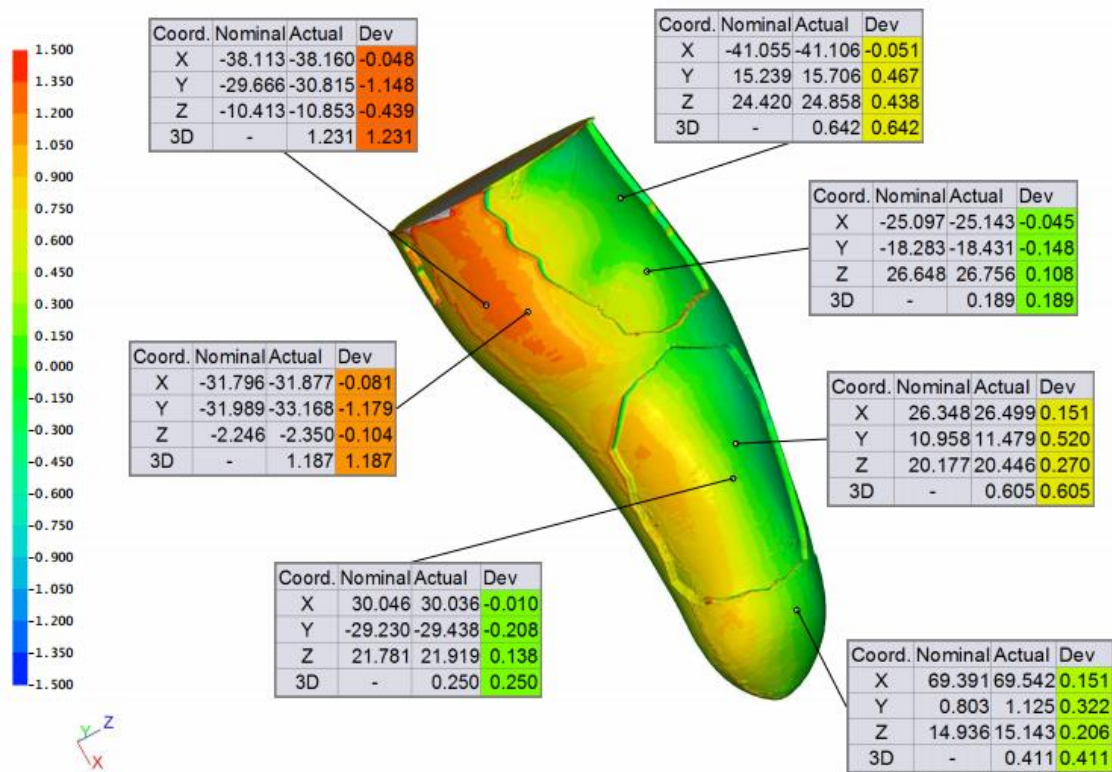
Figure-7.9: Point-to-Point deviation with actual CAD model

Chapter Summary

A framework for modeling and topology optimization of prosthetic sockets has been developed resulting in improved fabrication accuracy for the individual patients.

CHAPTER 8
CONCLUSIONS AND FUTURE SCOPE

Introduction

This chapter includes the conclusions of the work done along with objectives, conclusions based on research work presented in this thesis followed by the scope for future work in this field.

8.1   Contribution of the research work

This theoretical and experimental investigation of prosthetic socket research reported in this thesis consists of five parts:

The first part has provided a novel digital and rapid route for eliminating manual measurements and provides a way for automation of the traditional manual process. The impracticability of scanning working surface of the PoP was overcome by axially splitting mold which facilitated accessibility for scanner beams. The split half later successfully assembled through software without loss of socket accuracy. Present study proposed two unified solutions using different CAD methodologies for modelling and analyzing a Freeform surface from a raw unorganized point cloud. In the first approach, digital model was generated with default settings of used software. For the second approach, developed digital model was based on the user expertise to achieve an upgraded and enhanced the surface model. The methodologies are useful in capturing original surface model accurately and improving the conventional reverse engineering process appropriately. The integration of rapid prototyping in the processes ensured dimensional accuracy and speed.

The second part has reported improvement of the design of the BK prosthetic socket through FE Analysis. A scientific understanding of pressure-displacement intensity at socket-limb interface is essential for improvement of prosthetic socket design. The results provide significant insight into the socket design and a roadmap for customization of the sockets. Although stress–strain patterns and magnitudes have shown similar behavior for all patients, however, the patient-specific solution is needed for comfortable socket design as peak value of stress was found to vary.

This work presents a method for stress analysis of transtibial prosthesis socket for improving the socket fit with residual limb and redistribute pressure from the critical regions. In socket design, aspect ratio is a decisive parameter to an optimized thickness of the socket.

The third part describes a new methodology that has been developed using low-cost piezo-resistive flexiforce sensor for quantitatively analyzing pressure distribution at eight specific regions. Six clinically significant cases were considered for pressure prediction under different loading conditions. In this context, advanced intelligence tools such as regression analysis and population-based GA has been employed. From the results, it was found that a patient's weight plays a major role in pressure evaluation followed by stump length. The present approach significantly evaluates pressure variation for different loading conditions. The adopted methodology helped in providing pressure monitoring system for socket fitting which will help in better-designe of prosthetic sockets to ensure enhanced patient satisfaction.

The fourth part of this thesis was an investigation on the effects of patient's physiological parameters on maximum pressure developed at transtibial prosthesis limb/socket interface. Significant control factors affecting the pressure have been identified through successful implementation of analysis of variance (ANOVA). The results presented in this study will give a prosthetics a quantitative tool to analyze the maximum possible pressure, which could be developed at limb/socket interface for a patient during different conditions. The experimental results of the ANOVA are also validated with GA, and it was found that a patient's weight is a vital parameter that decides the amount of pressure at stump-socket interface followed by stump length and height. Thus, the prosthetist can ensure the endurance of the prosthesis socket without leading to any harmful situation for transtibial amputees.

The fifth part of this thesis was to produced optimized socket geometries with near-perfect strength-to-weight ratios. The result of comparison chart of AM socket and PoP socket using INSPECTIONPLUS revealed a maximum dimensional deviation of -3 to +3%, though medical field demands close tolerance.

8.2   Scope for future work

The following aspects could also be incorporated in this research work that should be taken up in the future:

1.   The present study can be further explored by attempting digital manufacturing of socket through high-end AM machine and 3D scanner with 50-micron accuracy.

2.   The topology optimization techniques used to reduce volume of the socket can be manufactured by different additive methods.

3.   The present study may be extended further to optimize both digital manufacturing system and developed analysis algorithm, to achieve more perfect results and a more user independent system.

4.   The present study can be extended further to measuring gait cycle of amputees walking with prostheses.

REFERENCES

1.   Abu Osman, N.A., Spence, W.D., Solomonidis, S.E., Paul, J.P., Weir, A.M. (2010). Transducers for the determination of the pressure and shear stress distribution at the stump-Socket interface of trans-tibial amputees. *Proc. Inst. Mech. Eng. Part B J. Eng. Manuf.* 224 (8), 1239–1250.

2.   Abu Osman, N.A., Spence, W.D., Solomonidis, S.E., Paul, J.P., Weir, A.M. (2010). The patellar tendon bar! Is it a necessary feature? *Med. Eng. Phys.,* 32(7), 760-765.

3.   Alcaide-Aguirre, R.E., Morgenroth, D.C., Ferris, D.P. (2013). Motor control and learning with lower limb myoelectric control in amputees. *J. Rehabil. Res. Dev.* 50(5), 687-698.

4.   Al-Fakih, E.A., Abu Osman N.A., Eshraghi, A., Mahamd Adikan, F.R.. (2013). The Capability of Fiber Bragg Grating Sensors to Measure Amputees' Trans-Tibial Stump/Socket Interface Pressures. *Sensors.*13(8), 10348-10357.

5.   Al-Fakih, E.A., Abu Osman, N.A., Mahmad Adikan, F.R. (2016). Techniques for Interface Stress Measurements within Prosthetic Sockets of Transtibial Amputees: A Review of the Past 50 Years of Research. Sensors, 16(7), 11-19.

6.   Ali, S., Abu Osman, N.A., Eshraghi, A., Gholizadeh, H., Wan Abas, W.A.B.B. (2013). Interface pressure in transtibial socket during ascent and descent on stairs and its effect on patient satisfaction. *Clin. Biomech.* 28(9-10), 994-999.

7.   Ali, S., Osman, N.A.A., Mortaza, N., Eshraghi, A., Gholizadeh, H., Abas, W.A.B.B.W. (2012). Clinical investigation of the interface pressure in the trans-tibial socket with dermo and seal-in x5 liner during walking and their effect on patient satisfaction. *Clin. Biomech.* 27(9), 943-948.

8.   Almeida, H., Brtolo, P. (2013). Topological optimisation of scaffolds for tissue engineering. Procedia Engineering, 59, 298–306.

9.   Amali, R., Noroozi, S., Vinney, J., Sewell, P. Andrews, S. (2006). Predicting interfacial loads between the prosthetic socket and the residual limb for below knee amputees – a case study. *Strain.* 42(1), 3-10.

10.   Andrysek J. (2010). Lower-limb prosthetic technologies in the developing world: A review of literature from 1994–2010. *Prosthetics and Orthotics International.* 34(4), 378–398.

11.   Baars, E.C.T., Geertzen, J.H.B. (2005). Literature review of the possible advantages of silicon liner socket use in trans-tibial prostheses, *Prosthetics and Orthotics International.* 29(1), 27-37.

12.   Bansal, G., Bhatia, D., Joshi, D., Anand, S., Tewari, RP. (2011) Coordination between lower limb muscles in different locomotion activities, *Int. J. Biomedical Engineering and Technology.* 6(2), 129-141.

13.   Berlemont, M., Weber, R., Willot, J.P. (1969). Ten years of experience with the immediate application of prosthetic devices to amputees of the lower extremities on the operating table, *Prosthet Orthot Int.* 3, 8-18.

14.   Bibb, R., Freeman, P., Brown, R., Sugar, A., Evans P., Bocca, A. (2000). An investigation of three-dimensional scanning of human body surfaces and its use in the design and manufacture of prostheses, Proceedings of the Institution of Mechanical Engineers, Part H. *Journal of Engineering in Medicine.* 214(6), 589-594.

15.   Boonhong, J. (2007). Validity and reliability of girth measurement (circumference measurement) for calculating residual limb volume in below-knee amputees. *Chula Med J.* 51, 77–88.

16.   Bouten, D. C., Colin, D., Oomens C. W. J. (2010). Pressure Ulcer Research, Current and Future Perspectives, Springer. *Berlin, Germany.*

17.   Bowker, H.K., Quigly, J.W. (1992). Prosthetic Management: Overview, Methods, and Materials. *Prosthetic and Rehabilitation Principles, Mosby-Year Book.* 67-79.

18.   Brackett, I. Ashcroft, and R. Hague. (2011). Topology optimization for additive manufacturing. Pages 348–362.

19.   Buis, A.W., Blair, A., Convery, P., Sockalingam, S., McHugh, B. (2003). Pilot study: Data-capturing consistency of two transtibial casting concepts,

using a manikin stump model: A comparison between the hands on PTB and hands-off ICECAST compact concepts. *Prosthetics and orthotics International.* 27(2), 100-106.

20. Buis, A.W.P., Condon, B., Brennan, D., McHugh, B., Hadley, D. (2006). Magnetic resonance imaging technology in transtibial socket research: A pilot study. *Journal of Rehabilitation Research & Development JRRD.* 43(7), 883-890.

21. Challis, A., Roberts, J., Grotowski, L., Zhang, C., Sercombe, T. (2010). Prototypes for bone implant scaffolds designed via topology optimization and manufactured by solid freeform fabrication. Advanced Engineering Materials, 12(11), 1106–1110.

22. Chen, M., Schellekens, S., Zhou, J., Cadman, W., Li, R., Appleyard, Q. (2011). Design optimization of scaffold microstructures using wall shear stress criterion towards regulated flow-induced erosion. Journal of Biomechanical Engineering, 133(8).

23. Collins, D.M., Karmarkar, A., Relich, R., Pasquina, P.F., Cooper, R.A (2006). Review of Research on Prosthetic Devices for Lower Extremity Amputation. 34(5), 379-438.

24. Colombo G., Filippi, S., Rizzi, C., Rotini, Rotini, F. (2010). A new design paradigm for the development of custom-fit soft sockets for lower limb prostheses. *Computers in Industry*, 61(6), 513-523.

25. Colombo, G., Berretti, M., Bonacini, D. and Magrassi, G. (2006). Reverse and rapid prototyping techniques to innovate prosthesis socket design, Paper presented at SPIE-IS&T Electronic Imaging, *SPIE*, Vol. 6056, 60560P.

26. Colombo, G., Facoetti, G., Gabbiadini, S., Rizzi, C. (2013) Socket modelling assistant for prosthesis design, *International Journal of Computer Aided Engineering and Technology*, 5(2-3), 216-241.

27. Colombo, G., Morotti, R., Rizzi, C. (2014). FE Analysis of Contact between Residual Limb and Socket during Simulation of Amputee Motion. Computer-Aided Design and Applications. 11(4), 381-388.

28. Commean, P.K, Smith, K.E., Cheverud, J.M., Vannier, M.W. (1996). Precision of surface measurements for below-knee residua. *Archives of Physical Medicine and Rehabilitation,* 77(5), 477-486.

29. Convery, P and Buis, AWP (1999). Socket/stump interface dynamic pressure distributions recorded during the prosthetic stance phase of gait of a transtibial amputee wearing a hydrocast socket. *Prosthetics and Orthotics International,* 23(2), 107-112.

30. Convery, P., Buis, A.W., Wilkie, R., Sockalingam, S., Blair, A., McHugh, B. (2003). Measurement of the consistency of patellar tendon-bearing cast rectification, *Prosthetics and orthotics International.* 27(3), 207-213.

31. Convery, P., Buis, A.W.P. (1998) Conventional patellar-tendon-bearing (PTB) socket/stump interface dynamic pressure distribution recorded during the prosthetic stance phase of gait of a trans-tibial amputee. Prosthetic Orthotic International, 22, 193-198.

32. Cugini, U, Bertetti, M., Bonacini, D., Corradini, C., Magrassi, G. (2006). Innovative Implementation in Socket Design: Digital Models to Customize the Product. In: Proceedings of ArtAbilitation, vol. 1, 54–61, ISBN: 87-7606r-r015-2.

33. Cummings, D., (1996). Prosthetics in the developing world: a review of the literature, *Prosthetics and Orthotics International*, 20(1), 51-60.

34. Dean, D, Saunders, CG (1985). A software package for design and manufacture of prosthetic sockets for transtibial amputees. *IEEE Trans Biomed Eng,* 32(4), 257-262.

35. Deb, K. (1998). Genetic algorithm in search and optimization: the technique and applications, in: Proceedings of International Workshop on Soft Computing and Intelligent Systems, Calcutta, India, 58–87.

36. Demet, K, Martinet, N, Guillemin, F, Paysant, J, Andre J-M (2003). Health related quality of life and related factors in 539 persons with amputation of upper and lower limb. *Disabil Rehabil,* 25(9), 480-6.

37. Dev, R., Singh, AK. (2015). Distortion analysis of EMG signal using LabVIEW as an effective tool, *Int. J. Biomedical Engineering and Technology*, 19(2), 187-204.

38. Dias, M., Guedes, J., Flanagan, C., Hollister, S., Fernandes, P. (2014). Optimization of scaffold design for bone tissue engineering: A computational and experimental study. Medical Engineering and Physics, 36(4), 448–457.

39. Dillingham T. R., Pezzin L. E., and MacKenzie E. J. (2002). Limb amputation and limb deficiency: epidemiology and recent trends in the United States, *Southern Medical Journal*, 95(8), 875–883.

40. Dillingham, T.R.., Pezzin, L. E., MacKenzie, E. J., Burgess, AR. (2001). Use and satisfaction with prosthetic devices among persons with trauma-related amputations: A long-term outcome study, American Journal of Physical Medicine and Rehabilitation, 80(8), 563-571.

41. Dou, P., Jia, X., Suo, S., Wang, R and Zhang M. (2006). Pressure distribution at the stump/socket interface in transtibial amputees during walking on stairs, slope and non-flat road. *Clinical Biomechanics.* 21(10), 1067–1073.

42. Dougherty, G., Digital image processing for medical applications. (2009). Cambridge University Press.

43. Douglas T., Solomonidis S., Sandham W., Spence W., (2002). Ultrasound Imaging in Lower Limb Prosthetics. IEEE Transactions On Neural Systems And Rehabilitation Engineering, 10(1), 11-21.

44. Douglas, T.S., Solomonidis, S.E., Lee, V.S.P. Spence, W.D., Sandham, W.A., Hadley, D.M. (1998). Automatic segmentation of magnetic resonance images of the trans-femoral residual limb, Medical Engineering & Physics 20(10), 756–763.

45. Duchemin, L., Bousson, V., Raossanaly, C., Bergot, C., Laredo, J.D., Skalli, W., Mitton, D., (2008). Prediction of mechanical properties of cortical bone by quantitative computed tomography, *Medical Engineering & Physics*, 30(3), 321–328.

46. Dumbleton, T., Buis, A.W.P., McFadyen, A., McHugh, B.F., McKay, G., Murray, K.D., Sexton, S., (2009). Dynamic interface pressure distributions of two transtibial prosthetic socket concepts, *Journal of Rehabilitation Research & Development*, 46(3), 405-416.

47. Eberhart, H.D., McKennon, J.C. (1960). Suction-socket suspension of the above-knee prosthesis, in Klopsteg PE, Wilson PD: Human Limbs and Their Substitutes. McGraw-Hill International Book Co, New York, 1954. *Reprinted by Hafner Press, New York*.

48. Emmelmann, C., Sander, P., Kranz, J., Wycisk, E. (2011). Laser additive manufacturing and bionics: Redefining lightweight design, 12, 364–368.

49. Engsberg, J.R., Clynch, G.S., Lee, A.S., Allan, J.S., Harder J.A. (1992). A CAD CAM method for custom below-knee sockets, *Prosthetics and Orthotics International* 16(3), 183-188.

50. Engsberg, J.R., Springer, M.J., Harder, J.A. (1992). Quantifying interface pressures in below-knee amputee sockets. *J Assoc Child Prosthet Orthot Clin*. 27(3), 81-88.

51. Facoetti, G., Gabbiadini, S., Colombo, G., Rizzi, C. (2010). Knowledge-based system for guided 158odelling of sockets for lower limb prostheses, Computer Aided Design Application 7(5), 723-737.

52. Faulkner, V.W., Walsh, N.E. (1989). Computer Designed Prosthetic Socket from Analysis of Computed Tomography Data, *Journal of Prosthetics & Orthotics* 1(3), 154-164.

53. Faustini, M. C., Neptune, R. R., Crawford, R. H., Rogers, W. E., and Bosker, G., (2006). An Experimental and Theoretical Framework for Manufacturing Prosthetic Sockets for Transtibial Amputees, *IEEE Trans. Neural Syst. Rehabil. Eng.,* 14 (3), 304–310.

54. Faustini, M. C., Neptune, R. R., Crawford, R. H., Stanhope, S. J., (2008). Manufacture of Passive Dynamic Ankle-Foot Orthoses Using Selective Laser Sintering, *IEEE Trans. Biomed. Eng*., 55 (2), 784–790.

55. Faustini, M.C., Neptune, R., Crawford, R.H. (2006). The quasi-static response of compliant prosthetic sockets for transtibial amputees using finite element methods, Medical Engineering & Physics, 28(2), 114-121.

56. Faustini, M.C., Richard, H.C., Richard, R. N., William, E. R., Gordon, B. (2005). Design and analysis of orthogonally compliant features for local contact pressure relief in transtibial prostheses, *Journal of Biomechanical Engineering*. 127(6), 946-951.

57. Fernie, G.R., Griggs G., Bartlett, S, Lunau, K. (1985). Shape sensing for computer aided below-knee prosthetic socket design. *Prosthet Orthot Int*. 9(1), 12–16.

58. Foort, J. (1979). Socket design for the above-knee amputee. *Prosthetics and Orthotics Int*; 3(2), 73-81.

59. Frillici, F.S., Rissone P., Rizzi C., Rotini F. (2008). The role of simulation tools to innovate the prosthesis socket design process, *Intelligent Production Machines and Systems, Whittles Publishing*, 612–619, ISBN: 978-1904445-52-4.

60. Fuh, J.Y.H., Feng, W., Wong, Y.S. (2006). Modeling, analysis and fabrication of below-knee prosthetic sockets using rapid prototyping, in Gibson I (ed.), Advanced Manufacturing Technology for Medical Applications: Reverse Engineering, Software Conversion and Rapid Prototyping, Engineering Research Series, *John Wiley & Sons*.

61. Geil, M. (2007). Consistency, precision and accuracy of optical and electromagnetic shape-capturing systems for digital measurement of residual-limb anthropometrics of persons with transtibial amputation, *Journal of Rehabilitation Research and Development*. 44(4), 515-524.

62. Geil, M. D. (2005). Consistency and accuracy of measurement of lower-limb amputee anthropometrics. *Journal of Prosthetics & Orthotics,* 42(2), 131-140.

63. Gholizadeh, H., Abu Osman, N.A., Eshraghi, A., Ali, S., (2014). Transfemoral prosthesis suspension systems: A systematic review of the literature. *American journal of Physical Medicine and Rehabilitation*, 93(9), 809-823.

64. Gibson, I., editor. (2005). Advanced manufacturing technology for medical applications: reverse engineering, software conversion and rapid prototyping. John Wiley & Sons.

65. Goh JCH, Lee PVS, Chong SY. (2004). Comparative study between patellar-tendon-bearing and pressure cast prosthetic sockets. *Journal of Rehabilitation Research & Development*. 41(3B), 491–501.

66. Goh, J.C., Lee, P.V., Ng P. (2002). Structural integrity of polypropylene prosthetic sockets manufactured using the polymer deposition technique, Proceedings of the Institution of Mechanical Engineers, Part H: *Journal of Engineering in Medicine* 216(6), 359-368.

67. Goh, J.C.H., Lee, P.V.S and Chong, S.Y. (2003). Stump/socket pressure profiles of the pressure cast prosthetic socket. *Clinical Biomechanics*. 18(3), 237–243.

68. Golbranson, F., Wirta, R., Kuncir, E., Lieber, R., Oishi, C. (1988). Volume changes occurring in postoperative below-knee residual limbs. *J Rehabil Res Dev*. 25(2), 11–18.

69. Goswami, J., Lynn, R., Street, G., Harlander, M. (2003). Walking in a vacuum-assisted socket shifts the stump fluid balance, *Prosthetics & Orthotics International*, 27(2), 107-113.

70. Guest, J. K., Prevost, J. H. (2006). Optimizing multifunctional materials: design of microstructures for maximized stiffness and fluid permeability. International Journal of Solids and Structures, 43(22):7028–7047.

71. Guest, J. K., Prevost, J. H. (2007). Design of maximum permeability material structures. Computer Methods in Applied Mechanics and Engineering, 196(4), 1006–1017.

72. Hachisuka, K., Dozono, K., Ogata, H., Ohmine, S., Shitama, H., Shinkoda, K. (1998). Total surface bearing below-knee prosthesis: Advantages, disadvantages, and clinical implications, Archives of Physical Medicine & Rehabilitation, 79(7), 783-789.

73. He, P., Xue, K., Chen, Q., Murka, P., Schall, S. (1996). A PC-based ultrasonic data acquisition system for computer-aided prosthetic socket design. *IEEE Trans Rehabil Eng*. 4(2):114–19.

74. He, P., Xue, K., Murka, P. (1997). 3-D imaging of residual limbs using ultrasound. *J Rehabil Res Dev*. 34(3), 269–78.

75. Herbert, N., Simpson, D., Spence, W, Ion, W. (2005). A preliminary investigation into the development of 3-D printing of prosthetic sockets, *Journal of Prosthetics and Orthotics* 42(2), 141-146.

76. Hopkinson, N., Dickens, P.M. (2003). Analysis of rapid manufacturing-using layer manufacturing processes for production, Proceedings of the Institute of Mechanical Engineers, Part C: *Journal of Mechanical Engineering Science* 217 (C1), 31-39.

77. Horgan, O., MacLachlan, M. (2004). Psychosocial adjustment to lower-limb amputation: a review. *Disability and Rehabilitation.* 26(14-15), 837–850.

78. Houston, V.L. (1992). Automated Fabrication of Mobility Aids (AFMA): Below-knee CASD/CAM Testing and Evaluation Program Results, *Journal of Rehabilitation Research and Development* 29 (4), 78-124.

79. Hsu, L.H., Au, H.W., Chou, Y.L., Huang, G.F. (2001). Recognition for the boundary of pressure-tolerant and pressure-relief areas on the scanned points of residual limb, Biomedical engineering applications, basis & communications 13, 276-282.

80. Hsu, L.H., Hsu, F.M., Chou, Y.L., Hsu, L.Y. Leong, H., Huang, K.F. (2001). An algorithm to construct the CAD model of a residual limb. Biomedical engineering applications basis and communication, 13(3), 149-158.

81. Hsu, L.H., Hsu, L.Y., Chou, Y.L., Chien, C.W., Huang, G.F. (2000). Automated shape modification for the cadmodel of residual limb, Biomedical engineering applications, basis & communications 14: 251.

82. Hsu, L.H., Huang, G.H., Lu, C.T., Hong, D.Y., Liu, S.H. (2010). The Development of a Rapid Prototyping Prosthetic Socket Coated with a Resin Layer for Transtibial Amputees, Prosthetics and orthotics International 34:37.

83. Jaime, A.V., Patino, F.R.J. (2012). Incidence of the boundary condition between bone and soft tissue in a finite element model of a transfemoral amputee, Annals of Biomedical Engineering, 36(4), 405-414.

84. Jensen, J.S., Craig, J.G., Mtalo, L.B., Zelaya, C.M. (2004). Clinical field follow-up of high density polyethylene (HDPE) – Jaipur prosthetic technology for trans-femoral amputees. Prosthetics and Orthotics International, 28, 152-16

85. Jensen, J.S., Poetsma, P.A., Thanh, N.H. (2005). Sand-casting technique for trans-tibial prostheses. *Prosthetics and Orthotics International* August 29(2), 165–175.

86. Jia, X., Zhang, M., Lee, W.C.C. (2004). Load transfer mechanics between transtibial prosthetic socket and residual limb-Dynamic effects, *Journal of Biomechanics,* 37(9), 1371–1377.

87. Johansson, S., Oberg, T. (1998). Accuracy and precision of volumetric determinations using two commercial CAD systems for prosthetics: A technical note. *J Rehabil Res Dev*. 35(1), 27–33.

88. Kang, P., Kim, J., and Roh, J. (2006). Pressure Distribution in Stump/Socket Interface in Response to Socket Flexion Angle Changes in Transtibial Prostheses with Silicone. Liner. *PTK*. 13(4).

89. Kay, H.W., Newman, J.D. (1975). Relative incidences of new amputations. *Orthot Prosthet*, 29:3-16.

90. Kim, W.D., Lim, D., Hong, K.S. (2003). An evaluation of the effectiveness of the patellar tendon bearing bar in the trans-tibial patellar-tendon-bearing prosthesis socket. *Prosthet Orthot Int*. 27(1), 23–35.

91. Kovacs, L., Eder, M., Volf, S., Raith, S., Pecher, M., Pathak, H., Müller, C., and Gottinger, F. Patient-Specific Optimization of Prosthetic Socket Construction and Fabrication Using Innovative Manufacturing Processes: A Project in Progress. In Materialise World Conference 2010. Leuven, Belgium.

92. Krishna, V.G., Rao, L.B. (2015). Modelling and analysis of a synovial joint, *Int. J. Biomedical Engineering and Technology*, 17(2), 178-191.

93. Krouskop, T.A. (1987). Computer aided design of a prosthetic socket for an above-knee amputee. *Journal of Rehabilitation Research and Development* 24(2), 31–38.

94. Kruth, J. P., Badrossamay, M., Yasa, E., Deckers, J., Thijs, L., Van Humbeeck, J. (2010). Part and material properties in selective laser melting of metals. In Proceedings of the 16th International Symposium on Electromachining.

95. Lacroix, D., Pantino, J.F.R. (2011). Finite element analysis of donning procedure of a prosthetic transfemoral socket, *Annals of Biomedical Engineering*. 39 (12), 2972-2983.

96. Lee, A.J.C. (1992). The place of numerical and experimental methods in biomedical engineering. In: Middleton, J., Pande, G.N., Williams, K.R. (Eds.), Recent Advances in Computer Methods in Biomechanics and Biomedical Engineering. *Books and Journal International Ltd.*, Swansea, 1–7.

97. Lee, V.S.P., Solomonidis, SE, Spence, W.D. (1997). Stump-socket interface pressure as an aid to socket design in prostheses for trans-femoral amputees-a preliminary study. *Proc Inst Mech Eng,* 211(2), 167-180.

98. Lee, W.C.C., Frossard, L. A., Hagberg, K., Haggstrom, E., Gow, D. L., Steven, G., Branemark, R. (2008). Magnitude and variability of loading on the osseointegrated implant of transfemoral amputees during walking, *Medical engineering and physics*, 30(7), 825-833.

99. Lee, W.C.C., Zhang, M. (2007). Using computational simulation to aid in the prediction of socket fit: a preliminary study, *Medical Engineering and Physics*, 29(8), 923–929.

100. Lee, W.C.C., Zhang, M., Jia, X., Cheung, J.T.M. (2004). Finite element 163odelling of the contact interface between trans-tibial residual limb and prosthetic socket, *Medical Engineering & Physics,* 26(8), 655–662.

101. Legro, M.W., Reiber, G., del Aguila, M., Ajax, M.J., Boone, D.A., Larsen, J.A., Smith, D.G., Sangereozan, B. (1999). Issues of importance reported by persons with lower limb amputation and prostheses, *Journal of Rehabilitation Research and Development*, 36(3) 155-163.

102. Lei, N., Moon, S., Bi, G. (2011). Additive manufacturing and topology optimization to support product family design. Pages 505–510, 2014.

103. Lemaire E.D. (1994). A CAD analysis programme for prosthetics and orthotics, *Prosthet. Orthot. Int.*, 18(2), 112-117.

104. Lemaire E.D., Johnson, F., (1996). A quantitative method for comparing and evaluating manual prosthetic socket modifications. *IEEE Trans Rehabil Eng* 4(4), 303-309.

105. Lenka, P.K., Choudhury, A. R. (2011). Analysis of transtibial prosthetic socket materials using finite element method. *Journal of Biomedical Science and Engineering*, 4(12), 762-768.

106. Lilja, M., Johansson, S., Oberg, T. (1999). Relaxed versus activated stump muscles during casting for tran-tibial prostheses. *Prosthet Orthot Int.* 23:13–20.

107. Lilja, M., Oberg, T. (1995). Volumetric determinations with CAD/CAM in prosthetics and orthotics: Errors of measurement. *J Rehabil Res Dev.* 32(2),141–48.

108. Lilja, M., Oberg, T. (1997). Proper time for definitive transtibial prosthetic fitting. *J Prosthet Orthot.* 9(2), 90–95.

109. Lin, Y.P., Wang, C.T., Dai. K.R. (2005). Reverse engineering in CAD model reconstruction of customized artificial joint", *Medical engineering and physics*, 27(2), 189-193.

110. Linde, H.V.D., Hofstad, C.J., Geurts, A.C.H, Postema, K., Geertzen, J.H.B., Limbeek JV. (2004). A systematic literature review of the effect of different prosthetic components on human functioning with a lower-limb prosthesis. *Journal of Rehabilitation Research & Development.* 41(4), 555-570.

111. Linlin, Zhang, Ming Zhu, Ling Shen, Feng Zheng (2013). Finite Element Analysis of the Contact Interface Between Trans-femoral Stump and Prosthetic Socket, 35th Annual International Conference of the IEEE EMBS Osaka, Japan, 3 – 7 July,

112. Lyon, C.C., Kulkarni, J, Zimerson, E., Van Ross, E., Beck, M.H. (2000). Skin disorders in amputees. *Journal of the American Academy of Dermatology.* 42(3), 501-507.

113. Mak, A.F.T., Zhang, M., Boone, D.A. (2001). State-of-the-art research in lower-limb prosthetic biomechanics-socket interface, *Journal of Rehabilitation Research and Development*, 38(2), 161-174.

114. McGarry, T, McHugh, B, Buis, A, McKay, G. (2008). Evaluation of the effect of shape on a contemporary CAD system. *Prosthet Orthot Int.*; 32(2), 145–54.

115. McGarry, T., McHugh, B. (2005). Evaluation of a Contemporary CAD/CAM System, *Prosthetics & Orthotics International* 29(3), 221.

116. Michael, J.W. (1986). Upper limb powered components-current concepts. *Clin Prosthet Orthot,* 10:66-74.

117. Montgomery, John, T., Meagan, R. Vaughan, Richard, H. Crawford (2010). Design of an actively actuated prosthetic socket. *Rapid Prototyping Journal*, 16(3), 194-201.

118. Moo, E.K., Abu Osman, N.A., Pingguan-Murphy, B., Wan Abas, W.A.B., Spence, W.D., Solomonidis, S.E., (2009). Interface pressure profile analysis for patellar tendon-bearing socket and hydrostatic socket, *Acta of Bioengineering and Biomechanics*, 11(4), 37-43.

119. Muir, M. (2013). Multidisciplinary optimisation of a business jet main exit door hinge for production by additive manufacturing. In The 8th UK Altair Technology Conference.

120. Muller, M, Staats, TB, Leach, M, Fothergill, I. (2007). Total surface bearing transtibial socket design impression techniques. *J Proc*. Available at http://www.oandp.org/publications/jop/2007/2007-49.asp.

121. Murdoch, G., Bennett, W. A. (1996). *Amputation: Surgical Practice and Patient Management*. Boston: Butterworth-Heinemann.

122. Murphy, E.F., Wilson, A.B. (1962). Anatomical and physiological considerations in below-knee prosthetics, *Artificial Limbs*, 6(2), 4-15.

123. Nawijn, S.E, van der Linde, H., Emmelot, C.H. Hofstad C.J. (2005): Stump management after transtibial amputation: A systematic review. Prosthetics & Orthotics International, 29(1), 13-26.

124. Neumann, E.S., Brink, J., Yalamanchili, K., Lee, J.S. (2013). Regression estimates of pressure on transtibial residual limbs using load cell measurements of the forces and moments occurring at the base of the socket. *Journal of Prosthetics and Orthotics*. 25(1), 1–12.

125. Ng, P, Lee, P.S.V., Goh, J.C.H. (2002). Prosthetic sockets fabrication using rapid prototyping technology. Rapid Prototyping Journal, 8 (1), 53 – 59.

126. Nicholas, P.F., Brian, J.S., Carolyn, C.S., Richard, R.N. (2009). Topology optimization and freeform fabrication framework for developing prosthetic

feet 20th Annual International Solid Freeform Fabrication Symposium. University of Texas at Austin, pp. 607-619.

127. Nielsen, C.C. (1991). A survey of amputees: functional level and life satisfaction, information needs, and the prosthetist's role. *J Prosthet Orthot*; 3(3), 125–130.

128. Novicov, A., Foort, J. (1982). Computer aided socket design for amputees. ConfBiosteriometrics-82, Appendix 5, University of British Columbia, Vancouver, Canada, 1-4.

129. Oberg K, Kofman, J, Karisson, A, Lindström, B, Siglad, G. (1989). The CAPOD system—A Scandinavian CAD/CAM system for prosthetic sockets. *J Prosthet Orthot*. 1(3), 139–48.

130. Oberg, T., Lilja, M., Johansson, T., Karsznia, A. (1993). Clinical Evaluation of Trans-tibial Prosthesis Sockets: Comparison between CAD CAM and Conventionally Produced Sockets, Prosthetics and orthotics International 17:164.

131. Pandey, R., Pattanaik, L.N. (2014). A fuzzy QFD approach to implement reverse engineering in prosthetic socket development. Int. J. Industrial and Systems Engineering, 17(1), 1-14.

132. Peters, E.J., Lipsky, B.A., Aragon-Sanchez, J. (2016). Interventions in the management of infection in the foot in diabetes: a systematic review, *Diabetes Metabolism Res Reviews*, 32(1), 145-153.

133. Pilkey W. D., Formulas for Stress, Strain, and Structural Matrices. New York: Wiley, 1994.

134. Poeggel, S., Tosi, D., Duraibabu, D., Leen, G., McGrath, D., Lewis, E. (2015). Optical fibre pressure sensors in medical applications. *Sensors*, 15, 17115–17148.

135. Polliack AA, Craig DD, Sieh RC, Landsberger S, Mcneal DR. (2002). Laboratory and clinical tests of a prototype pressure sensor for 166odellin assessment of prosthetic socket fit. Prosthet Orthot Int. 26(1), 23-34.

136. Portnoy, S., Kristal, A., Gefen, A., Siev-Ner, I. (2012). Outdoor dynamic subject-specific evaluation of internal stresses in the residual limb: Hydraulic

energy-stored prosthetic foot compared to conventional energy-stored prosthetic feet, *Gait Posture*, 35(1), 121-125.

137. Portnoy, S., Siev-Ner, I., Yizhar, Z. (2009). Surgical and Morphological Factors that Affect Internal Mechanical Loads in Soft Tissues of the Transtibial Residuum, Annals of Biomedical Engineering, 37(12), 2583-2605.

138. Portnoy, S., Yarnitzky, G., Yizhar, Z., Kristal, A., Oppenheim, U., Siev-Ner, I., Gefen, A. (2007). Real-time patient-specific finite element analysis of internal stresses in the soft tissues of a residual limb: A new tool for prosthetic fitting, Annals of Biomedical Engineering, 35(1), 120–135.

139. Powelson, T., Yang, J. (2012). Literature review of prosthetics for transtibial amputees, *Int. J. Biomechatronics and Biomedical Robot*ics, 2(1), 50-64.

140. Qin, S. F., Prieto, P. A., Wright, D. K. (2008). A Novel Form Design and CAD Modelling Approach, Elsevier, *Computer in Industry* 59(4), 364-369.

141. Radcliffe, C. W., and J. Foort (1961). The patellar-tendon-bearing below-knee prosthesis, Biomechanics Laboratory, University of California (Berkeley and San Francisco).

142. Radcliffe, C.M., Johnson N.C., Foort, J. (1957). Some experiences with prosthetic problems of above-knee amputees. *Artif Limbs*; spring; 41-75.

143. Rajtukova, V., Hudak, R., Zivcak, J., Halfarova, P., and Kudrikova, R. (2014). Pressure Distribution in Transtibial Prostheses Socket and the Stump Interface. *Procedia Engineering*. 96, 374 – 381.

144. Roark R. J.and Young W. C., Formulas for Stress and Strain.New York: McGraw-Hill, 1975.

145. Rogers, B., Bosker, G. W., Crawford, R. H., Faustini, M. C., Neptune, R.R., Walden, G., and Gitter, A. J., (2007). "Advanced trans-tibial socket fabrication using selective laser sintering". Prosthetics and Orthotics International, 31(1), 88-100.

146. Rogers, B., Stephens, S., Gitter, A., Bosker, G. Crawford, R. (2000). Double-wall, transtibial prosthetic socket fabricated using selective laser sintering: a case study. *J Prosthet Orthot* 12(3), 97 – 100.

147. Rovick, J. (1992). An additive fabrication technique for the computer-aided manufacturing of sockets. *7th World Congress of the International Society for Prosthetics and Orthotics, Chicago, IL.*

148. Rovick, J., Chan, R., Van Vorhis, R., Childress, D. (1992). Computer-aided manufacturing in prosthetics: Various possibilities using industrial equipment. *In Proceedings of the 7th World Congress of the International Society for Prosthetics and Orthotics.*

149. Ryait, H.S., Arora, A.S., Agarwal, R. (2012). Realisation of SEMG-based multi-functional prototype elbow prosthesis, *Int. J. Biomedical Engineering and Technology*, 9(1), 72-87.

150. Safari, M.R., Tafti, N., Aminian, G. (2015). Socket interface pressure and amputee reported outcomes for comfortable and uncomfortable conditions of patellar tendon bearing socket: A pilot study. *Assist. Technol.* 27(1), 24–31.

151. Sagawa, Y., Turcot, K., Armand, S., Thevenon, A., Vuillerme, N., Watelain, E. (2011). Biomechanics and physiological parameters during gait in lower-limb amputees: a systematic review, *Gait Posture*, 33(4), 511–26.

152. Sander, J.E., (1995). Interface mechanics in external prosthetics: review of interface stress measurement techniques, *Medical and biological engineering and computing*, 33(4), 509-516.

153. Sanders JE, Daly CH, Burgess EM. (1992). Interface shear stresses during ambulation with a prosthetic limb. *Journal of Rehabilitation Research and Development.* 29(4), 1-8.

154. Sanders, J.E. (2007). CAD/CAM transtibial prosthetic sockets from central fabrication facilities: how accurate are they? *Journal of Rehabilitation Research and Development* 44(3), 395-405.

155. Sanders, J.E., Daly, C.H. (1993). Normal and shear stresses on a residual limb in a prosthetic socket during ambulation: comparison of finite element results with experimental measurements. *Journal of Rehabilitation Research and Development*, 30(2), 191–204.

156. Sanders, J.E., Fatone, S. (2011). Residual limb volume change: systematic review of measurement and management, *Journal of Rehabilitation Research and Development*, 48(8), 949–986.

157. Sanders, J.E., Lam, D., Dralle, A., Okumura, R., 1997, Interface pressures and shear stresses at thirteen socket sites on two persons with transtibial amputation, *Journal of Rehabilitation, Research and Development*, 34(1), 19-43.

158. Sanders, J.E., Lam, D., Dralle, A.J. and Okumura, R. (1997). Interface pressures and shear stresses at thirteen socket sites on two persons with transtibial amputation. *Journal of Rehabilitation Research and Development*. 34(1), 19–43.

159. Sanders, J.E., Lee, GS. (2008). A means to accommodate residual limb movement during optical scanning: A technical note. *IEEE Trans Neural Syst Rehabil Eng*. 16(5), 505–519.

160. Sanders, J.E., Rogers E.L., Sorenson, E.A., Lee, G.S. (2007). Abrahamson. CAD/CAM trans-tibial prosthetic sockets from central fabrication facilities: how accurate are they? *J. Rehabil. Res. Dev*. 44 (3), 395–405,

161. Sanders, J.E., Severance, M.R., Myers, T.R., Ciol, M.A. (2011). Central fabrication: carved positive assessment. *Prosthet Orthot Int*. 35(1):81–89.

162. Sanders, J.E., Zachariah, S.G., Jacobsen, A.K. and Fergason, J.R. (2005). Changes in interface pressures and shear stresses over time on transtibial amputee subjects ambulating with prosthetic limbs: comparison of diurnal and six-month differences. *Journal of Biomechanics*. 38(8):1566–1573.

163. Sang, Y., Li, X., Luo, Y. (2016). Biomechanical design considerations for transradial prosthetic interface: A review, Proceedings of the Institution of Mechanical Engineers, *Part H: Journal of Engineering in Medicine*, 230(3), 239-250.

164. Saunders, C.G., Foort, J., Bannon, M., Dean, D., Panych, L. (1985). Computer aided design of prosthetic sockets for belowknee amputees. *Prosthetics and Orthotics International*, 9, 17-22.

165. Sayed, A.M.E., Hamzaid, N.A., Kenneth Tan, Y.S., Abu Osman, N.A. (2015) Detection of Prosthetic Knee Movement Phases via In-Socket Sensors: A

Feasibility Study, Hindawi Publishing Corporation the *Scientific World Journal*, 923286, 13 pages.

166. Schreiner, R.E., Sanders, J.E. (1995). A silhouetting shape sensor for the residual limb of a below-knee amputee. *IEEE Trans Rehabil Eng.*, 3(3), 242–53.

167. Selles, R.W., Janssens, P.J., Jongenengel, C.D., Bussmann, J.B. (2005). A randomized controlled trial comparing functional outcome and cost efficiency of a total surface-bearing socket versus a conventional patellar tendon-bearing socket in transtibial amputees, *Archives of Physical Medicine & Rehabilitation*, 86(1),154-161.

168. Sengeh, D.M., Herr, H. A. (2013). Variable-impedance prosthetic socket for a transtibial amputee designed from magnetic resonance imaging data. JPO: *Journal of Prosthetics and Orthotics,* 25(3), 129-137.

169. Sewell, P., Noroozi, S., Vinney, J., Amali, R. (2012). Andrews S. Static and dynamic pressure prediction for prosthetic socket fitting assessment utilising an inverse problem approach. *Artificial Intelligence in Medicine,* 54(1), 29–41.

170. Seymour, N., (2002). Transtibial components-Clinical decision making, prosthics and orthotics, SUNY upstate medical university, Syracuse, New york, 8, 175-208.

171. Shankar, S., Manikandan, M., Kalayarasan, M. (2014). Dynamic contact analysis of total hip prosthesis during the normal active walking cycle, *Int. J. Biomedical Engineering and Technology*, 15(2), 114-127.

172. Shankar, S., Prakash, L., Kalayarasan, M. (2013). Finite element analysis of different contact bearing couples for human hip prosthesis, *Int. J. Biomedical Engineering and Technology,* 11(1), 66-80.

173. Shrivastava, P., Pavri, K. (2015). Frontal Plane Analysis At Knee In Transtibial Amputation. International *Journal of Pharma and Bio Sciences*; 6(2), 595 – 601.

174. Silver-Thorn, M.B., Steege, J.W., Childress, D.S. (1996). A review of prosthetic interface stress investigations, Journal of Rehabilitation Research and Development, 33(3), 253–266.

175. Singh R, Hunter J, Philip A. (2007). Fluid collections in amputee stumps: A common phenomenon. *Arch Phys Med Rehabil.* 88(5), 661–63.

176. Smith, D., Burgess, E.M., The use of CAD/CAM technology in prosthetics and Orthotics Current clinical models and a view to the future, *Journal of Rehabilitation Research & Development.* 38(3), 327-334.

177. Smith, E.J., Anstey, J.A., Venne, G, Ellis, R.E. (2013). Using additive manufacturing in accuracy evaluation of reconstructions from computed tomography, Proceedings of the Institution of Mechanical Engineers, Part H: *Journal of Engineering in Medicine,* 227(5), 551-559.

178. Smith, K.E., Commean, P.K., Bhatia, G., Vannier, M.W. (1995). Validation of spiral CT and optical surface scanning for lower limb stump volumetry. *Prosthet Orthot Int.* 19(2), 97–107.

179. Smith, K.E., Commean, P.K., Robertson, D.D., Pilgram, T., Mueller, M.J. (2001). Precision and accuracy of computed tomography foot measurements, *Arch Phys Med Rehabil,* 82(7), 925-9.

180. Smith, K.E., Commean, P.K., Vannier, M.W. (1996). In vivo 3D measurement of soft tissue change due to lower limb prostheses using spiral computed tomography. *Radiology* 200, 843–850.

181. Smith, K.E., Vannier, M.W., Commean, P.K. (1995). Spiral CT volumetry of below knee residua. IEEE Trans. Rehabil. Eng. 3(3), 235–241.

182. Song, B., Dong, S., Deng, S., Liao, H., Coddet, C. (2014). Microstructure and tensile properties of iron parts fabricated by selective laser melting. Optics & Laser Technology, 56, 451-460.

183. Spaeth, J.P. (2006). Laser imaging and computer-aided design and computer-aided manufacturing in prosthetics and Orthotics, Physical medicine and rehabilition clinic of north America 17(1), 245-263.

184. Staats, T.B., Lundt, J. (1987). The UCLA total surface bearing suction below-knee prosthesis, Clinical Prosthetics and Orthotics, 11(3), 118-130.

185. Steege, J.W., Scnur, D.S. (1987). Finite element analysis as a method of pressure prediction at the below knee socket interface. In: Proceedings of RESNA 10th Annual Conference, California, 814–816.

186. Steege, J.W., Scnur, D.S., Childress, D.S. (1987). Prediction of pressure at the below knee socket interface by finite element analysis. In: ASME Symposium on the Biomechanics of Normal and Pathological Gait, Boston, BED 4, 39–43.

187. Steege, M.B.J.W., Childress, D.S. (1996). A review of prosthetic interface stress investigations, *Journal of Rehabilitation Research and Development,* 33(3), 253-266.

188. Stefanescu, D.M. (2011). Wheatstone bridge-the basic circuit for strain gauge force transducers. In *Handbook of Force Transducers*; Springer: Berlin, Germany, 347–360.

189. Tay, F.E., Manna, M.A., Liu, L.X. (2002). A CASD/ CASM method for prosthetic socket fabrication using the FDM technology, *Rapid Prototyping Journal* 8(4), 258-262.

190. Tiwana, M.I., Redmond, S. J., Lovell, N. H. (2012). A review of tactile sensing technologies with applications in biomedical engineering. *Sens. Actuators A Phys. 179*, 17–31.

191. Tomlin, M., Meyer, J. (2011). Topology optimization of an additive layer manufactured (alm) aerospace part. In The 7th Altair CAE Technology Conference, Gaydon.

192. Torres Moreno, R., Lemaire, E.D., Wood, I.R., Vazquezvela Sanchez, E., Martel, G.G., Morrison, J.B., Daly, C.H. (1995). The evolution of C A D / C A M technology in the design and manufacture of lower limb prosthetic sockets. Revista de la Sociedad Mexicana de Medicina Fisica y Rehabilitation 7 (4), 85-100.

193. Turner-Smith, A. (1997). Structured light surface measurement techniques," Orr J, Shelton J. Optical measurement methods in biomechanics. Germany: Chapman & Hall, 39-58.

194. Tzeng, M.J., Hsu, L.H., Chang, S.H. (2015). Development and evaluation of a CAD/3DP process for transtibial socket fabrication, Biomedical engineering: applications, basis and communications 27(5), 1550044.

195. Vannier, M.W., Commean, P.K., Smith, K.E. (1997). Three-dimensional lower-limb residual measurement systems error analysis, *Journal of Prosthetics & Orthotics* 9:67.

196. Varady, T., Martin, R.R., Cox, J. (1997). Reverse Engineering of Geometric Models – an Introduction, *Computer-aided Design* 29(4), 255.

197. Villalpando, L., Eiliat, H., Urbanic, R. (2014). An optimization approach for components built by fused deposition 173odelling with parametric internal structures. 17, 800–805.

198. Webb, S. (1988). The physics of medical imaging, Taylor & Francis.

199. Williams, R.B., Porter, D, Roberts, V.C., Regan, J.F. (1992). Triaxial force transducer for investigating stresses at the stump/socket interface. *Med Biol Eng Comput* 30(1), 89-96.

200. Wilson, A., Schuch, C., Nitschke, R. (1987). A variable volume socket for below-knee prostheses. *Clin Prosthet Orthot.* 11(1), 11–19.

201. Wilson, A.B. (1989). *Limb Prosthetics*. New York: Demos Medical Pub.

202. Winarski, D.J., Pearson, J.R. (1987). Least-square matrix correlations between stump stress and prosthesis load for below-knee amputees. *J. Biomech. Engng*, 109,238- 246.

203. Wu, C.L., Chang, C.H., Hsu, A.T., Lin, C.C., Chen, S.I., Chang, G.L. (2003). A proposal for the pre-evaluation protocol of below-knee socket design: integration pain tolerance with finite element analysis. *J. Chin. Inst. Eng.* 26(6), 853–860.

204. Yigiter, K., Sener, G., Bayar, K. (2002). Comparison of the effects of patellar tendon bearing and total surface bearing sockets on prosthetic fit and rehabilitation", *Prosthetics and Orthotics International,* 26(3), 206-212.

205. Zachariah, S.G., Sanders, J.E. (2000). Finite element estimates of interface stress in the transtibial prosthesis using gap elements are different form those using automated contact, *Journal of Biomechanics*, 33(7), 895–899.

206. Zachariah, S.G., Sanders, J.E. (2001). Standing interface stresses as a predictor of walking interface stresses in the trans-tibial prosthesis. Prosthet Orthot Int. 25(1), 34-40.

207. Zegard, T., Paulino G.H. (2014). GRAND- Ground structure based topology optimization for arbitray 2D domains using MATLAB. Structural and Multidisciplinary optimization, 50(5), 861-882.

208. Zhang M, Lord M, Turner-Smith AR, Roberts VC. Development of a nonlinear finite element modelling of the below-knee prosthetic socket interface. Med Eng Phys 1995;17(8):559–66.

209. Zhang, M., Arthur, F.T.M., Roberts, V.C. (1998). Finite element modelling of a residual lower-limb in a prosthetic socket: a survey of the development in the first decade, *Medical Engineering & Physics* 20(5), 360–373.

210. Zhang, M., Mak, F.T., Chung, A.I.K, Chung, K.H. MRI investigation of musculoskeletal action of transfemoral residual limb inside a prosthetic socket. 1998 Proceedings of the 20th Annual International Conference of the IEEE Engineering in Medicine and Biology Society. 20:2741Y2743.

211. Zhang, M., Roberts, C. (2000). Comparison of computational analysis with clinical measurement of stresses on below-knee residual limb in a prosthetic socket. *Medical Engineering & Physics*. 22(9), 607–612.

212. Zhang, M., Turner-Smith, A.R., Tanner A and Roberts VC. (1998). Clinical investigation of the pressure and shear stress on the transtibial stump with a prosthesis. *Medical Engineering & Physics*, 20(3), 188–198.

213. Zhang, M., Turner-Smith, Roberts, V.C. and Tanner A. (1996). Frictional action at lower limb/prosthetic socket interface. *Medical Engineering & Physics*. 18(3), 207–214.

214. Ziegler-Graham K., MacKenzie E.J., Ephraim, P.L., Travison, T.G., Brookmeyer, R. (2008). Estimating the prevalence of limb loss in the United States: 2005 to 2050. *Arch Phys Med Rehabil,* 89(3), 422-429.

PAPERS PUBLISHED/ACCEPTED BASED ON THIS WORK

Peer Reviewed International Journal Publications:

1. Nayak C., Singh A., Chaudhary H., 2017, "Sensor based transtibial socket pressure determination using regression analysis and genetic algorithm", *Journal of Advanced Manufacturing Systems* (under review).

2. Nayak C., Singh A., Chaudhary H., 2017, "An Investigation on Effects of Amputee's Physiological Parameters on Maximum Pressure developed at the Prosthetic Socket Interface using Artificial Neural Network". *Technology and Health Care*. IOS press (Accepted) (Issue not assigned).

3. Nayak C., Singh A., Chaudhary H., 2017, "Topology Optimization of Transtibial Prosthesis Socket using Finite Element Analysis", *International Journal of Biomedical Engineering and Technology,* 24(4):323-337.

4. Nayak C., Singh A., Chaudhary H., Tripathi A., 2016, "A novel approach for customized prosthetic socket design", *Biomedical engineering applications, basis & communications,* 28 (3):1650022 (1-10). DOI 10.4015/S1016237216 500228

5. Nayak C., Singh A., Chaudhary H., 2016, "Pressure distribution at lower limb/prosthetic socket interface", *International Journal of Pharma and Bio Sciences,* 7(3):(B) 1258-1262.

6. Pathak V., Nayak C., Singh A., Chaudhary H., 2016, "A virtual reverse engineering methodology for accuracy control of transtibial prosthetic socket", *Biomedical engineering applications, basis & communications*, 28(4):1650037 (1-9).

7. Pathak V., Nayak C., Singh A., Chaudhary H., 2016, "An integrated reverse engineering approach for accuracy control of free-form objects", *Archive of Mechanical Engineering, De Gruyter*, 63(4):635-651.

International/National Conferences

1. Nayak C., Singh A., Chaudhary H., 2015, "Mesh Generation From Point Cloud Data For Transtibial Prosthesis Socket Using Altair Hypermesh", Altair Technology Conference 2015 (I-ATC2015), *Modelling & visualization*, July 14-15, Bangalore, India.

2. Nayak C., Singh A., Chaudhary H., 2015, "Stress analysis of transtibial prosthetic socket thickness using finite element method", *Indian Conference on Applied Mechanics (INCAM)*, IIT Delhi, 13-15 July 2015.

3. Nayak C., Singh A., Chaudhary H., 2014, "Customized prosthetic socket fabrication using 3D scanning and printing", *International Conference on Additive Manufacturing,* September 1-2, Bangalore, India.

4. Nayak C., Singh A., Chaudhary H., 2014, "A Review on Stump-Socket Interface Pressure Distribution", *National Conference on Bio- Mechanical Sciences,* (NCBMS 2014) March 7-8, Bhubaneswar, India, I.K. International Publishing House Pvt. Ltd. ISBN: 978-93-82332-86-2: 253-258.

5. Nayak C., Singh A., Chaudhary H., 2013, "Using Reverse Engineering and Rapid Prototyping to compare the PTB and TSB Socket Design for lower limb prosthesis", *International Conference on Additive Manufacturing*, October 6-7, Bangalore, India.

BRIEF BIO-DATA OF THE AUTHOR

Name   : **Chitresh Nayak**

Date of birth   : August 09, 1980

Address for correspondence : Kamal Singh ka Bagh, Nayak Kothi, Gwalior

            (Madhya Pradesh) India – 474001

Education:

Degree	Discipline	Institute	Board/ University	Percentage	Year
Senior Secondary	PCM	Shanti Nikatan School Hoshangabad	MP Board	61	1998
B.E	Mechanical Engineering	SRCEM Gwalior	RGPV Bhaopal	73	2002
M.Tech	Production Technology	MITS Gwalior	RGPV Bhaopal	73.73	2008
Ph.D	Mechanical Engineering	Malaviya National Institute of Technology Jaipur	Autonomous	8.33 (Course work)	Thesis submitted in Dec 2016

Teaching/Industrial/Research Experience:

University / Institute	Duration	Post
MNIT, Jaipur, (Rajasthan)	January 2013-December 2016	Ph.D. Research Scholar
Amity University, Madhya Pradesh, Gwalior	July 2012-January 2013	Assistant Professor in Department of Mechanical & Automation Engineering
Amity University Rajasthan, Jaipur	August 2008-July 2012	Lecturer/ Sr. Lecturer in Department of Mechanical & Automation Engineering
Maharana Pratap College of Technology, Gwalior	August 2007-August 2008	Lecturer in Department of Mechanical Engineering
Magnum Steel Plant	July 2004-July 2006	Production Engineering